# Expression and function of erythropoietin and its receptor in invertebrate nervous systems

DISSERTATION

zur Erlangung des mathematisch-naturwissenschaftlichen Doktorgrades

"Doctor rerum naturalium"

der Georg-August-Universität Göttingen

vorgelegt von

Daniela Gocht

aus Dresden

Göttingen 2009

Referent: Prof. Dr. Ralf Heinrich
Koreferentin: Prof. Dr. Dr. Hannelore Ehrenreich
Tag der mündlichen Prüfung: 29.Okt. 2009

# Table of contents

## 3 The effect of erythropoietin on the regeneration of auditory receptor fibres in the grasshopper *Chorthippus biguttulus*



## 4 Effects of erythropoietin on cultured insect brain cells

# Introduction to the scientific project

The cytokine erythropoietin (EPO) is a glycoprotein of 30.4kDa that was first described as the main regulator of erythropoiesis (red blood cell production) (Erslev 1953). EPO is predominantly produced by the fetal liver and adult kidney in dependency of the oxygen availability (Dame et al. 1998; Zanjani et al. 1977). Hypoxic conditions increase EPO production and its release into the bloodstream. Circulating EPO binds to its receptor (EPOR) expressed on erythroid progenitor cells in the bone marrow and promotes the generation of erythrocytes by stimulation of proliferation, inhibition of apoptosis, and accelerated differentiation (Jelkmann 1992).

The detection of EPO and its receptor in non-hematopoietic tissues, including the brain of mammals, lead to the identification of previously unknown functions of EPO signalling beyond its role in the production of red bood cells (Tan et al. 1992; Sasaki et al. 2001). Various *in vivo* and *in vitro* studies on mammals revealed an important role of the EPO/EPOR signalling system in the protection of the CNS against harmful stimuli and the regeneration of neuronal cells after injury. Although the hematopoietic EPOR was detected in the CNS, newly employed EPO variants were uncapable of binding the hematopoietic EPOR but retained the neuroprotective effect (Erbayraktar et al. 2003; Leist et al. 2004; Wang et al. 2004; Belayev et al. 2005; Coleman et al. 2006; Villa et al. 2007; Wang et al. 2007). These results indicate that EPO limits the damage caused by injury to various tissues including the nervous system by signalling through a non-hematopoietic receptor. Brines et al. (2004) revealed the importance of a receptor constellation involving the EPOR and the common beta receptor (CβR) subunit for the neuroprotective effect mediated by EPO. The possible existence of a specific EPOR in mammalian central nervous systems and the detection of EPO in lower vertebrates such as several fish species (Chou et al. 2004; Chu et al. 2007), suggested that the EPO/EPOR signalling system may have been evolved before the emergence of vertebrates and its original role may have been to protect the nervous system against pathogens and other damaging stimuli.

The purpose of this doctoral thesis was to investigate whether an analoque to the vertebrate EPO/EPOR sigalling pathway may be present in organisms without erythropoiesis and whether EPO may mediate neuroprotective and neuroregenerative effects on injured nervous tissue of invertebrates.

*Specific aim of the project I*

Since all previous studies concerning the EPO/EPOR signalling system were performed on *in vivo*- and *in vitro* preparations of mammalian nervous tissue, methods for the functional analysis of EPO and EPOR in the CNS of invertebrates had to be established. One aspect of my doctoral thesis dealt with the potential neuroprotective effect of human recombinant EPO (rhEPO) on primary cultured locust brain cells (chapter 4). A necessary prerequisite for this study was (i) to investigate optimal conditions for cultivation of dissociated locust brain cells (ii) to distinguish between different cell types in the cultures (e.g. neurons and glia) and (iii) to

assess the vitality of adherent cells. The respeptive studies are described in the first chapter of this doctoral thesis.

*Specific aim of the project II*

The expression of EPO and EPOR in cells of mammalian nervous systems was previously investigated with specific antibodies against both proteins (Masuda et al. 1994; Morishita et al. 1997; Juul et al. 1998, 1999; Bernaudin et al. 1999; Sirén et al. 2001; Weber et al. 2002; Yu et al. 2002; Knabe et al. 2004). The same antibodies were used to label cells that express EPO- and EPOR-like epitopes in the central nervous systems of mice, annelids (*Hirudo medicinalis*), crustaceans (*Procambarus spec.*) and insects (*Drosophila melanogaster*, *Locusta migratoria*). In addition, Western blot analysis was performed to compare the molecular weight of the proteins detected in the different species. The results of these studies are described in the second chapter of this doctoral thesis.

*Specific aim of the project III*

Nerve crush injuries in the peripheral nervous system of mammals change the expression pattern of EPO and EPOR both in glial and neuronal cells (Campana & Myers 2001; Li et al. 2005; Toth et al. 2008). The activation of the EPO/EPOR signalling pathway results in an induction of mechanisms that support survival and regeneration of the damaged tissues. The aim of this study was to investigate whether crushing of an insect peripheral nerve also alters the expression of invertebrate analogues of EPO and EPOR and whether application of EPO promotes the anatomical and functional regeneration of axotomised auditory receptor fibres. The results of this project are described in the third chapter of this doctoral thesis.

*Specific aim of the project IV*

Various *in vitro* studies revealed a neuroprotective effect of rhEPO under hypoxic conditions and a promotive effect of rhEPO on the regeneration of neurites of cultured mammalian neurons (Lewczuk et al. 2000; Sinor & Greenberg 2000; Sirén et al. 2001; Böcker-Meffert et al. 2002; Ruscher et al. 2002; Wen et al. 2002; Kretz et al. 2005; Zhong et al. 2007). None of the previous studies investigated the neuroprotective and neuroregenerative effect of rhEPO on cultured insect or any other invertebrate brain tissue. The purpose of this project was to determine the potential protective effect of rhEPO on cell viability of primary cultured locust brain cells and a neuronal cell line from *Drosophila melanogaster* under both normoxic and hypoxic conditions. In addition, the promotive effect of rhEPO on neurite outgrowth of cultured locust neurons was analysed. The results of this project are described in the fourth chapter of this doctoral thesis.

# 1 Recognition, presence and survival of locust central nervous glia and neurons in situ and in vitro

## 1.1 Introduction

Neurons and glia interact dynamically to enable information processing in both vertebrate and invertebrate central nervous systems. Although glia has been studied in only relatively few invertebrate species, their functions and underlying mechanisms seem to be very similar to those of vertebrate glia (reviewed by: Laming et al. 2000; Kretzschmar & Pflugfelder 2002; Villegas et al. 2003; Edenfeld et al. 2005). During development and regeneration after central nervous damage, glial cells regulate survival, differentiation and maturation of neurons. Glia directly modulate the growth of axons and dendrites and shape the organisation of neuropils by defining their borders and ensheathing synapses and compartments that are commonly affected by diffusible signals. In mature nervous systems, glial cells provide structural and metabolic support for neurons, electrically insulate neurons, regulate synaptic efficacy by clearance of signalling molecules and contribute to nervous plasticity and the generation of behaviour. In addition, glial cells establish blood- (or haemolymph-) brain barriers and some types are competent to perform immune-like functions.

The most commonly used classification of insect glia distinguishes neuropil glia, cortex glia, surface glia and peripheral glia, based on the location of glial cells within the central nervous system or their morphology rather than physiological characteristics (Ito et al. 1995; Freeman & Doherty 2006; Parker & Auld 2006). It is assumed that the number of glia and the degree of glial differentiation increase with phylogeny (Radojcic & Pentreath 1979; Laming et al. 2000), but reliable data about the glia-to-neuron ratio in invertebrate nervous systems is only available for very few species. Various studies agree that the glia-to-neuron ratio is approximately 10:1 in the human brain and 2 to 2.5:1 in brains of rodents (Pfrieger & Barres 1995; Bass et al. 2004). Within the invertebrates, nervous systems of nematodes seem to contain higher numbers of neurons than glial cells (glia : neuron ratio is 0.17:1 in *C. elegans* (Shaham 2006)) while in annelids glial cells may outnumber neurons by far (glia : neuron ratio is 45:1 in the horse leech *Haemopsis sanguisuga* (Kai-Kai & Pentreath 1981)). The proportion of glial cells in insect central nervous systems is quite variable, even when identical species were considered in different studies. Glia-to-neuron ratios in insects have been estimated to range from 0.25:1 to 8:1 (e.g. Carlson & Saint Marie 1990; Ito et al. 1995; Pfrieger & Barres 1995). A reason for this variability lies in the lack of universal glia-specific markers. Although a number of antibodies, lectins and other molecular markers specifically

label insect glial cells, none of the currently available markers universally labels all types of glia through all developmental stages of a given species (Meyer et al. 1987; Halter et al. 1995; Hähnlein et al. 1996; Boyan & Williams 2004; Gibson et al. 2004; Parker and Auld 2006; Heil et al. 2007). The most commonly used antibody for labelling glial cells in the developing and adult CNS of *Drosophila* is directed against the homeodomain-containing transcription factor Reversed polarity (Repo). The Repo antibody labels all glial cells except the midline glia in *D. melanogaster* (Halter et al. 1995, also see Figure 1). While anti-Repo immunohistochemistry has been used as a universal glial marker in both juvenile and adult tissues of some insect species such as *D. melanogaster* (Halter et al. 1995), *Manduca sexta* (Gibson et al. 2004) and *Apis mellifera* (Hähnlein & Bicker 1997), the antibody labelled glial cells only in early developmental stages of *Locusta migratoria* (Boyan et al. 2002) and *Schistocerca gregaria* (Boyan & Williams 2004).

While the functions of glial cells and their interactions with neurons during developmental formation of the insect nervous system have been extensively studied in flies and moths (reviews by: Oland & Tolbert 2003; Edenfeld et al. 2005; Parker & Auld 2004, 2006) and the roles of glial cells in the separation of central nervous tissues from haemolymph have been studied with some detail (reviews by: Carlson et al. 2000; Stork et al. 2008), their contributions to signalling processes and maintenance of mature central nervous systems are generally poorly characterised. Various studies reported that glial cells are especially sensitive to mechanical dissociation of central nervous tissue leading to a low abundance of surviving glial cells in primary cell cultures (Levi-Montalcini et al. 1973; Beadle et al. 1982; Vanhems and Delbos 1987). Nevertheless, the morphology of glial cells from adult cockroaches (Howes et al. 1989), pupal honeybees (Gascuel et al. 1991) and locust embryos (Vanhems & Delbos 1987) has been studied *in vitro* and a number of functional studies revealed that insect glial cells express high affinity transporters for L-glutamate, GABA and histamine (Campos-Ortega 1974; Borycz et al. 2002; Soustelle et al. 2002, Freeman et al. 2003), respond to neuronal transmitters (Giles & Usherwood 1985; Schofield & Treherne 1985; Leitch et al. 1993) and may require neuron-derived trophic signals for survival and differentiation (Hidalgo et al. 2001; Bergmann et al. 2002; Sen et al. 2004). A prerequisite for *in vitro* studies on primary cell cultures from insect nervous systems is the reliable distinction of glial and neuronal cell bodies, which is especially problematic in fresh cell cultures, where both cell types assume spherical shapes and lack characteristic processes (Beadle et al. 1982, 1987). A simple and widely used method to identify glial cells in histological studies is based on the absence of anti-horseradish peroxidase (HRP) immunoreactivity, which labels the pan-neuronal expressed surface protein Nervana (Jan & Jan 1982; Sun and Salvaterra 1995a, b) and this method has recently been adopted to identify cultured glial cells (Loesel et al. 2006).

The present study demonstrates that the absence of anti-HRP immunoreactivity is not sufficient to identify cultured cell bodies as glia but must be complemented by viability testing. Since dead or dying cultured cells, glia and neurons alike, loose their membranes and with them the HRP-like antigens like Nervana, only cells that are both viable and anti-HRP immunonegative should be considered to be of glial type. Furthermore, this study

demonstrates that the staining pattern of the nuclear marker DAPI is a reliable means to assess the viability of cultured central nervous cells. The above-mentioned methods were used to determine the glia-to-neuron ratios in brains of *Locusta migratoria* and characterise differentiation, survival and the shift in composition of primary cell cultures derived from locust brains.

# 1.2 Material and Methods

Unless otherwise mentioned, all chemicals were either purchased from Sigma-Aldrich (Steinheim, Germany) or Merck (Darmstadt, Germany).

### 1.2.1 Animals

Locusts, *Locusta migratoria* (L.), were purchased from a commercial animal breeder (Schätzle Terraristik, Karlsruhe, Germany) and maintained in colonies at 18-21°C on a 12h/12h day/night cycle. All experiments were carried out with fourth-instar nymphs of *L. migratoria*. For anti-Repo immunocytochemistry wild type fruit flies (*Drosophila melanogaster*, Canton-S) were used. The animals were reared in 175 ml breeding vials (Greiner Bio-One, Solingen, Germany) on an approximately 2 cm thick layer of commercial Nekton-*Drosophila*-food concentrate (Günter Enderle Nekton-Produkte, Pforzheim, Germany) with tap water and vinegar added. Fruit flies maintained at 25°C and 65% relative humidity on a 16h/8h day/night cycle.

### 1.2.2 Anti-HRP immunohistochemistry

*Anti-HRP immunohistochemistry on vibratome sections*. Nymphs of *L. migratoria* were anaesthetised by cooling and their brains dissected in cold saline containing 140 mM NaCl, 10 mM KCl, 4 mM $NaH_2PO_4$ x 2 $H_2O$, 5 mM $Na_2HPO_4$, 2 mM $CaCl_2$ x 2 $H_2O$ and 90 mM Saccharose, adjusted to 6.8 pH. Dissected brains were fixed with 4% paraformaldehyde dissolved in phosphate buffer (PB) for 2 h at room temperature (RT), embedded in albumin-gelatine and postfixed in 4% paraformaldehyde overnight at 4°C. Frontal sections (= horizontal with respect to the neuro axis) of 40µm thickness were cut with a vibrating blade microtome (VT 1000 S, Leica, Bensheim, Germany). The tissue sections were permeabilised in phosphate buffered saline (PBS) containing 1% Triton X-100 for 2 days at 8°C and nonspecific binding of the antibody was reduced by blocking in 2% normal goat serum (NGS, GE-Healthcare, Freiburg, Germany) and 3% bovine serum albumin (BSA, MPI Biomedical, Heidelberg, Germany) dissolved in PBS-1% Triton for 2h at RT. For neuronal staining, anti-HRP serum (rabbit α-HRP) was applied to the sections at a dilution of 1:500 at 8°C for 2 days. After washing several times with PBS, a Cy2-coupled secondary antibody (Cy2 goat α-rabbit IgG, Rockland, Gilbertsville, USA) at a dilution of 1:300 was used to visualise immunoreactivity. For nuclear staining, tissue sections were incubated for 30 minutes at RT with 100µg/ml 4`-6-diamino-2-phenylindole (DAPI) dissolved in PBS. Following several washes in PBS and transfer to PBS with glycerol (1:1), fluorescence was analysed with a conventional fluorescence microscope (Zeiss Axioskop, Jena, Germany) equipped with a Spot CCD camera (Intas, Göttingen, Germany or Invisitron, Sterling Heights, USA). All figures were generated using Adobe Photoshop 7.0.

*Anti-HRP immunohistochemistry on microtome sections.* Brains of *L. migratoria* were dissected and fixed as described above. After dehydration through an ethanol series the

tissue was embedded in paraffin wax and serially cut with a microtome (Reichert-Jung 1130Biocut, Nußloch, Germany) to 5µm sections. After rehydration and washing several times with PBS-1%Triton, the brain slices were incubated with blocking buffer (2% NGS, 3% BSA in PBS-1%Triton) for 2h at RT. The anti-HRP serum (rabbit α-HRP) was dissolved in blocking buffer at a dilution of 1:1000 and applied to the sections over night at RT. After three times of washing with PBS-1%Triton the Cy2-coupled secondary antibody was added (Cy2 goat α-rabbit IgG, Rockland, Gilbertsville, USA) at a dilution of 1:500 for 2h at RT to visualise immunoreactivity. For nuclear staining, tissue sections were incubated with 50µg/ml DAPI dissolved in PBS for 30 minutes at RT.

### 1.2.3 Double immunohistochemistry of anti-Repo and anti-HRP

Brains were dissected and fixed as described above. The tissue was embedded in 5% agarose (double labelling was not possible on albumin-gelatine embedded brain sections) and cut horizontally with a vibrating blade microtome (VT 1000 S, Leica, Bensheim, Germany) into slices of 40µm thickness. The brain sections were permeabilised in PBS containing 1% Triton X-100 for 2 days at 8℃ and no nspecific binding of the antibody was reduced by blocking in 10% normal donkey serum (NDS, Dianova, Hamburg, Germany) and 0.25% bovine serum albumin (BSA, MPI Biomedical, Heidelberg, Germany) dissolved in PBS-1% Triton for 2h at RT. Anti-Repo (mouse α-Repo, 1:50) and anti-HRP serum (rabbit α-HRP, 1:500, Sigma-Aldrich, Steinheim, Germany) were applied to the sections at RT for 2 days. After washing several times with PBS, fluorescence coupled secondary antibodies (Cy2 donkey α-rabbit IgG (Rockland, Gilbertsville, USA), Cy3 donkey α-mouse IgG (Jackson Immuno Research, Suffolk, England)) were used to visualise immunoreactivity. For nuclear staining, tissue sections were incubated with DAPI as described above. Following several washes in PBS and transfer to PBS with glycerol (1:1), fluorescence was analysed with a conventional fluorescence microscope equipped with a Spot CCD camera. All figures were generated using Adobe Photoshop 7.0.

### 1.2.4 Analysis of glia-to-neuron ratio *in situ*

To evaluate the glia-to-neuron ratio in brains of *L. migratoria*, paraffin embedded and microtome cut (5µm) brain slices were used. After anti-HRP immunostaining the fluorescence was analysed with a conventional fluorescence microscope (Zeiss Axioskop, Jena, Germany) equipped with a Spot CCD camera (Intas or Invisitron). Every fourth section of a complete series of brain slices of three animals was examined. High resolution pictures of one brain hemisphere without optic lobes and peripheral nerve roots of anti-HRP immunofluorescence and DAPI-staining were taken and superimposed using Photoshop 7.0 (Adobe). Locations of neuronal and glial cell bodies were individually marked, counted (ImageJ 1.3v, NIH) and their numbers graphed with Microsoft Excel.

### 1.2.5 Preparation of primary cell cultures

Brains without optic lobes were dissected and transferred to sterile culture medium (Leibowitz L-15, Gibco, Invitrogen, Karlsruhe, Germany) containing 0.5% gentamicin (GM).

To exclude haemocytes from cell cultures, brains were washed three times with fresh L15-0.5% GM. To ease dissociation of cells, brains were treated with a collagenase/dispase (Gibco, Invitrogen, Karlsruhe, Germany) solution (1mg/ml in L15-0.5% GM) for 15-20 minutes at 29°C. The reaction was stopped by washing twice with 250µl/brain of Hanks' balanced salt solution (HBBS, Gibco, Invitrogen, Karlsruhe, Germany). Afterwards the tissue was gently titurated by repeated passage (~15-20 times) through the tip of a 100µl Eppendorf pipette (Eppendorf, Wesselin-Berzdorf, Germany). After brief spinning (3000 x g) in a bench-top centrifuge (Quick Spin 7000, Süd-Laborbedarf, Gauting, Germany) the supernatant containing cellular debris was discarded while the pellet of dispersed cells was resuspended in 200µl/brain of L15-0.5% GM. The cell suspension was plated on concavalin-coated (1µg/ml) cover slips (100µl/coverslip, Hartenstein, Würzburg, Germany), which were placed in sterile plastic culture dishes (35 x 10mm, Corning Inc., Sigma-Aldrich, Steinheim, Germany). Cells were allowed to adhere to the bottom of the cover slip for 90 minutes. Afterwards the culture dishes were filled up with 2ml L15-0.5% GM containing 5% fetal calf serum (FCSG, PAA laboratories, Cölbe, Germany) and placed in a humidified culture chamber at 29°C (Heraeus, Hanau, Germany). The medium was replaced every four days. To evaluate the growth of neurites, particular cultured neurons were observed with relief contrast optics and repeatedly, photographed with a digital camera (Olympus DP 12-2, Hamburg, Germany). Neurite lengths were measured with the program NeuronJ 1.1.0 (macro for ImageJ 1.37v, National Institute of Health).

### 1.2.6 Phalloidin staining and anti-HRP immunocytochemistry of cultured cells

For Phalloidin staining and immunostaining against HRP, 5-12 days old primary cell cultures were fixed for 15 minutes in 4% paraformaldehyde dissolved in PB and rinsed three times with PBS and two times with PBS-0.1% Triton. To reduce nonspecific binding of the anti-HRP antibody, cells were treated with blocking buffer (3% BSA, 2% NGS in PBS-0.1% Triton) for 1h at RT. Cultures were incubated over night at 8°C with the anti-HRP serum (rabbit α-HRP) at a dilution of 1:500. After several washing steps with PBS a Cy3-coupled second antibody (Cy3 goat α-rabbit IgG, Rockland, Gilbertsville, USA) was added at a dilution of 1:1000 for 1h at RT. For staining the actin skeleton of the cells, the culture dishes were subsequently incubated with Alexa Fluor488 phalloidin (Invitrogen, Karlsruhe, Germany) at a dilution of 1:100 for 2 days at 8°C. For nuclear staining, the cells were incubated with DAPI (100µg/ml) for 30 minutes at RT. Following several washes in PBS and transfer to PBS with glycerol (1:1), fluorescence was analysed as described above.

### 1.2.7 Glia-to-neuron ratio *in vitro*

To identify the ratio of neurons and glial cells in primary cell cultures, 10 *L. migratoria* brains were dissected, their cells dissociated and pooled and allocated in similar portions to 20 cell culture dishes. Subsequently, cells were allowed to adhere on the bottom of the concavalin-coated cover slips and maintained as described above. Starting at day 0, after cells adhered to the ground, cells of three culture dishes were fixed for analyses on every other day (day 0, 2, 4, 6, 8 and 10). Cell cultures were stained with anti-HRP and DAPI (as described above)

and analysed with a conventional fluorescence microscope (Zeiss Axioskop) equipped with a Spot CCD camera (Intas or Invisitron). DAPI- and anti-HRP immunofluorescence were individually photographed and subsequently merged. Cell counts were performed on 24 photographs per culture dish. The overall area that was analysed in this way consisted of two continuous rows of pictures passing to the right and the left of the centre of the cover slip. This procedure assured the inclusion of both densely and sparsely overgrown regions in the analysis. The data of cell counts were transferred to a spreadsheet (Microsoft Excel) to generate an initial diagram. All values were expressed as means ± SD (standard deviation). The diagram was reformatted and labelled with Photoshop 7.0 (Adobe).

### 1.2.8 Electron microscopy of primary cultured cells

For ultrastructural analysis, cells were plated on concavalin-coated lumox™ multiwell plates (In Vitro Systems & Services GmbH, Göttingen, Germany), filled up with 2ml L15-0.5% GM containing 5% FCSG and placed in a humidified culture chamber at 29℃ for four days. The cells were fixed for 30 minutes at 10℃ with 2.5% g lutardialdehyde in 0.05M Na-cacodylate buffer (Merck, Darmstadt, Germany), washed for several times and postfixed with 2% osmic acid (Merck, Darmstadt, Germany) in the same buffer solution for 30 minutes at 10℃. Afterwards the cells were dehydrated through an ethanol series and blockstained for 30 minutes with a saturated solution of uranyl acetate (Serva, Heidelberg, Germany) in 70% ethanol at RT. The bottom foil of the lumox™ multiwell plates was cut into small pieces and flat-embedded in Araldite (Serva, Heidelberg, Germany). Sections of 60-70nm thickness were cut with a diamond knife (Diatome AG, Biel, Schweiz) in parallel to the plane of growth and sections were mounted on Formvar-coated slot-grids (Plano, Wetzlar, Germany). Transmission electron microscopic analysis was performed with a Zeiss 902 microscope (Zeiss, Jena, Germany), with specimen cooling by $N_2$, under low and high magnifications.

# 1.3 Results

### 1.3.1 Identification of glial cells in the insect brain

The most commonly used antibody for labelling glial cells in insects is directed against the homeodomain-containing transcription factor Reversed polarity (Repo). In the fly *Drosophila melanogaster* glia can be identified by presence of the specific glia marker anti-Repo and the absence of the specific neuronal marker anti-HRP (Figure 1). Following criteria used in earlier studies on different species (e.g. Hoyle 1986; Ito et al. 1995; Cantera & Trujillo-Cenoz 1996; Jones 2001), three major categories of glial cells were identified on the basis of their location. The surface glia, that together with the unstained neural lamella forms the perineurium which functions as the blood-brain barrier, ensheaths the entire brain (Figure 1a). The neuropil glia was found within central neuropil regions (Figure 1b) and the cortex glia was present among neuronal cell bodies in all regions of the peripheral brain cortex (Figure 1c). But the anti-Repo serum did not stain all types of glia (Figure 1d-f, white asterisks) and can therefore not be used as a reliable marker for all types of a fruitfly`s glial cells.

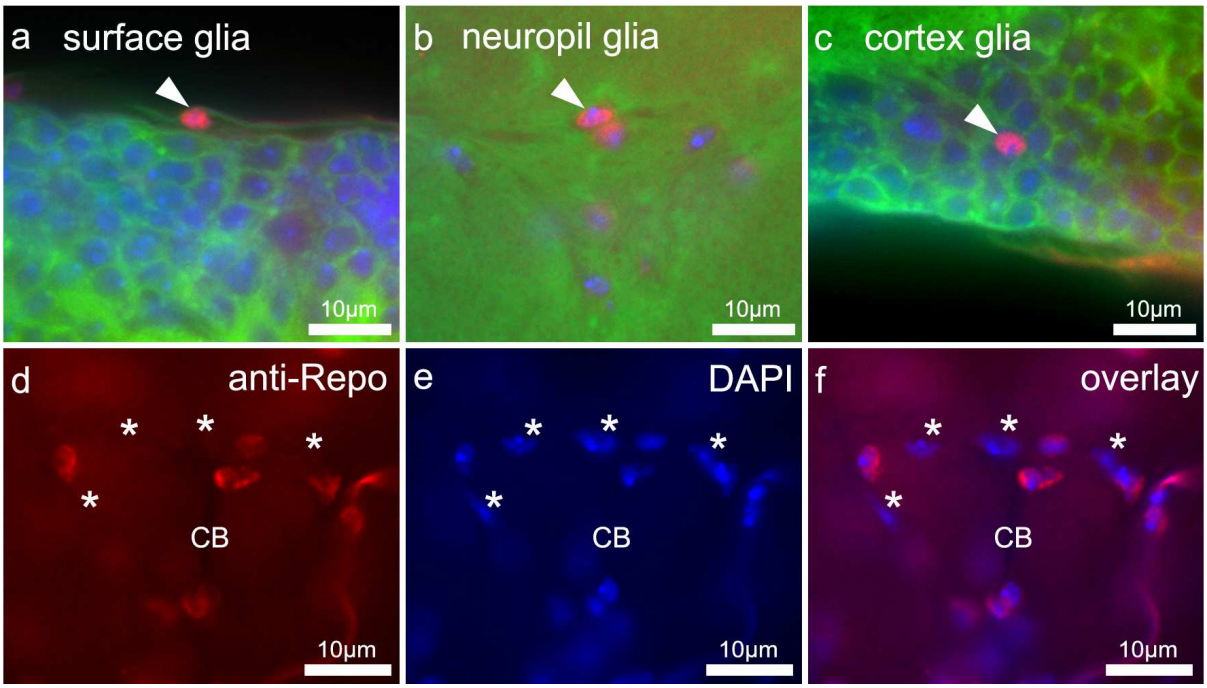


**Figure 1:** Brain sections of *D. melanogaster* labelled with the glia marker anti-Repo (red fluorescence), the neuronal marker anti-HRP (green fluorescence) and the nuclear marker DAPI (blue fluorescence). **a-c:** White arrowheads mark the different types of glia in the brain: surface glia (a), neuropil glia (b) and cortex glia (c). **d-f:** Glia in the central neuropil region of the brain (central complex). White asterisks mark glial cells that are stained with DAPI (e) but not with anti-Repo serum (d, f).

Since no universal glia marker is available for insects, numerous studies identified glial cells only by the absence of a specific neuronal surface marker that can be visualised by an antibody against horseradish peroxidase (HRP) (Jan & Jan 1982). Frontal sections through

brains of *L. migratoria* were labelled with anti-HRP serum and the nuclear marker DAPI. Fluorescent labelling revealed the typical partition of arthropod central nervous systems into the peripheral cortex, where most cell bodies are located and central regions containing neuropils and tracts (Figure 2). Central regions housed only a few cell bodies that usually lined the borders of individual neuropils and were rarely detected within particular neuropils. Glial cell bodies were identified by both the presence of nuclear DAPI staining and the absence of neuron-specific anti-HRP immunofluorescence.

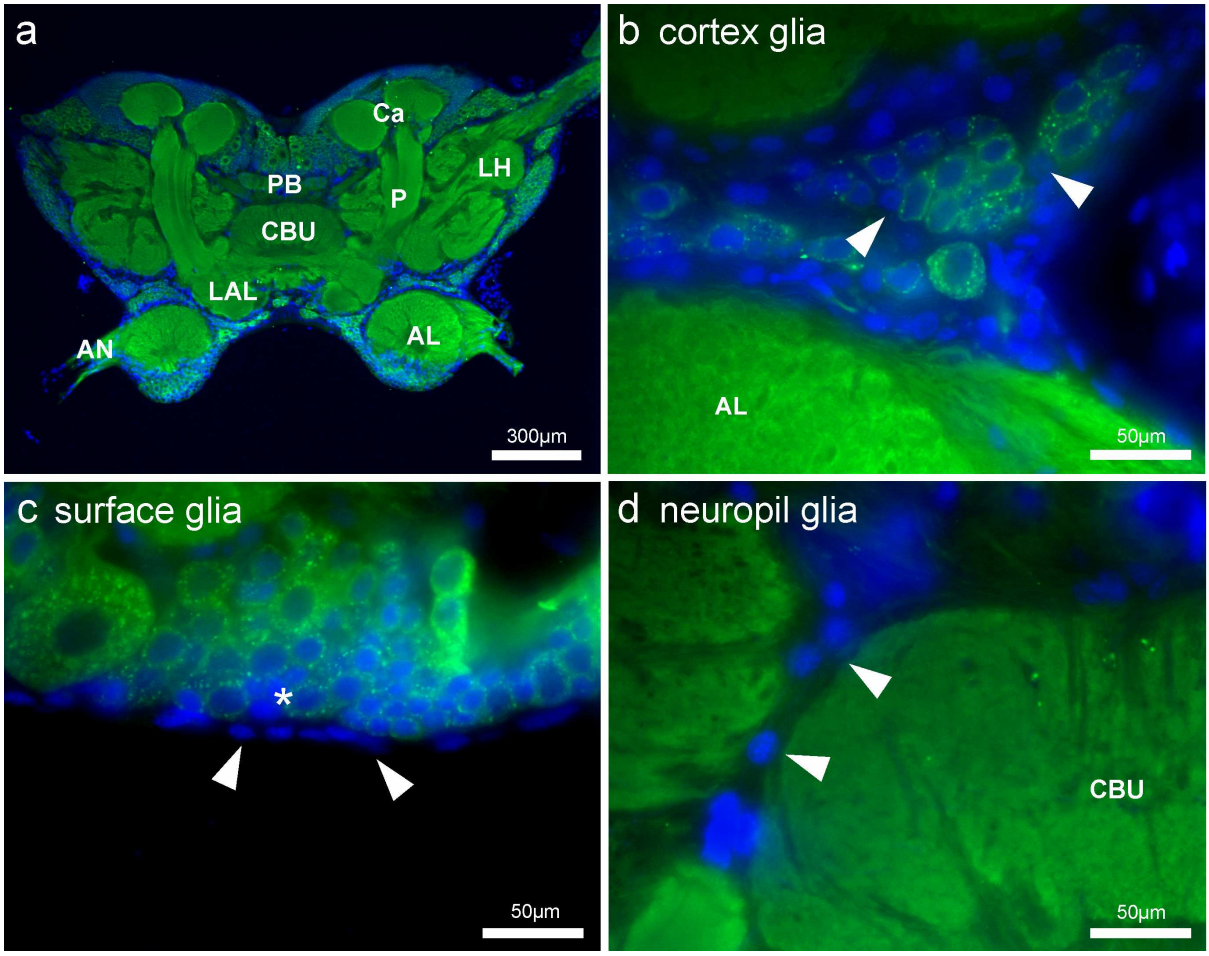


**Figure 2:** Types of glia in the brain of *Locusta migratoria*. Frontal sections through the brain labelled by anti-HRP immunofluorescence (green) and DAPI nuclear stain (blue). **a:** Complete section showing the distribution of cell bodies in peripheral cortex and between brain neuropils. **b:** Cortex glia (marked by arrowheads) in the lateral protocerebrum dorsal to the antennal lobe. **c:** Surface glia (marked by arrowheads) with flat nuclei ventral to the inferior protocerebrum. Asterisk placed next to a cortex glial cell with round nucleus. **d:** Neuropil glia (marked by arrowheads) in between the central complex upper division and adjacent neuropils. Arrowheads and asterisk in b-d mark glial cells that contain the DAPI signal but do not express the HRP-antigen.
AL antennal lobe, AN antennal nerve, Ca calyces of mushroom bodies, P pedunculus of mushroom body, CBU central body upper division, PB protocerebral bridge, LAL lateral accessory lobe, LH lateral horn

Similar to the *Drosophila* brain three major categories of glial cells in the brain of *L. migratoria* were classified on the basis of their locations. Cortex glia (or cell body glia) was present among neuronal cell bodies in all regions of the peripheral brain cortex (Figure 2b), although their cytoplasmic protrusions that separate neurons or groups of neurons from each

other were not specifically labelled. Surface glia was found to ensheath the entire brain (Figure 2c). In comparison with the cortex glia, surface glia was recognised as a chain of elongated nuclei lining the outer border of the peripheral cortex. Neuropil glia was detected between individual neuropils (e.g. between the central body upper division and laterally adjacent neuropils (Figure 2d)) and at the border between the peripheral cortex and central neuropil regions (Figure 2b).

### 1.3.2 Ratio of neurons to glial cells in the locust brain

In order to evaluate the relative proportions between neurons and glia, brains of *L. migratoria* were sectioned into slices of 5 µm thickness and labelled with anti-HRP antibodies and DAPI. The numbers and locations of glial and neuronal cells within a hemibrain were determined in every fourth section. Analysis of every fourth section prevented double counts of the same nuclei in subsequent sections, since even the largest nuclei found in neurosecretory neurons had diameters of less than 20 µm and appeared in at most three consecutive brain sections. As shown in Figure 3 glial cells (marked with white dots) were clearly identified by the presence of nuclear DAPI staining and the absence of neuron-specific anti-HRP immunofluorescence. Even flat nuclei of glial cells located in between of densely packed neurons could be individually counted on photographs with high magnification (Figure 3b, c).

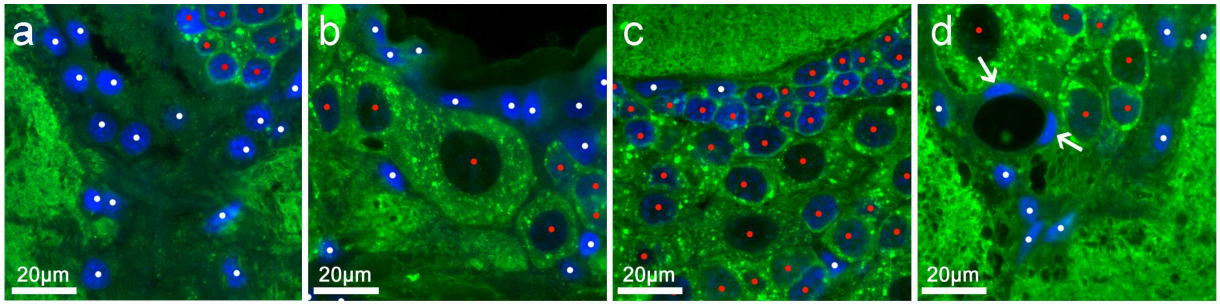


**Figure 3a-d:** Detailed view of locust brain sections labelled by anti-HRP immunofluorescence (green) and DAPI nuclear stain (blue). Glial cells (marked with white dots) are identified by the presence of nuclear DAPI staining together with the absence of neuron-specific anti-HRP immunofluorescence. Nuclei of anti-HRP immunopositive neurons are marked with red dots. Tracheal cells that are also not labelled with anti-HRP can be distinguished from glial cells by their close association with tracheal tubes (d, arrows).

A second type of non-neuronal cell within the central nervous system of insects is the tracheal cell (Loesel et al. 2006). Tracheal cells can be distinguished from glial cells by their close association with tracheal tubes invading the brain and characteristically elongated nuclei (Figure 3d). Less than 10 cells per section were identified as tracheal cells and were not included in glial cell numbers.

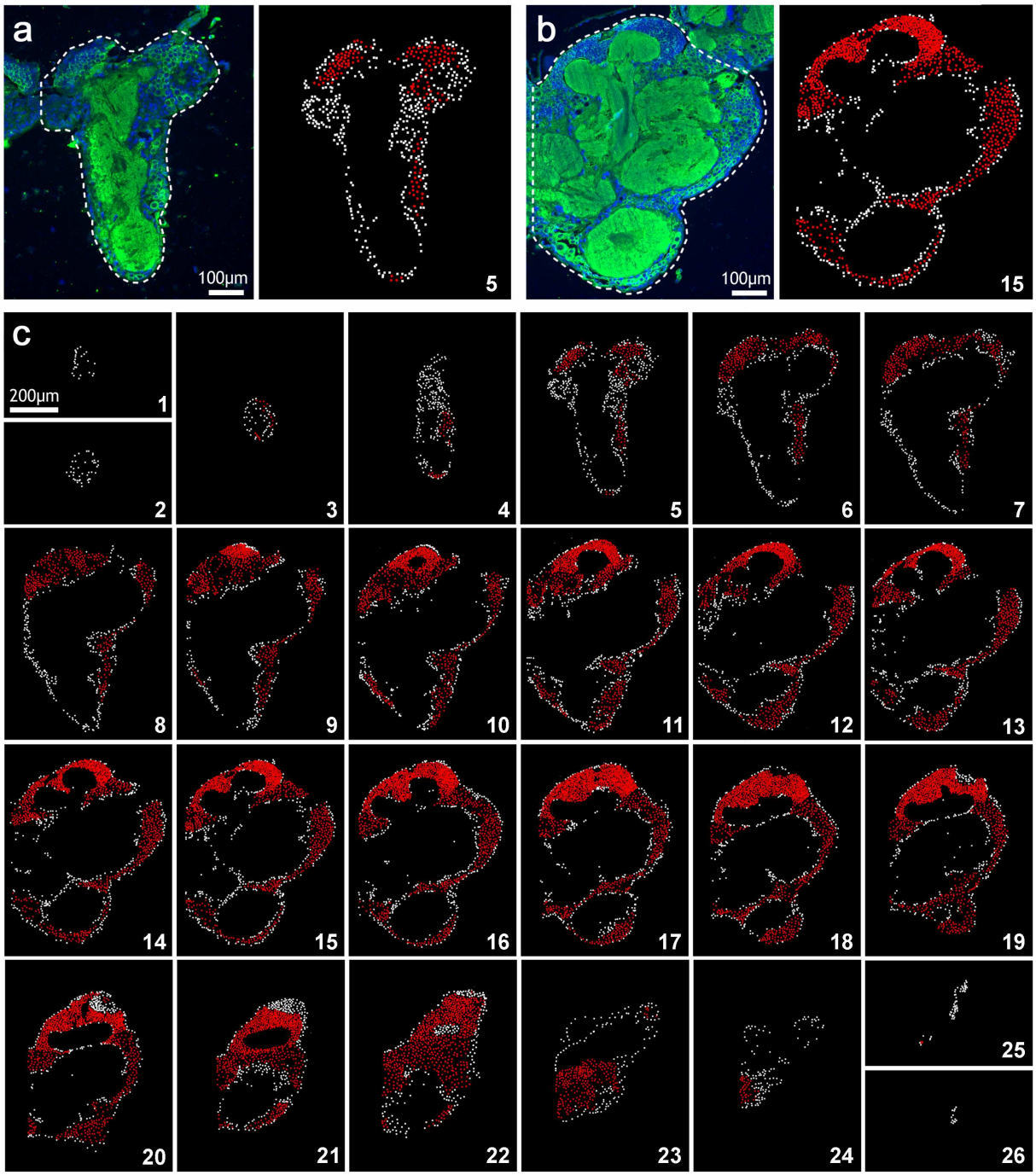


**Figure 4:** Complete series of evaluated sections of one *L. migratoria* brain. **a, b:** Two paraffin sections through the brain of *L. migratoria* labelled by anti-HRP immunofluorescence (green) and DAPI nuclear stain (blue). Dotted lines frame one brain hemisphere excluding the optic lobe and peripheral nerve roots, in which the locations of glial (white dots) and neuronal (red dots) nuclei were determined. **c:** Distribution of glial and neuronal cells in a series of frontal sections (from rostral to caudal) through the brain. Every fourth section of the complete series (altogether 104 sections of 5 µm thickness) is displayed.

Figure 4a-c displays the complete series of evaluated sections of one *L. migratoria* hemibrain. Two labelled histological sections, one from the rostral portion of the brain and one through its central part, illustrate the evaluated hemiganglionic region (Figure 4a, b). As seen in these two examples and the complete series of sections, glial cell bodies dominate in peripheral rostral and caudal sections while neurons are more abundant in sections through

central parts of the brain. Neuronal cell bodies were especially densely packed in regions dorsal to the mushroom body calyces that house the somata of Kenyon cells. In contrast, central neuropil areas were completely free of neuronal cell bodies but contained considerable numbers of glial cells that seemed to line the borders of individual neuropils (best seen in Figure 4c). Three brains were analysed with the same detail in order to determine the numbers of neuronal and glial cell bodies in every fourth histological frontal section. The results are summarised in Figure 5.

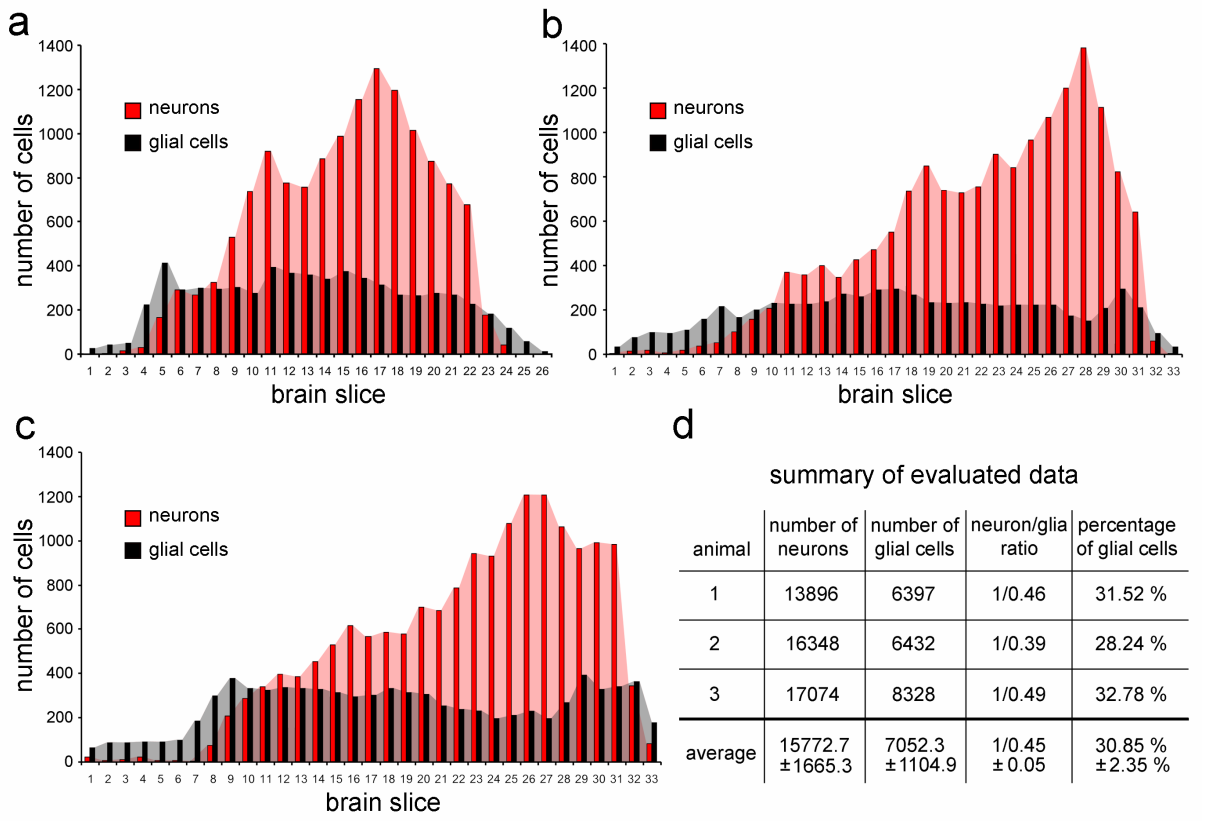


| animal | number of neurons | number of glial cells | neuron/glia ratio | percentage of glial cells |
|---|---|---|---|---|
| 1 | 13896 | 6397 | 1/0.46 | 31.52 % |
| 2 | 16348 | 6432 | 1/0.39 | 28.24 % |
| 3 | 17074 | 8328 | 1/0.49 | 32.78 % |
| average | 15772.7 ±1665.3 | 7052.3 ±1104.9 | 1/0.45 ±0.05 | 30.85 % ±2.35 % |

**Figure 5:** Numbers of glial and neuronal cells in series of frontal sections through the brain of *Locusta migratoria*. **a-c:** Three brains were sectioned from rostral to caudal into 5 µm thick slices and numbers of glial and neuronal nuclei in one hemisphere (excluding optic lobes and roots of peripheral nerves) were determined in every fourth section. **d:** Summary and comparison of cell counts from the three brains displayed in a-c.

As indicated by the different numbers of evaluated sections the three brains differed in their rostral-to-caudal dimensions from approximately 520 µm (brain a) to 660 µm (brains b and c) and the total numbers of cells varied accordingly. In all three brains glial cells were more abundant than neurons in the most rostral and the most caudal sections, while neurons dominated in sections through the central parts. Although total numbers of counted cell nuclei varied (Figure 5d), the ratio of glial to neuronal cell bodies was quite similar in all three brains (average glia-to-neuron ratio is 0.45 ± 0.05:1). This suggests that almost a third (30.85% on average) of all *L. migratoria* brain cells are of glial phenotype.

### 1.3.3 Identification of glial cells in primary cultures of locust brain cells

In order to evaluate whether anti-HRP immunocytochemistry can be used to reliably distinguish between cultured neurons and glial cells, as it has been suggested by a previous study (Loesel et al. 2006), central brains of *L. migratoria* were dissected, dissociated and transferred into primary cell cultures. After two days in cell culture, approximately 40% of the cells expressed HRP-associated immunofluorescence and were therefore identified as neurons (Figure 6a). According to Loesel and coworkers (Loesel et al. 2006), who used the lack of anti-HRP immunoreactivity as a sufficient criterion to identify a glial cell, the remaining approximately 60% of cultured cells should have been classified as glia. But nuclei that were not associated with surrounding anti-HRP immunoreactivity showed different patterns of DAPI staining (Figure 6c). Some nuclei contained a discontinuous patchy distribution of DAPI fluorescence that was similar to the nuclei of HRP-expressing neuronal cells. In contrast, other nuclei were uniformly labelled by DAPI and in most cases smaller than the ones with discontinuous staining (Figure 6c, e). When cultures were incubated with trypan blue to determine cell viability, all cells with uniformly DAPI-labelled nuclei accumulated the dye indicating that they were dead or in the process of dying. In contrast, all cells with discontinuous nuclear DAPI staining excluded the trypan blue indicating their viability (Figure 6d, e). Most dead cells' nuclei were entirely devoid of surrounding cytoplasm. Nuclei with uniform DAPI distribution were only occasionally associated with fragments of HRP immunoreactive tissue, suggesting that these were nuclei of dead neurons whose membranes had degraded which caused the loss of cytoplasm. This was confirmed by electron microscopy of primary cultured cells. As shown in Figure 6f, viable cells contained large nuclei with loose distribution of electron dense heterochromatin, which resembled the patchy nuclear staining with DAPI. These nuclei were surrounded with cytoplasm containing numerous organelles and membranous compartments and were enclosed by an intact cytoplasmic membrane. In contrast, condensed nuclei with uniform electron dense appearance and a seemingly intact nuclear membrane either appeared completely isolated or were surrounded by loose cellular debris that was not enclosed by cytoplasmic membranes (Figure 6g).This suggests the assumption that nuclei with uniform DAPI staining are remnants of cells that lost their cytoplasm upon degradation of their cytoplasmic membranes. Since the neuronal surface marker HRP is contained in cytoplasmic membranes, the absence of HRP immunoreactivity is not sufficient to identify a nucleus as part of a glial cell. Remnants of neurons that lost their cytoplasmic membranes would appear identical. Only in combination with a method that confirms the presence of intact cellular membranes (e.g. a viability test such as the pattern of DAPI staining or a method that directly visualises cytoplasmic membranes or other functional cytoplasmic components such as the actin skeleton) is the absence of HRP expression a reliable indicator for glial cells.

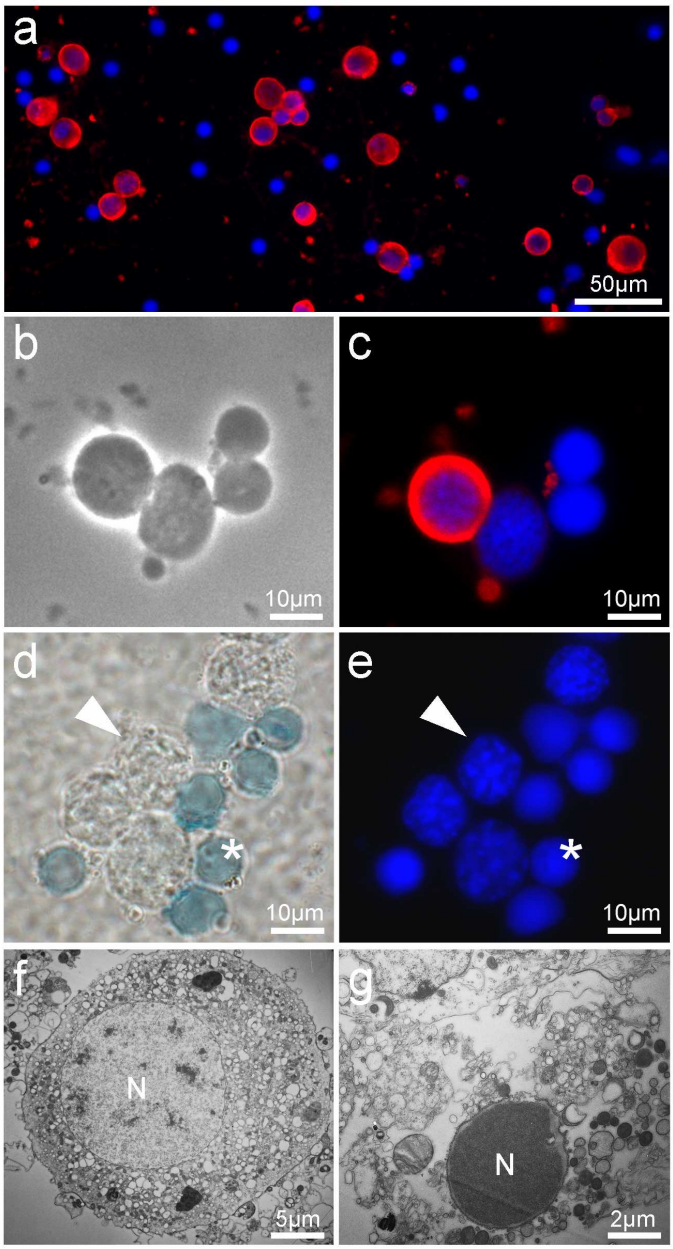


**Figure 6:** Distinction of glial and neuronal cells in primary cell culture of locust brains. **a:** Cultured cells labelled with the neuron-specific anti-HRP antibody (red fluorescence) and the nuclear marker DAPI (blue fluorescence). **b, c:** Freshly cultured cells appear similar in phase contrast. Anti-HRP immunoreactive cells (red fluorescence) contain nuclei with discontinuous DAPI staining (blue fluorescence). Nuclei of cells that do not express the HRP antigen are either discontinuously or uniformly labelled by DAPI. **d, e:** All cell bodies with discontinuous nuclear DAPI staining excluded the dye trypan blue (arrowhead), while all cell bodies with uniform nuclear DAPI fluorescence accumulated the dye and were identified as dead or dying (asterisk). **f, g:** Electron microscopy revealed a discontinuous distribution of electron dense heterochromatin in nuclei of intact cells (f). Nuclei were embedded in cytoplasm containing numerous organelles and membranous compartments which were enclosed by an intact cytoplasmic membrane. In contrast, nuclei of dead cells (g) lacked surrounding cytoplasm and cytoplasmic membrane (only the nuclear membrane is visible) and contained a uniform distribution of electron dense chromatin.
N nucleus

Primary cell cultures from *L. migratoria* brains were observed for prolonged periods of culturing. Cultures that were maintained for up to 21 days still contained large numbers of physiologically intact cells. During enzymatic and mechanical dissociation, brain cells entirely loose their processes and the remaining cell bodies assume a round shape in fresh cultures. At this stage, glial cells resemble neurons and cannot be reliably distinguished by light microscopic comparison (Figure 6b). As described above, the lack of anti-HRP immunoreactivity in combination with discontinuous nuclear DAPI staining that confirms the viability of the cell readily identifies glial cells in culture. With increasing time in cell culture, glial and neuronal cells assume different morphologies. Neurons retained the round shape of their cell bodies and regenerated HRP-immunoreactive neurites with or without swellings along the concavalin-coated cover slips (Figure 8a-d). The first neurites appeared after six hours in culture and their extensions and arborisation patterns increased continuously. Observations of individual neurons revealed cumulative growth rates of all their neurites of

156.74 ± 85.80µm within the first 24 hours (n = 130 cells of 7 different culture dishes). Physiologically intact neurons displayed progressive growth of their neurites during the first ten days in cell culture. Later on neurite outgrowth of most neurons ceased, some neurites were usually retracted and the neurons assumed a relatively stable morphology. The time lapse-observation of cultured cells in Figure 7 shows a neuron that initially regenerated some neurites until day four and died at day six (black arrow). After disintegration of its cytoplasmic membrane on day seven all remnants of the cell detached and vanished from the bottom of the culture dish by day eight.

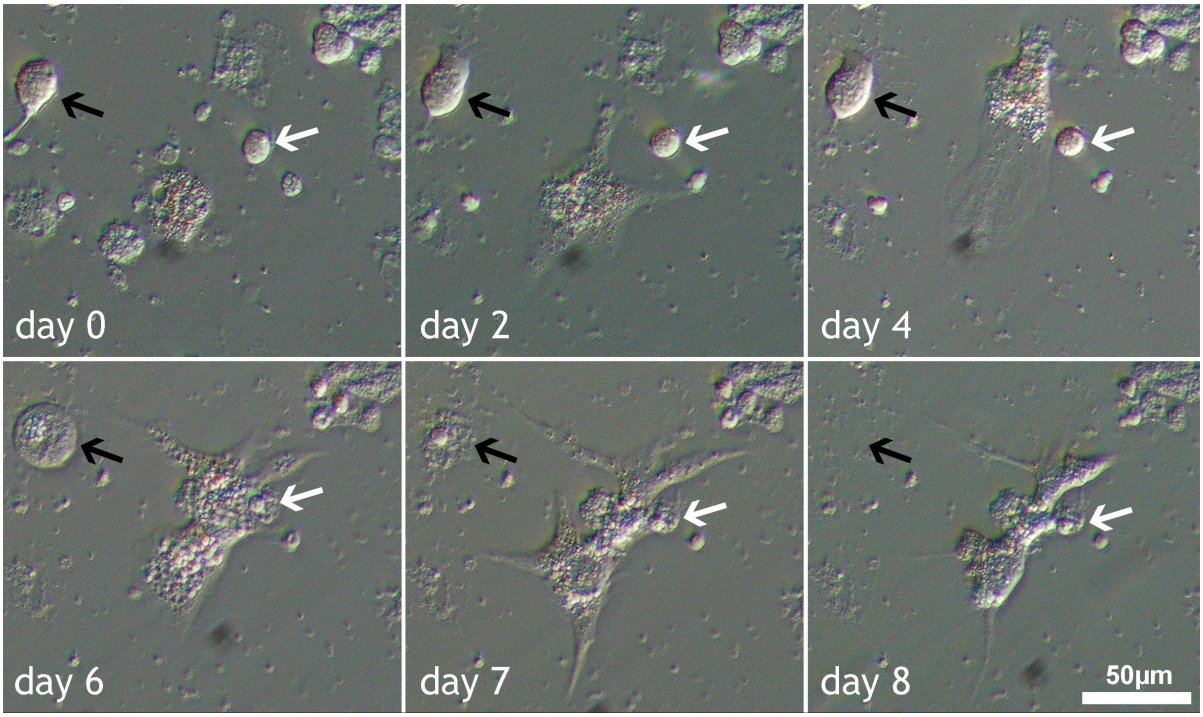


**Figure 7:** Time lapse observation of a cultured glial cell and adjacent neurons in relief contrast microscopy. The glial cell in the centre had a flat appearance and phagocytosed an adjacent cell body (white arrow). Another nearby neuron (black arrow) died at day 6. After disintegration of its cytoplasmic membrane (day 7) the nucleus and other cellular remnants detached from the bottom of the culture dish (day 8).

The morphology of cultured glial cells was visualised by incubation with labelled phalloidin which binds to filamentous actin (Figure 8). Glial cell bodies appeared flat and were surrounded by flat extensions of cytoplasm (Figure 8a). Some glial cells formed clusters whose emerging membranous extensions could not be associated with particular cells (Figure 8b). As shown in the time lapse-recording in Figure 7, glial cell morphology was highly variable and remained flexible throughout its survival in culture. One of the functions of glial cells *in vivo* is to remove degenerating cells and cellular debris by phagocytosis. The observations shown in Figure 7 suggest that cultured glial cells from locust brains may retain their phagocytotic activity in dissociated cell culture. The cell body marked by white arrows is enclosed by the glial cell on day 6 and subsequently incorporated. Probably following the phagocytotic incorporation of membranous neuronal structures some glial cells expressed anti-HRP immunoreactivity in cytosolic inclusions. Figure 8d-d`` shows a glial cell with HRP-immunoreactive inclusions. One neurite of a co-cultured neuron sharply terminates right at

the site of contact with the glial cell, suggesting that part of the incorporated HRP-immunoreactive material might have originated from the previously more extended neurite.

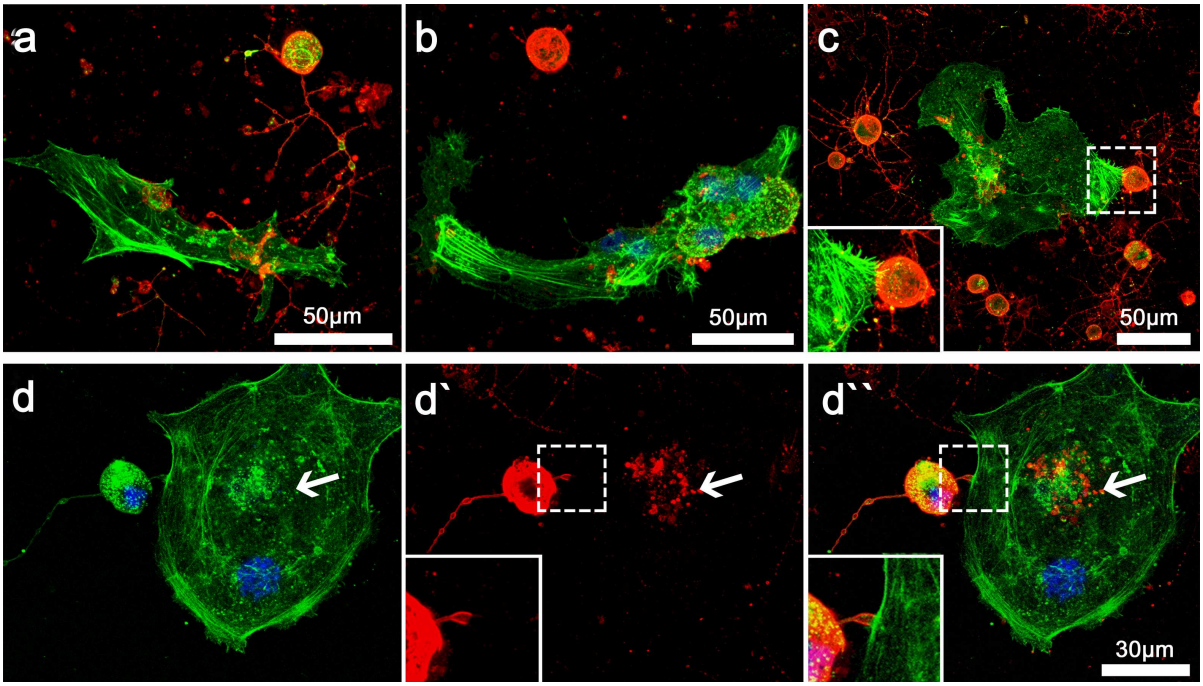


**Figure 8a-c:** Four day old primary cell culture labelled with anti-HRP serum (red) to identify neuronal cells. Filamentous actin was labelled with phalloidin (green) to reveal the morphology of glial cells. Nuclei were stained with DAPI (blue). **d-d``:** Cultured cells of locust brains labelled with anti-HRP, phalloidin and DAPI. The combination of the three labels identifies a neuron with bipolar processes and a glial cell with a flat and expanded morphology (d``). The upper neurite of the labelled neuron ends exactly where it contacts the glial cell (d` and d``). The glial cell contains a number of HRP-immunoreactive inclusions (white arrows) that may represent incorporated remnants of the previously more extended neurite.

### 1.3.4 Ratio of neurons to glial cells in primary cultures of locust brain cells

In order to assess the survival of glial cells and neurons, cells from 10 *L. migratoria* brains were initially pooled and evenly distributed to 20 cultures. Starting with fresh cultures whose cells were given time to attach to the concavalin-coated bottom, the numbers of neurons, glial cells and dead/dying cells were determined in three cultures on every second day until 10 days of culture time. Since cultured cells have to be fixed to evaluate their viability, it was not possible to monitor cell death in individual cultures to determine absolute numbers of dying cells over time in a particular culture. Some cells died immediately due to severe damage during the process of dissociation. After establishment of cultures, a small proportion of cells are in the process of dying at any given time. Some of the dying cells displayed apoptosis-like features such as condensation of DNA (Figure 9, day 0, asterisks), fragmentation (Figure 9, day 1, arrowhead) and shrunken nuclei (Figure 9, day 2 and 4, arrowheads).

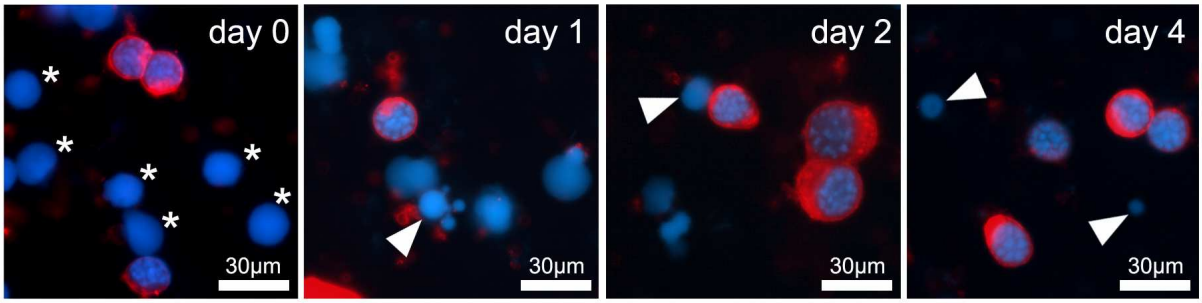


**Figure 9:** Time lapse observation of cultured locust brain cells labelled with anti-HRP (red fluorescence) and the nuclear marker DAPI (blue fluorescence). In fresh cultures dead cells show intense condensation of chromatin (day 0, asterisks). Within the first 24 hours fragmentation of dead cells` nuclei was observed (day 1, arrowhead). In older cultures the nuclei of dead cells were of smaller diameter than nuclei of living cells (day 2-4, arrowheads).

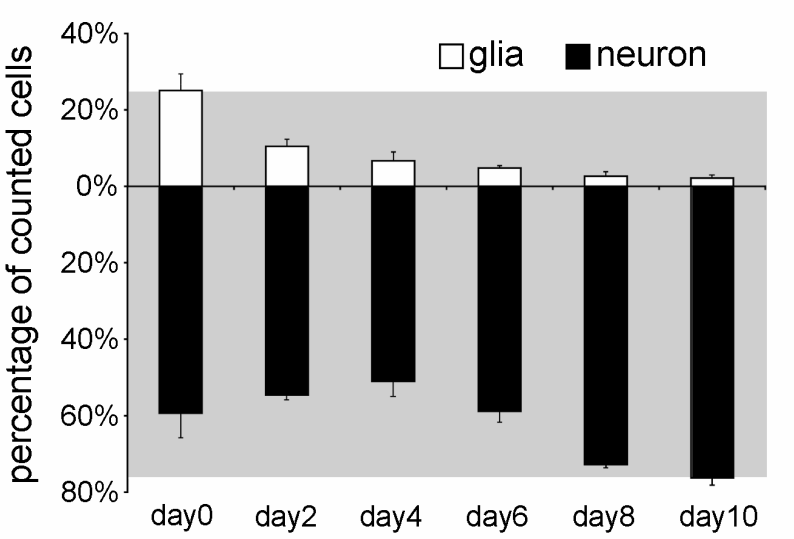


**Figure 10:** Glia-to-neuron ratio after different duration in primary cell culture. The proportion of viable glial cells continuously decreases from 25.1% right after culturing to 2.2% after 10 days in culture. In contrast, proportion of alive neurons decreases from 59.4% to 51.0% during the first four days in cell culture and then increases to 76.2% until day ten. As indicated by the grey background which marks the range of 100% (=total number of nuclei in the cultures), the proportion of dead or dying cells increases from 15.6% right after culturing to 42.3% on culture day four. Relative numbers of dead or dying cells decrease 21.6% until day ten, suggesting that dead cell bodies and their nuclei either completely degrade or detach from their substrate and vanish from the analysis. Analysis is based on n = 3 culture dishes per day and the following total numbers of evaluated cells: $n_{day0}$ = 518; $n_{day2}$ = 770; $n_{day4}$ = 1007; $n_{day6}$ = 508; $n_{day8}$ = 566; $n_{day10}$ = 382.

The glia-to-neuron ratios after different durations of culturing are shown in Figure 10. Fresh cultures (day 0) contained 15.6% dead or dying cells (Figure 10). The proportion of dead cells increased to 42.3% until day four and subsequently decreased to 21.5% after 10 days of culture. The decrease of dead or dying cells suggests that after degradation of their cellular membranes and loss of cytoplasm, also the nuclei degrade or detach from the concavalin-coated substrate and escape subsequent cell counts. Nuclei of dead cells disappeared after shrinkage from the bottom of culture dishes within 4-6 days (Figure 9). The proportion of viable neurons changes inversely to the number of dead or dying cells. Their relative abundance drops from 59.4% in fresh cultures to 51.0% after four days in culture and then gradually increases to 76.2% in ten day old cultures. In contrast, the proportion of alive

glial cells continuously decreased from 25.1% in fresh cultures to only 2.2% in ten day old cultures. The glia to neuron ratio of 1:2.4 in fresh cultures changes to a ratio of 1:35 within ten days. Exposure of primary cell cultures from locust brains to culture conditions that are commonly used for *in vitro* studies on insect central nervous system preparations promotes the survival of neurons more effectively than that of glial cells.

# 1.4 Discussion

*Glia-to-neuron ratio in the brain of locusts*

Glial cells are essential for the formation, maintenance and function of complex nervous systems. Glia may have evolved to separate neural circuits dedicated to different functions, enabling the coordinated performance of different behaviours. It is widely assumed that more complex behaviours require higher numbers of neurons combined with a higher proportion and diversity of glial cells in nervous systems and that the number and degree of glia differentiation increases with phylogeny (Laming et al. 2000; Edenfeld et al. 2005; Heiman & Shaham 2007). But information about both the numbers and physiological functions of glial cell types is scarce for lower vertebrates and invertebrates including insects, compared with the detailed information on numerous molecular subtypes of mammalian glia and their roles in healthy and diseased central nervous systems (Garden & Möller 2006; Bribián & Castro 2007; Pinto & Götz 2007; Rossi et al. 2007; DeKeyser et al. 2008).

Glia-to-neuron ratios have been estimated in only a few insect species and even studies on the same species reported variable proportions ranging from 0.25:1 to 8:1 (e.g. Carlson & Saint Marie 1990; Ito et al. 1995; Pfrieger & Barres 1995). The present study revealed a glia-to-neuron ratio of approximately 1:2 in central brains of the locust *L. migratoria*. Identification of glial cells in histological sections was based on the absence of neuron-specific anti-HRP immunoreactivity. The HRP-antigen is expressed on the surfaces of all insect and probably many other invertebrate neurons and its immunohistochemical detection is a simple, reliable and widely used method to identify insect neurons (Jan & Jan 1982; Sun & Salvaterra 1995a, b). Insect central nervous systems contain neurons, glia and comparatively few tracheal cells that can be distinguished by elongated nuclei and association with tracheal walls (Figure 3d, Loesel et al. 2006). Therefore, insect glial cells can be identified in histological sections as discontinuously DAPI-stained nuclei that lack surrounding HRP-immunopositive cytomembranes (Figure 2; Loesel et al. 2006). The determination of absolute numbers of neurons and glial cells in an organism's nervous system is methodically laborious and has only been achieved in the relatively simple nervous system of the nematode *Caenorhabditis elegans* (Shaham 2006). In the assessment of cell numbers in *L. migratoria* brains, some cells whose nuclei did not appear in any of the sections may have missed. Nevertheless, the method used in this study to determine the numbers of neurons and glial cells in histological sections provides a good estimate of the relative proportions of both cell types for the following reasons. Firstly, series of sections through the entire brain were analysed to account for the different proportions of neurons and glial cells in peripheral and central regions of the brain. Secondly, sections of only 5 µm thickness were used that contained only a single layer of cells in which individual nuclei were easily distinguishable (Figure 3a-d). Thirdly, every fourth histological section was evaluated to prevent multiple counts of large nuclei, which had diameters of up to 18 µm. The glia-to-neuron ratio that was determined for the *L. migratoria* brain is supported by similar percentages of the glial cells in the three brains analysed (30.85% ± 2.35; Figure 5). Both glial and neuronal cell bodies were predominantly located in the cortex region, with glial cells

outnumbering the neurons in the most peripheral layers. Additional glial cell bodies were found to line up along the borders of central brain neuropils such as the central complex and the calyces of the mushroom bodies. Based on their locations, glial cells in the locust brain fit into the three classes of central nervous glia that have been defined by previous studies on various insect species (summarised by Ito et al. 1995; Freeman & Doherty 2006; Parker & Auld 2006). Ectoderm-derived surface glia form the blood-brain barrier that ensheaths the central nervous system and accounts for the high proportion of glial cells in the most peripheral layers (reflected in the sections through peripheral layers of *L. migratoria* brains; Figure 5). Cortex glia are embedded within the cortex region and extend processes that surround neuronal cell bodies and their primary neurites and contact the blood-brain barrier. Neuropil glia mark the borders of central neuropils to the cortex region or to other central neuropils and extend sheath-like membranous structures that surround axons and synapses within the neuropils. Since universal markers that reveal the morphology of insect glial cells are not available, only the positions of their cell bodies could be determined, which provides little information about the functions of particular glial cells in the nervous system.

*Identification of cultured insect glial cells*

In order to promote a functional analysis of insect glia, a number of attempts have been made to study their physiology in primary cell cultures. Various studies indicated that glial cells are very sensitive to mechanical tissue dissociation, may be lost through adherence to vessels and tools during dissociation, may only survive in co-cultures with neurons and may only differentiate typical morphologies under optimal culture conditions (Levi-Montalcini et al. 1973; Hicks et al. 1981; Giles & Usherwood 1985; Beadle et al. 1987; Vanhems & Delbos 1987; Kreissl & Bicker 1992). While cultured mammalian glial cells and neurons mutually promote each others survival (Raff et al. 1993) the importance of glia and neurons for mutual support of survival and differentiation in insect primary cell cultures is largely unknown, although various *in vivo* studies suggested the exchange of signals that regulate growth, apoptosis and differentiation (Buchanan & Benzer 1993; Jones et al. 1995; Rössler et al. 1999; Hidalgo et al. 2001; Oland & Tolbert 2003). Therefore, *in vitro* studies on both glial cells and neurons would benefit from identification of these cell types at any time of the culture period. Especially in freshly dissociated cultures, where glial and neuronal cell bodies assume a spherical shape and lack processes, morphological differences of both cell types are not always obvious (Giles & Usherwood 1985; this study). A recent study (Loesel et al. 2006) adopted anti-HRP immunocytochemistry to study insect cell cultures and identified cells that lacked this neuron-specific membrane marker as glial cells. While this is a valid method to identify glial cells in nervous tissues where almost all cells are viable prior to fixation (see above), the absence of anti-HRP immunoreactivity alone is not sufficient to distinguish between cultured glial cell bodies and remnant nuclei of dead neurons whose membranes have already disintegrated (Figure 6). Since both neurons and glial cells can be severely damaged during the culturing procedure, many of them die and disintegrate (Beadle et al. 1982, 1987; this study). Therefore viability testing is essential to distinguish HRP-negative glial cells from membraneless remnants of any type of dead cells. Only viable cell

bodies that are surrounded by an anti-HRP immunonegative cytoplasmic membrane can be reliably identified as glial cells in primary cultures from insect central nervous tissues.

The results of this study indicate that the pattern of DAPI nuclear staining is a reliable indicator of cell viability. DAPI binds to the minor groove of DNA and its staining pattern reflects the distribution of chromatin inside the nucleus (Wilson et al. 1990). For direct comparison the widely used trypan blue assay was applied and as excepted, dead or compromised cells which accumulated trypan blue contained nuclei with continuous DAPI labelling while cells with intact membranes that excluded trypan blue contained a discontinuous or patchy DAPI-associated fluorescence (Figure 6). Similar observations were made in primary cell cultures from *Drosophila melanogaster* central nervous systems (unpublished results) and condensation of DNA has been detected by DAPI staining in apoptotic cells of *D. melanogaster* (Chao & Nagoshi 1999; Cavaliere et al. 1998) and cell cultures derived from mammalian central nervous tissues (Hu et al. 2002; Daniel & DeCoster 2004). Trypan blue staining may be critical since it involves the exposure of unfixed cell cultures to a toxic dye that by itself may compromise cell viability. The method may also be rather insensitive since the dye only accumulates in severely compromised cells (Altman et al. 1993; Falkenhain et al. 1998). Moreover, trypan blue labelling is not persistent and therefore cannot be combined with other cellular markers. Assessment of viability by DAPI nuclear staining is performed on fixed tissues or fixed dissociated cells and seems to be a sensitive method to detect degradation of DNA before other morphological and functional signs of degeneration, including membrane permeability for trypan blue, manifest. Since the fluorescent signal persists, DAPI staining can be combined with other immunocytochemical or histochemical labelling procedures.

*The portion of glial cells in primary cultures of locust brain cells*

Directly after culturing, primary cell cultures from *L. migratoria* central brains contained 15.6% of cell bodies that adhered to the concavalin-coated bottom but died from damage by enzymatic and mechanic dissociation. By the fourth day of culturing, the proportion of dead cells increased to 42.3% and then decreased to 21.6% by day 10 (Figure 10). This suggests that a portion of those cells that were classified as viable immediately after culturing may have been compromised to such extent that they died during subsequent days. The subsequent reduction of dead cells in cultures can only be explained by a removal of dead cells from the analysis following detachment of their nuclei from the substrate. Whether phagocytotic activities of cultured glial cells significantly contribute to the removal of cellular debris including dead cell's nuclei or even promote the destruction of physiologically impaired cells could not be determined in the present studies, although evidence was found that cultured insect glial cells are capable to enclose and incorporate entire cell bodies (Figure 7). Occasionally glial cells contained HRP-immunoreactive vesicles that could have resulted from incorporation of neuronal membranes (Figure 8d``). Various studies on *D. melanogaster* suggested that apparently all types of glial cells throughout all developmental stages including the adult have the capacity to phagocytose apoptotic cells (Sonnenfeld & Jacobs 1995; Cantera & Technau 1996; Kretzschmar & Pflugfelder 2002). Irrespective of the

underlying mechanism, the fact that dead cells vanish from cultured cellular populations growing on a substrate may considerably impact the outcome of pharmacological studies that investigate the survival of differently treated cells. The results of the present study indicate that nuclei of dead cells disappear from the substrate within 4-6 days (Figure 9).

In freshly dissociated primary cell cultures of locust central brains, glial cells accounted for 29.8% of all living cells. Similar proportions of glial cells (30.8%) were found in histological sections through *L. migratoria* brains (see Figure 5 and first part of the discussion). Matching glia-to-neuron ratios *in situ* and *in vitro* suggest that this protocol prevents a disproportionate loss of glial cells due to particular sensitivity to mechanical dissociation and enhanced adherence to pipettes and other tools. Both possibilities have been suggested to account for the previously described low abundance of glial cells in cell cultures from insect nervous systems (Levi-Montalcini et al. 1973; Hicks et al. 1981; Beadle et al. 1987; Kirchhof & Bicker 1992). However, the proportion of glial cells steadily decreased from 29.7% of living cells in freshly dissociated cultures to only 2.8% of all surviving cells after ten days in culture. This suggests that the culture conditions used in this and other previously conducted studies support the survival of neurons better than that of glial cells, leading to a gradual disappearance of glial cells from locust brain cell cultures. Other studies reported similar problems to maintain insect glial cells in dissociated long-term cultures (Hicks et al. 1981) and one study identified fetal calf serum as a component of the medium that reduces glial cell survival during the first week of culturing (Vanhems and Delbos 1987). Since glial cells survived well in close association with neurons (Beadle et al. 1987; Keen et al. 1994), embryonic tissues (Hicks et al. 1981; Vanhems & Delbos 1987) or other cell types (Howes et al. 1989, 1993), signals derived from co-cultured cells seem to be of vital importance. This may reflect conditions in intact insect nervous systems, where survival of glial cells has been demonstrated to depend on trophic factors from nearby neurons and the lack of these factors initiated apoptosis (Jacobs 2000; Hidalgo et al. 2001; Bergmann et al. 2002; Sen et al. 2004; Learte et al. 2008). In addition, some studies indicated that neurons also depend on glial signals that determine differentiation (Jones et al. 1995), growth (Keen et al. 1994) and survival (Buchanan & Benzer 1993; Jones et al. 1995; Booth et al. 2000; Shepherd 2000). A progressive reduction of glial cells in long-term cell cultures may therefore change the conditions for cultured neurons and may impose an additional variable by which glia may influence the outcome of pharmacological studies. But since thorough *in vitro* investigations of mutual interactions have so far not been performed, the importance of glia for survival of insect neurons in primary cell cultures remains unclear. By introducing methods that reliably identify glial cells in primary cell cultures from various insects and developmental stages and determinate cell viability by a persisting fluorescence signal that allows combination with additional immunocytochemical markers, the present study may support future functional characterisations of insect glia. These future studies should carefully take into account the possibility that the compositions of cell cultures may change during prolonged culture periods due to conditions that prefer survival of particular cell types and the loss of dead cells from the analysis, which might affect the outcome of pharmacological studies.

# 1.5 References


Altman SA, Randers L, Rao G (1993) Comparison of trypan blue dye exclusion and fluorometric assays for mammalian cell viability determinations. Biotechnol Prog 9:671-674

Bass NH, Hess HH, Pope A, Thalheimer C (2004) Quantitative cytoarchitectonic distribution of neurons, glia, and DNA in rat cerebral cortex. J Comp Neurol 143:481-490

Beadle CA, Bermudez I, Beadle DJ (1987) Amino-acid uptake by neurones and glial cells from embryonic cockroach brain growing *in vitro*. J Insect Physiol 33:761-768

Beadle DJ, Hicks D, Middleton C (1982) Fine structure of *Periplaneta americana* neurons in long-term culture. J Neurocytol 11:611-626

Bergmann A, Tugentman M, Shilo BZ, Steller H (2002) Regulation of cell number by MAPK-dependent control of apoptosis: a mechanism for trophic survival signaling. Dev Cell 2:159-170

Booth GE, Kinrade EF, Hidalgo A (2000) Glia maintain follower neuron survival during *Drosophila* CNS development. Development 127:237-244

Borycz J, Borycz JA, Loubani M, Meinertzhagen IA (2002) Tan and ebony genes regulate a novel pathway for transmitter metabolism at fly photoreceptor terminals. J Neurosci 22:10549-10557

Boyan GS, Williams JL (2004) Embryonic development of the sensory innervation of the antenna of the grasshopper *Schistocerca gregaria*. Arthropod Struct Dev 33:381-397

Boyan GS, Williams JL, Posser S, Braunig P (2002) Morphological and molecular data argue for the labrum being non-apical, articulated, and the appendage of the intercalary segment in the locust. Arthropod Struct Dev 31:65-76

Bribián A, de Castro F (2007) Oligodendrocytes: their embryonic origin, migration and therapeutic implications. Rev Neurol 45(9):535-46

Buchanan RL, Benzer S (1993) Defective glia in the *Drosophila* brain degeneration mutant drop-dead. Neuron 10:839-850

Campos-Ortega JA (1974) Autoradiographic localization of 3H-gamma-aminobutyric acid uptake in the lamina ganglionaris of *Musca* and *Drosophila*. Z Zellforsch Mikrosk Anat 147:415-431

Cantera R, Technau GM (1996) Glial cells phagocytose neuronal debris during the metamorphosis of the central nervous system in *Drosophila*. Development Genes and Evolution 206:277-280

Cantera R, Trujillo-Cenoz O (1996) Glial cells in insect ganglia. Microsc Res Tech 35:285-293

Carlson SD, Saint Marie RL (1990) Structure and Function of Insect Glia. Ann Rev Entomol 35:597-621

Carlson SD, Juang JL, Hilgers SL, Garment MB (2000) Blood barriers of the insect. Annu Rev Entomol 45:151–174

Cavaliere V, Taddei C, Gargiulo G (1998) Apoptosis of nurse cells at the late stages of oogenesis of *Drosophila melanogaster*. Dev Genes Evol 208:106-112

Cayre M, Buckingham SD, Strambi A, Strambi C, Sattelle DB (1998) Adult insect mushroom body neurons in primary culture: cell morphology and characterization of potassium channels. Cell Tissue Res 291:537-547

Chao S, Nagoshi RN (1999) Induction of apoptosis in the germline and follicle layer of *Drosophila* egg chambers. Mech Dev 88:159-172

Daniel B, DeCoster MA (2004) Quantification of sPLA2-induced early and late apoptosis changes in neuronal cell cultures using combined TUNEL and DAPI staining. Brain Res Brain Res Protoc 13:144-150

De Keyser J, Mostert JP, Koch MW (2008) Dysfunctional astrocytes as key players in the pathogenesis of central nervous system disorders. J Neurol Sci 267(1-2):3-16

Edenfeld G, Stork T, Klambt C (2005) Neuron-glia interaction in the insect nervous system. Curr Opin Neurobiol 15:34-39

Falkenhain A, Lorenz TH, Behrendt U, Lehmann J (1998) Dead cell estimation - A comparison of different methods. In: Merten OW, Perrin P, Griffiths B (eds) New Developments and New Applications in Animal Cell Technology. Springer Netherlands, pp 333-336

Freeman MR, Delrow J, Kim J, Johnson E, Doe CQ (2003) Unwrapping glial biology: Gcm target genes regulating glial development, diversification, and function. Neuron 8:567-580

Freeman MR, Doherty J (2006) Glial cell biology in *Drosophila* and vertebrates. Trends Neurosci 29:82-90

Garden GA, Möller T (2006) Microglia biology in health and disease. J Neuroimmune Pharmacol 1:127–137

Gascuel J, Masson C (1991) Developmental study of afferented and deafferented bee antennal lobes. J Neurobiol 22:795-810

Gibson NJ, Hildebrand JG, Tolbert LP (2004) Glycosylation patterns are sexually dimorphic throughout development of the olfactory system in *Manduca sexta*. J Comp Neurol 476:1-18

Giles DP, Usherwood PN (1985) Locust nymphal neurones in culture: a new technique for studying the physiology and pharmacology of insect central neurones. Comp Biochem Physiol C 80:53-59

Hähnlein I, Bicker G (1996) Morphology of neuroglia in the antennal lobes and mushroom bodies of the brain of the honeybee. J Comp Neurol 367:235-245

Hähnlein I, Bicker G (1997) Glial patterning during postembryonic development of central neuropiles in the brain of the honeybee. Dev Genes Evol 207:29-41

Halter DA, Urban J, Rickert C, Ner SS, Ito K, Travers AA, Technau GM (1995) The homeobox gene repo is required for the differentiation and maintenance of glia function in the embryonic nervous system of *Drosophila melanogaster*. Development 121:317-332

Heil JE, Oland LA, Lohr C (2007) Acetylcholine-mediated axon-glia signaling in the developing insect olfactory system. Eur J Neurosci 26:1227-1241

Heiman MG, Shaham S (2007) Ancestral roles of glia suggested by the nervous system of *Caenorhabditis elegans*. Neuron Glia Biology 3:55-61

Hicks D, Beadle DJ, Giles DP, Usherwood PNR (1981) Ultrastructure of dissociated nerve cells of *Periplaneta americana* (L.) (Dictyoptera: Blattidae) growing in culture. Int J Insect Morphol Embryol 10:225-233

Hidalgo A, Kinrade EF, Georgiou M (2001) The *Drosophila* neuregulin vein maintains glial survival during axon guidance in the CNS. Dev Cell 1:679-690

Howes EA, Armett-Kibel C, Smith PJ (1993) A blood-derived attachment factor enhances the *in vitro* growth of two glial cell types from adult cockroach. Glia 8:33-41

Howes EA, Smith PJS, Treherne JE (1989) Adult insect glial culture: activation, substrate effects and proliferation. Tissue & Cell 21:759–772

Hoyle G (1986) Glial cells of an insect ganglion. J Comp Neurol 246:85-103

Hu S, Sheng WS, Lokensgard JR, Peterson PK (2002). Morphine induces apoptosis of human microglia and neurons. Neuropharmacol 42:829-836

Ito K, Urban J, Technau GM (1995) Distribution, classification, and development of *Drosophila* glial cells in the late embryonic and early larval ventral nerve cord. Roux's Arch Dev Biol 204:284–307

Jacobs JR (2000) The midline glia of *Drosophila*: a molecular genetic model for the developmental functions of glia. Prog Neurobiol 62:475-508

Jan LY, Jan YN (1982) Antibodies to horseradish peroxidase as specific neuronal markers in *Drosophila* and in grasshopper embryos. Proc Natl Acad Sci USA 79:2700-2704

Jones BW (2001) Glial cell development in the *Drosophila* embryo. Bioessays 23:877-887

Jones BW, Fetter RD, Tear G, Goodman CS (1995) Glial cells missing: a genetic switch that controls glial versus neuronal fate. Cell 82:1013-1023

Kai-Kai MA, Pentreath VW (1981) The structure, distribution, and quantitative relationships of the glia in the abdominal ganglia of the horse leech, *Haemopis sanguisuga*. J Comp Neurol 202:193-210

Keen L, Amar M, Beadle DJ, Bermudez I (1994) Cockroach glial cell cultures: morphological development and voltage-gated potassium channels. Tissue Cell 26:209-221

Kirchhof B, Bicker G (1992) Growth properties of larval and adult locust neurons in primary cell culture. J Comp Neurol 323:411-422

Kreissl S, Bicker G (1992) Dissociated neurons of the pupal honeybee brain in cell culture. J Neurocytol 21:545-556

Kretzschmar D, Pflugfelder GO (2002) Glia in development, function, and neurodegeneration of the adult insect brain. Brain Res Bull 57:121-131

Laming PR, Kimelberg H, Robinson S, Salm A, Hawrylak N, Muller C, Roots B, Ng K (2000) Neuronal-glial interactions and behaviour. Neurosci Biobehav Rev 24:295-340

Learte AR, Forero MG, Hidalgo A (2008) Gliatrophic and gliatropic roles of PVF/PVR signaling during axon guidance. Glia 56:164-176

Leitch B, Watkins BL, Burrows M (1993) Distribution of acetylcholine receptors in the central nervous system of adult locusts. J Comp Neurol 334:47-58

Levi-Montalcini R, Chen JS, Seshan KR, Aloe L (1973) An *in vitro* approach to the insect nervous system. In: Developmental neurobiology of arthropods. Young D (eds) Cambridge University Press Cambridge, pp 5-36

Loesel R, Weigel S, Bräunig P (2006) A simple fluorescent double staining method for distinguishing neuronal from non-neuronal cells in the insect central nervous system. J Neurosci Methods 155:202-206

Meyer MR, Reddy GR, Edwards JS (1987) Immunological probes reveal spatial and developmental diversity in insect neuroglia. J Neurosci 7:512-521

Oland LA, Tolbert LP (2003) Key interactions between neurons and glial cells during neural development in insects. Annu Rev Entomol 48:89-110

Parker RJ, Auld VJ (2004) Signaling in glial development: differentiation migration and axon guidance. Biochem. Cell Biol. 82(6):694–707

Parker RJ, Auld VJ (2006) Roles of glia in the Drosophila nervous system. Semin Cell Dev Biol 17:66-77

Pfrieger FW, Barres BA (1995) What the fly's glia tell the fly's brain. Cell 83:671-674

Pinto L, Götz M (2007) Radial glial cell heterogeneity - the source of diverse progeny in the CNS. Prog Neurobiol 83:2–23

Radojcic T, Pentreath VW (1979) Invertebrate glia. Prog Neurobiol 12:115-179

Raff MC, Barres BA, Burne JF, Coles HS, Ishizaki Y, Jacobson MD (1993) Programmed cell death and the control of cell survival: lessons from the nervous system. Science 262:695-700

Rossi DJ, Brady JD, Mohr C (2007) Astrocyte metabolism and signaling during brain ischemia. Nat Neurosci 10:1377-1386

Rössler W, Oland LA, Higgins MR, Hildebrand JG, Tolbert LP (1999) Development of a glia-rich axon-sorting zone in the olfactory pathway of the moth *Manduca sexta*. J Neurosci 19:9865-9877

Schofield PK, Treherne JE (1985) Octopamine reduces potassium permeability of the glia that form the insect blood-brain barrier. Brain Res 360:344-348

Sen A, Kuruvilla D, Pinto L, Sarin A, Rodrigues V (2004) Programmed cell death and context dependent activation of the EGF pathway regulate gliogenesis in the *Drosophila* olfactory system. Mech Dev 121:65-78

Shaham S (2006) Glia-neuron interactions in nervous system function and development. Curr Top Dev Biol 69:39-66

Shepherd D (2000) Glial dependent survival of neurons in *Drosophila*. Bioessays 22:407-409

Sonnenfeld MJ, Jacobs JR (1995) Macrophages and glia participate in the removal of apoptotic neurons from the *Drosophila* embryonic nervous system. J Comp Neurol 359:644-652

Soustelle L, Besson MT, Rival T, Birman S (2002) Terminal glial differentiation involves regulated expression of the excitatory amino acid transporters in the *Drosophila* embryonic CNS. Dev Biol 248:294-306

Stork T, Engelen D, Krudewig A, Silies M, Bainton RJ, Klämbt C (2008) Organization and Function of the Blood–Brain Barrier in Drosophila. J Neurosci, 28:587-597

Sun B, Salvaterra PM (1995a) Characterization of nervana, a *Drosophila melanogaster* neuron-specific glycoprotein antigen recognized by anti-horseradish peroxidase antibodies. J Neurochem 65:434-443

Sun B, Salvaterra PM (1995b) Two *Drosophila* nervous system antigens, Nervana 1 and 2, are homologous to the beta subunit of $Na^+$, $K^+$-ATPase. Proc Natl Acad Sci USA 92:5396-5400

Vanhems E, Delbos M (1987) Differentiation of glial cells and neurite outgrowth obtained from embryonic locust central nervous system explants. Brain Res 411:129-138
Villegas SN, Poletta FA, Carri NG (2003) GLIA: A reassessment based on novel data on the developing and mature central nervous system. Cell Biol Int 27:599-609

Wilson WD, Tanious FA, Barton HJ, Jones RL, Fox K, Wydra RL, Strekowski L (1990) DNA sequence dependent binding modes of 4',6-diamidino-2-phenylindole (DAPI). Biochem 29:8452-8461

# 2 Immunohistochemical detection of erythropoietin and its receptor in the central nervous system of invertebrates

## 2.1 Introduction

The cytokine erythropoietin (EPO) was first characterised as the main regulator of erythropoiesis (Erslev 1953). EPO is a glycoprotein of 30.4kDa which is predominantly produced by the fetal liver and adult kidney (Zanjani et al. 1977; Dame et al. 1998). The major signal for the regulation of EPO production in the kidney is the availability of oxygen. Hypoxic conditions induce the accumulation of the transcription factor HIF-1 (hypoxia-inducible-factor-1) which promotes the enhanced transcription of EPO mRNA (Semenza 1994). Circulating EPO binds to its receptor (EPOR) expressed on erythroid progenitor cells in the bone marrow and activates the JAK/STAT signalling pathway (Ratajczak et al. 2001). This promotes the generation of erythrocytes by stimulation of proliferation, inhibition of apoptosis, and accelerated differentiation (Jelkmann 1992).

Over the past years, EPO and its receptor were also detected in non-hematopoetic tissues, including the brain of mammals (Tan et al. 1992; Sasaki et al. 2001). Since it is unlikely that renal EPO crosses the intact blood-brain barrier under physiological conditions (Marti et al. 1997), EPO has to be produced within the CNS. These findings suggested a biological role of paracrine and/or autocrine EPO/EPOR signalling in the central nervous system that is independent of the endocrine erythropoietic system. Astrocytes (Masuda et al. 1994, 1997; Marti 1996) and to a lesser extend also neurons (Morishita et al. 1997; Bernaudin et al. 1999, 2000) have been identified as central nervous production sites for EPO. Functional EPO receptor has been identified in a wide variety of brain cells including neurons, glial cells and capillary endothelial cells (Anagnostou et al. 1994; Yamaji et al. 1996; Bernaudin et al. 1999, 2000; Sirén et al. 2001; Sugawa et al. 2002). Furthermore, EPOR was detected in several neuronal cell lines, such as PC12 & SN6 (Masuda 1993), NT2 & hNT (Juul et al. 1998) and SK-N-MC (Assandri et al. 2004).

Both EPO and EPOR are expressed in the CNS of embryonic, fetal and adult rodents (Yasuda et al. 1993; Dame et al. 2000; Knabe et al. 2004) and humans (Juul et al. 1998; Juul et al. 1999). The expression of brain EPO and EPOR peaks at midgestation and decreases to a basal expression after birth (Liu et al. 1994; Sirén et al. 2001; Knabe et al. 2004). Furthermore, Yu et al. (2001, 2002) have shown that the lack of EPOR results in a reduction of neuronal progenitors and increased numbers of apoptotic cells in the brain of embryonic mice. This implicates an important role of EPO/EPOR signalling for neurodevelopment. The weak EPO and EPOR expression in adult brains can be upregulated by hypoxia (Tan et al.

1992; Bernaudin et al. 2000; Lewczuk et al. 2000), but also by metabolic disturbances that cause the accumulation of reactive oxygen species (Chandel et al. 1998) and by growth factors, such as IGF-I (insulin-like growth factor-I) (Masuda et al. 1997). Like in the fetal liver and adult kidney, EPO expression in the brain is regulated by the transcription factor HIF-1 (hypoxia-inducible-factor-1). In contrast to the upregulation of EPO in the kidney, the expression peak of EPO mRNA in the brain appears about two hours later and persists at a high level for a longer period of time (Chikuma et al. 2000). Various *in vitro* and *in vivo* studies showed that EPO has a direct neurotrophic and neuroprotective effect during and following hypoxia, ischemia or brain hemorrhage (for review see Dame et al. 2001; Buemi et al. 2002; Genc et al. 2004; Marti 2004; Arcasoy 2008).

Most studies on the expression of EPO and EPOR and their physiological functions in the CNS were performed in mammals. More recently a few studies characterised EPO and EPOR from teleost fishes and showed that both proteins are also expressed in the fish CNS (Chou et al. 2004; Chu et al. 2007; Paffett-Lugassy et al. 2007). There is accumulating evidence that the multitude of EPO/EPOR functions in nervous tissues is independent from effects on the maturation of red blood cells. The neuroprotective and neurotrophic functions of EPO and EPOR in the mammalian CNS may therefore be mediated by ancient evolutionary conserved mechanisms whose characterisation could be facilitated by studies on organisms without erythropoiesis, such as invertebrates.

In this study antibodies raised against mammalian EPO and EPOR were used to investigate the expression of erythropoietin and its receptor in the CNS of mice, annelids (*Hirudo medicinalis*), crustaceans (*Procambarus spec.*) and insects (*Drosophila melanogaster*, *Locusta migratoria*). Immunostainings of sectioned brains revealed uniform patterns of distinctly labelled neurons in all species studied. In addition, Western blot analysis was performed to compare the molecular weight of the proteins detected in the different species.

# 2.2 Material and Methods

Unless otherwise mentioned, all chemicals were either purchased from Sigma-Aldrich (Steinheim, Germany) or Merck (Darmstadt, Germany).

### 2.2.1 Animals

Locusts (*Locusta migratoria*) were purchased from a commercial animal breeder (Schätzle Terraristik, Karlsruhe, Germany) and maintained in colonies at 18-21°C on a 12h/12h day/night cycle. Leeches (*Hirudo medicinalis*) were obtained from a commercial supplier (Zaug GmbH, Biebertal, Germany) and kept in tanks filled with tap water at 10°C. Wild type fruitflies (*Drosophila melanogaster*, CantonS) were reared in 175 ml breeding vials (Greiner Bio-One, Solingen, Germany) on an approximately 2 cm thick layer of commercial Nekton-*Drosophila*-food concentrate (Günter Enderle Nekton-Produkte, Pforzheim, Germany) with tap water and vinegar added. Rearing conditions were maintained at 25°C and 65% relative humidity on a 16h/8h day/night cycle. Crayfish (*Procambarus spec.*) originating from a laboratory breeding were maintained at 26°C in tanks filled with tap water on a 12h/12h day/night cycle. Brains of mice (C57BL/6) were provided by Dr. T. Lübke (Department of Biochemistry II, Göttingen, Germany).

### 2.2.2 Anti-EPO and anti-EPOR immunohistochemistry

For the immunohistochemical studies the polyclonal goat anti-EPO antibody (N-19, Santa Cruz Biotechnology, Heidelberg, Germany) was used, which was raised against the N-terminus of human erythropoietin. The polyclonal rabbit anti-EPOR antibody (M-20, Santa Cruz Biotechnology, Heidelberg, Germany) was raised against the C-terminal cytoplasmic domain of EPOR of mouse origin.

*Immunohistochemistry on vibratome sections*. Dissected brains were fixed with 4% paraformaldehyde + 7.5% picric acid dissolved in phosphate buffer (PB) for 2h at room temperature (RT), embedded in albumin-gelatine or 5% agarose and postfixed in 4% paraformaldehyde overnight at 4°C. Sections of 40-50µm thickness were cut with a vibrating blade microtome (VT 1000 S, Leica, Bensheim, Germany). The tissue sections were permeabilised in phosphate buffered saline (PBS) containing 1% Triton X-100 for 2 days at 8°C and nonspecific binding of the antibody was reduced by blocking with 10% normal serum (rabbit serum for EPO antibody and goat serum for EPOR antibody, GE Healthcare, Munich, Germany) and 0.25% bovine serum albumin (BSA, MPI Biomedical, Heidelberg, Germany) dissolved in PBS with 1% Triton for 2h at RT. The first antibody (goat anti-EPO or rabbit anti-EPOR) was applied to the sections at a dilution of 1:75 at 8°C for 2 days. After washing several times with PBS, a biotinylated secondary antibody was used at a dilution of 1:100 for 2h at RT (biotinylated rabbit α-goat for the EPO antibody and biotinylated goat α-rabbit for the EPOR antibody). To visualise the immunoreactivity sections were either incubated with an avidin-biotin-peroxidase complex (ABC, Vectastain Elite PK-6100, Vector Laboratories,

Burlingame, USA) followed by a standard diaminobenzidine (DAB) reaction or a fluorophores coupled streptavidin (Rockland Immunochemicals, Gilbertsville, USA). For nuclear staining, tissue sections were incubated for 30 minutes at RT with 100µg/ml 4´-6-diamino-2-phenylindole (DAPI) dissolved in PBS. Following several washes in PBS and transfer to PBS with glycerol (1:1), DAB labelling or fluorescence were analysed with a conventional fluorescence microscope (Zeiss Axioskop, Jena, Germany) equipped with a Spot CCD camera (Invisitron, Sterling Heights, USA) or a laser-scanning confocal microscope (Leica TCS-4D). All figures were generated using Adobe Photoshop 7.0.

*Anti-HRP immunohistochemistry on microtome sections*. Dissected brains were fixed with 4% paraformaldehyde + 7.5% picric acid dissolved in PB for 2h at room temperature. After dehydration through an ethanol series, the tissue was embedded in paraffin wax and serially cut with a microtome (Reichert-Jung 1130 Biocut, Nußloch, Germany) into 8µm sections. After rehydration and washing several times with PBS-1%Triton, the brain slices were incubated with blocking buffer (5% normal serum, 3% BSA in PBS-1%Triton) for 2h at RT. The anti-EPO or anti-EPOR serum was dissolved in blocking buffer at a dilution of 1:100 and applied to the sections over night at RT. After three washes with PBS-1%Triton the biotinylated secondary antibody was added (biotinylated rabbit α-goat for the EPO antibody and biotinylated goat α-rabbit for the EPOR antibody) at a dilution of 1:300 for 2h at RT. To visualise the immunoreactivity the sections were washed three times and subsequently incubated with a Cy3-coupled streptavidin (Rockland Immunochemicals, Gilbertsville, USA) at a dilution of 1:400 for 2h at RT. For nuclear staining, tissue sections were incubated for 30 minutes at RT with DAPI dissolved in PBS. Finally the slices were dehydrated through an ethanol series, cleared in xylene and embedded in Entellan. Immunoreactivity was analysed as described above.

### 2.2.3 Western Blot analysis of EPO and EPOR

Central nervous systems of the various species used in this study were dissected and lysed in phosphate buffered saline (PBS) containing 1% Igepal, 0.5% sodium deoxycholate, 0.5mM phenylmethylsulphonyl fluoride (PMSF) and the protease inhibitor cocktail Complete mini (Roche Diagnostics GmbH, Mannheim, Germany). The lysates were cleared by centrifugation at 1500rpm for 15 min at 4℃ and protein content was quantified with a Bio-Rad protein assay kit using bovine serum albumin as a reference (Bio-Rad Laboratories, Munich, Germany). Samples of 20µg total protein were resolved by 12% sodium dodecyl sulphate polyacrylamide gel electrophoresis (SDS-PAGE) and transferred to a nitrocellulose membrane (Hybond C extra, Amersham-Pharmacia, Freiburg, Germany). The PageRuler™ prestained protein ladder (Fermentas, St. Leon-Rot, Germany) was used as molecular weight marker. The membrane was blocked in Tris buffered saline with 0.1% Tween 20 (TBST-T) and 5% skim milk powder (Bio-Rad Laboratories, Munich, Germany) for 1h at room temperature followed by overnight incubation with anti-EPO (N-19, Santa Cruz Biotechnology, Heidelberg, Germany) or anti-EPOR (M-20, Santa Cruz Biotechnology, Heidelberg, Germany) antibodies (all at 1:1000 dilution with 1% bovine serum albumin in TBS-T) at 4℃. Afterwards, the blots were rinsed for 30 min with TBS-T and incubated with a

peroxidase-conjugated secondary antibody (rabbit α-goat for the EPO antibody, goat α-rabbit for the EPOR antibody, Jackson ImmunoResearch Laboratories, Suffolk, UK) at 1:1000 dilution in TBS-T. Immunoreactive protein bands were visualised by an enhanced chemiluminescence detection system (ECL, Amersham Bioscience, Freiburg, Germany) according to the manufacturer's instructions.

# 2.3 Results

To study the expression of EPO and EPOR in the nervous system of invertebrates the polyclonal goat anti-EPO antibody (N-19, Santa Cruz Biotechnology) and the polyclonal rabbit anti-EPOR antibody (M-20, Santa Cruz Biotechnology) was used. Both antibodies have been used to label specific cells in the central nervous system of rats (Masuda et al. 1994; Morishita et al. 1997; Weber et al. 2002), mice (Bernaudin et al. 1999; Yu et al. 2002; Knabe et al. 2004) and humans (Juul et al. 1998, 1999; Sirén et al. 2001).

This study describes the presence of cells that contain EPO- and EPOR-like immunofluorescence in the central nervous systems of mice, annelids (*Hirudo medicinalis*), crustaceans (*Procambarus spec.*) and insects (*Drosophila melanogaster*, *Locusta migratoria*). Since the antibodies against EPO and EPOR were raised against mammalian proteins, the immunologically labelled proteins in the invertebrate CNS will be termed as *invertebrate analogs* of EPO and EPOR (*ia*EPO and *ia*EPOR).

### 2.3.1 Expression of EPO and EPOR in the central nervous system of mice

The brains of adult mice (C57BL/6) were cut with a vibrating blade microtome into slices of 50µm and frontal sections through the midbrain were either labelled with the anti-EPO serum (Figure 1, red fluorescence) or the anti-EPOR serum (Figure 2, red fluorescence) and the nuclear marker DAPI (blue fluorescence).

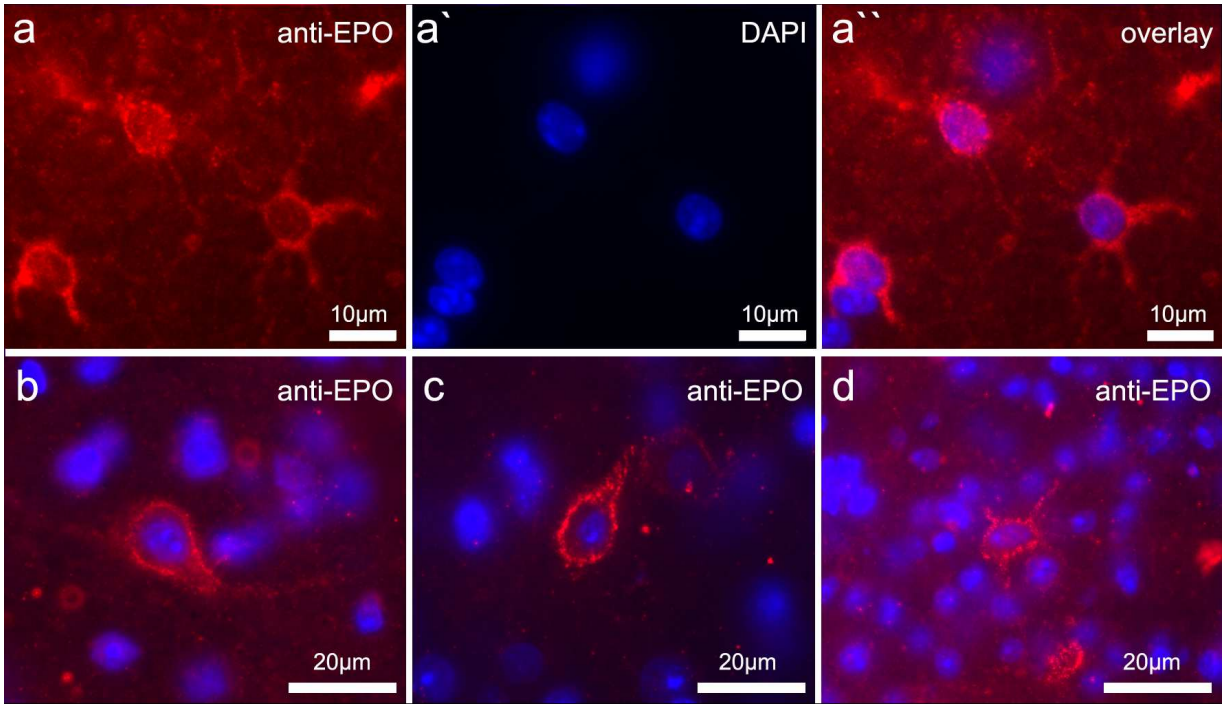


**Figure 1**: Frontal sections through the midbrain of a mouse labelled with anti-EPO serum (red fluorescence) and the nuclear marker DAPI (blue fluorescence). **a-a``:** EPO-immunopositive cells with a homogeneous, cytoplasmic staining. **b-d:** EPO-immunopositive cells with a granular staining concentrated in submembranous regions of cell bodies and neurites.

EPO immunoreactivity was detected in two different cell types in the midbrain of mice. Several immunopositive cells contained a homogeneous, cytoplasmic staining and morphological characteristics of astrocytes (Figure 1a-a``). Cells with a granular distribution of EPO immunoreactivity that was concentrated in submembraneous regions of cell bodies and processes appeared to be neurons (Figure 1b-d).

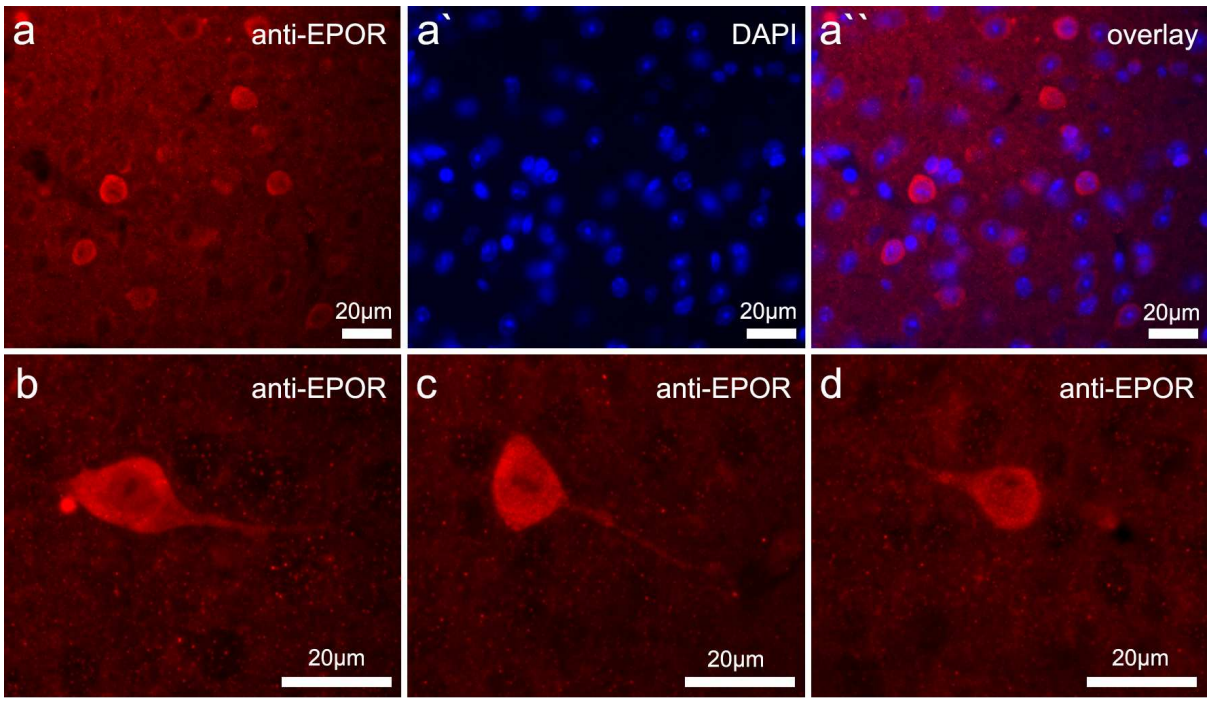


**Figure 2:** Frontal sections through the midbrain of a mouse labelled with anti-EPOR serum (red fluorescence) and the nuclear marker DAPI (blue fluorescence). **a-a``:** Overview of a midbrain section with a distinct, homogeneous and cytoplasmic expression of EPOR-like immunoreactivity in several cells. **b-d:** Detailed view of EPOR-immunopositive cells with neuronal morphology.

Sections of mouse midbrains were also labelled with anti-EPOR serum and several cells with a distinct, homogeneous, cytoplasmic expression of EPOR immunoreactivity were detected (Figure 2). Detailed analysis (Figure 2b-d) revealed a typical neuronal morphology.

### 2.3.2 Expression of *ia*EPO and *ia*EPOR in the central nervous system of *Hirudo medicinalis*

The central nervous system of the leech *H. medicinalis* comprises 32 ganglia, 4 of which are fused to the head ganglion and 7 to a tail ganglion. In between, 21 segmental ganglia are individually iterated along paired connectives (Nicholls & Essen 1974). Horizontal sections through the head ganglion and the segmental ganglia were labelled with anti-EPO (Figure 3) and anti-EPOR serum (Figure 4).

For *ia*EPO immunostaining segmental ganglia of leeches were cut horizontally with the vibratome into slices of 40µm thickness and labelled with the anti-EPO serum. EPO-like immunoreactivity was detected in serveral neuronal cells throughout all segmental ganglia. Figure 3a displays a section through a hemiganglion with two *ia*EPO-immunopositive cells (higher magnification in Figure 3a`). One of these cells shows a strong immunoreactivity in

the soma and weak immunoreactivity in its primary neurite (Figure 3a`, asterisk). The other cell contains EPO-like immunoreactivity concentrated in the vicinity of the cell membrane of the soma and its projections (Figure 3a`, arrowhead). In addition, fine and extensively branching fibres in the central neuropil region of the ganglion are distinctly labelled. Other examples of cells from different segmental ganglia that contained *ia*EPO immunoreactivity are summarised in Figure 3b-d.

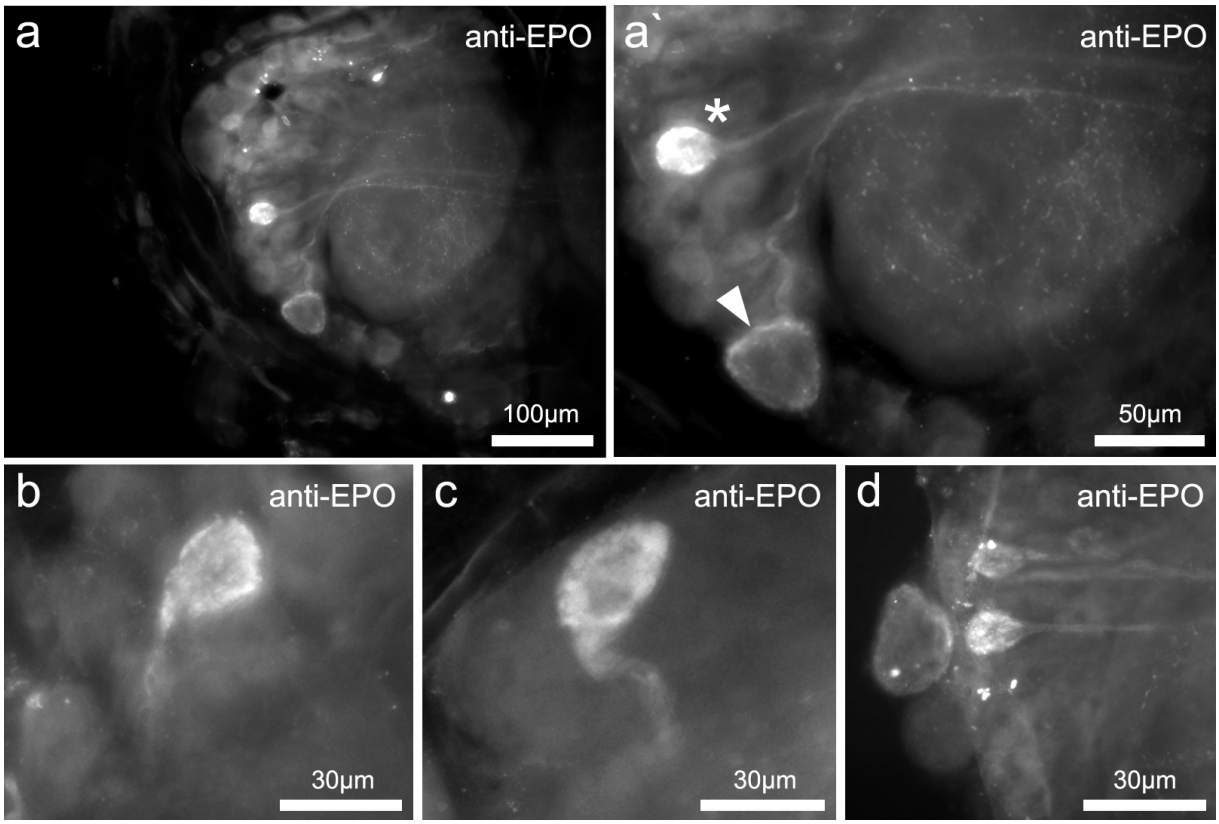


**Figure 3:** Horizontal sections through segmental ganglia of the leech *Hirudo medicinalis* labelled with anti-EPO serum. **a, a`:** Section through one hemiganglion with two *ia*EPO-immunopositive cells. Higher magnification in a` reveals one cell with an intensive cytoplasmic staining (asterisk) and one cell with staining restricted along the outer cell membrane (arrowhead). **b-d:** Detailed view of other *ia*EPO-immunopositive cells.

For *ia*EPOR immunoreactivity, the head ganglion of leeches was embedded in paraffin wax and horizontally cut into slices of 8µm thickness (Figure 4). A pair of strongly *ia*EPOR-immunopositive cells was detected in the most anterior part of the head ganglion, the supraesophageal ganglion (Figure 4a, arrowheads, higher magnification in 4a`, a``). Other *ia*EPOR-immunopositive cells were detected in the more posterior part of the head ganglion, the subesophageal ganglion (Figure 4b, c). All cells that contained EPOR-like immuno-reactivity had a distinct, homogeneous cytoplasmic staining.

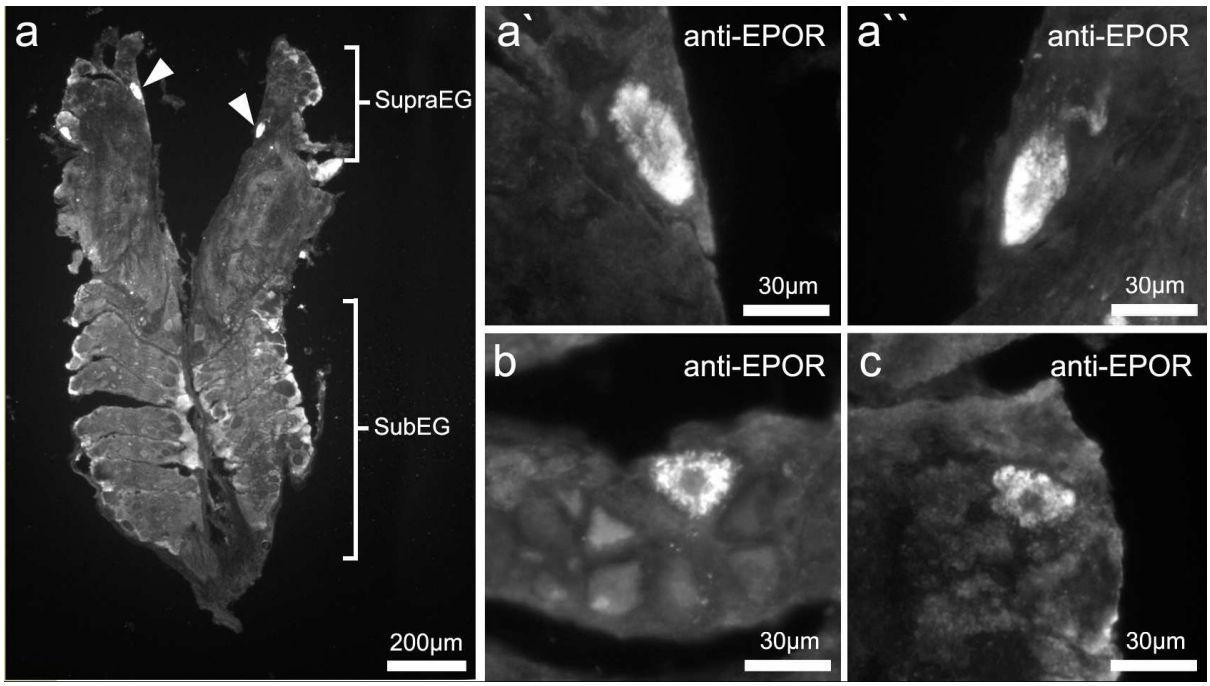


**Figure 4:** Horizontal section through the head ganglion of the leech *Hirudo medicinalis* labelled with anti-EPOR serum. **a-a``:** White arrowheads mark two *ia*EPOR-immunopositive cell bodies that are displayed at a higher magnification in a` and a``. **b, c:** Further examples of neuronal cells in the subesophageal ganglion that express *ia*EPOR immunoreactivity.
SupraEG: supraesophageal ganglion, SubEG: subesophageal ganglion

### 2.3.3 Expression of *ia*EPO and *ia*EPOR in the central nervous system of *Procambarus spec*.

Brain sections of the crayfish *Procambarus spec.* were labelled with anti-EPO serum and anti-EPOR serum and the immunoreactivity was either visualised with a diaminobenzidine (DAB) reaction (EPO, Figure 5) or fluorophore-coupled streptavidin (EPOR, Figure 6).

EPO-like immunoreactivity was detected both in fibres invading neuropil regions and in cell bodies of different cell types. Figure 5a and 5a` show a frontal section through a hemibrain with *ia*EPO-immunoreactive fibres that project in-between the olfactory and accessory lobe to central regions of the protocerebrum. Furthermore, *ia*EPO immunoreactivity with different patterns of distribution was detected in a number of cell bodies (Figure 5b-d). Various *ia*EPO-immunopositive cells showed a distinct staining in close association with the cell membranes of somata and neurites (Figure 5b, arrowhead). In contrast, entirely labelled cells with small somata (7-11µm) seemed to enclose the cell bodies of larger unlabelled cells (Figure 5c, arrowheads). A third type of *ia*EPO-immunopositive cells contained homogeneous staining throughout its entire cytoplasm (Figure 5d, arrowhead).

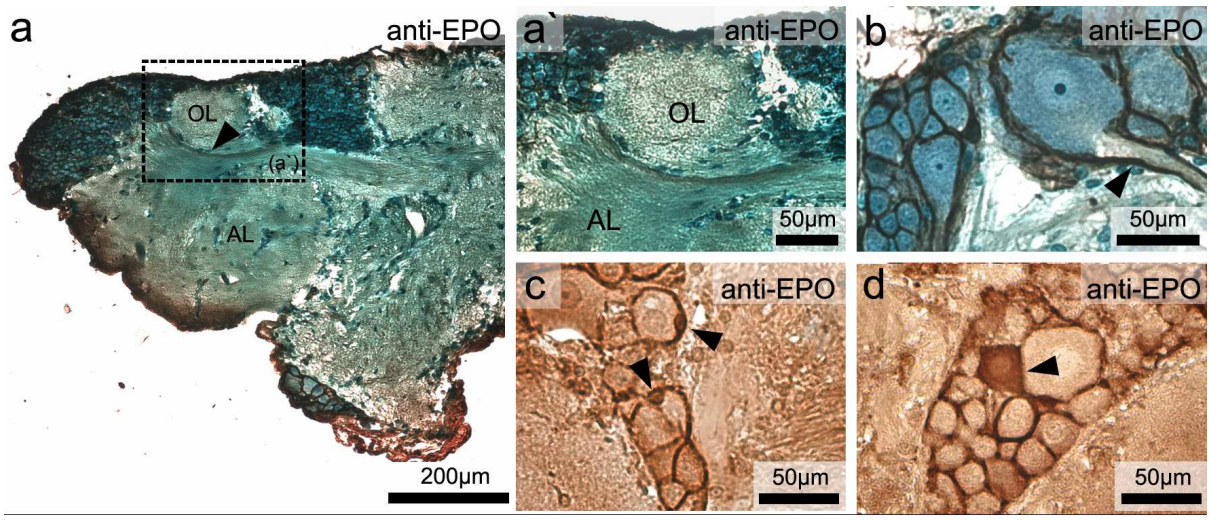


**Figure 5:** Frontal sections through the brain of *Procambarus spec.* labelled with anti-EPO serum (brown colour) and methylenblue. **a, a`:** Section through a hemibrain with *ia*EPO-expressing fibres in the deutocerebrum. The dashed line in a marks the region that is presented at higher magnification in a`. **b:** *ia*EPO-immunopositive cells with intensive staining associated with the membranes of somata and neurites (arrowhead). **c:** *ia*EPO-immunoreactive cells with small somata (arrowheads) enclose other cell bodies with labelled processes. **d:** *ia*EPO-immunopositive cell with homogeneous cytoplasmic staining (arrowhead).
OL: olfactory lobe, AL: accessory lobe

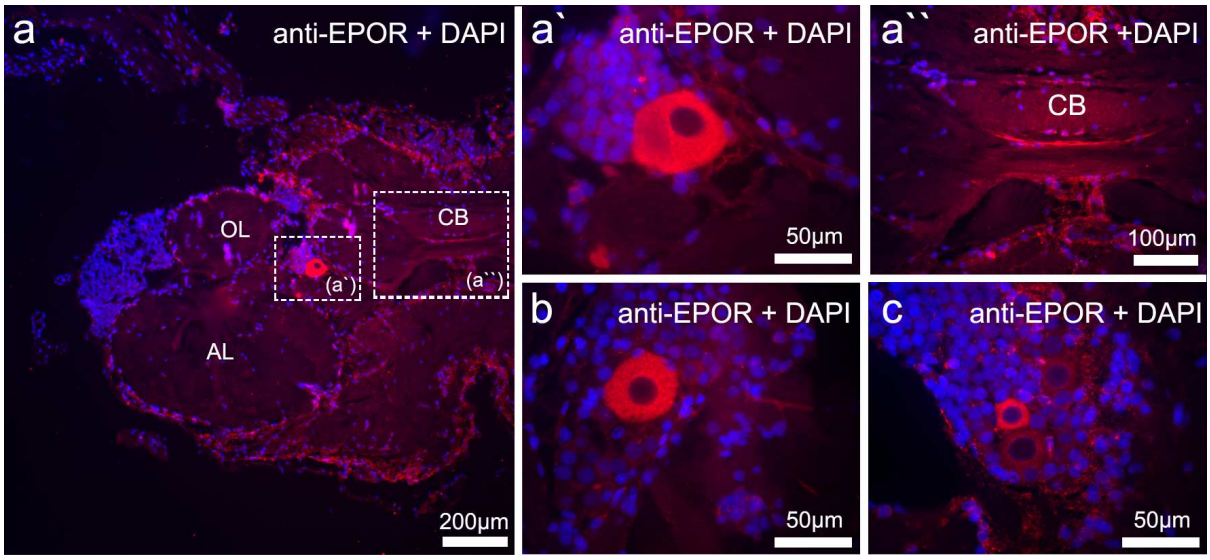


**Figure 6:** Frontal sections through the brain of *Procambarus spec.* labelled with anti-EPOR serum (red fluorescence) and the nuclear marker DAPI (blue fluorescence). **a-a``:** Section through a hemibrain showing an *ia*EPOR-immunolabelled cell body with a homogeneous cytoplasmic staining that is presented at higher magnification in a`. An *ia*EPOR-immunopositive fibre in the protocerebrum is presented at higher magnification in a``. **b, c:** Other examples of cells that displayed *ia*EPOR immunoreactivity located in the tritocerebrum of the brain.
OL: olfactory lobe, AL: accessory lobe, CB: central body

For *ia*EPOR immunohistochemistry the brain sections of *Procambarus spec.* were labelled with anti-EPOR serum (red fluorescence) and the nuclear marker DAPI (blue fluorescence). Figure 6a provides an overview of one section through a hemibrain with an *ia*EPOR-immunopositive cell located in a cluster of unlabelled cells lateral to the olfactory and accessory lobe (higher magnification in Figure 6a`). This cell has a homogeneous staining in

the cytoplasm of the soma. Furthermore, *ia*EPOR expressing fibres project posteriorly to the central body (higher magnification in Figure 6a``). Other cells that contained homogeneous cytoplasmic staining of *ia*EPOR were detected in the tritocerebrum of the brain (Figure 6b, c).

### 2.3.4 Expression of *ia*EPO and *ia*EPOR in the central nervous system of *Locusta migratoria*

The brains of *Locusta migratoria* were embedded in paraffin wax, cut with a microtome into sections of 8µm thickness and labelled with anti-EPO serum (Figure 7). Two different patterns of immunoreactivity were detected.

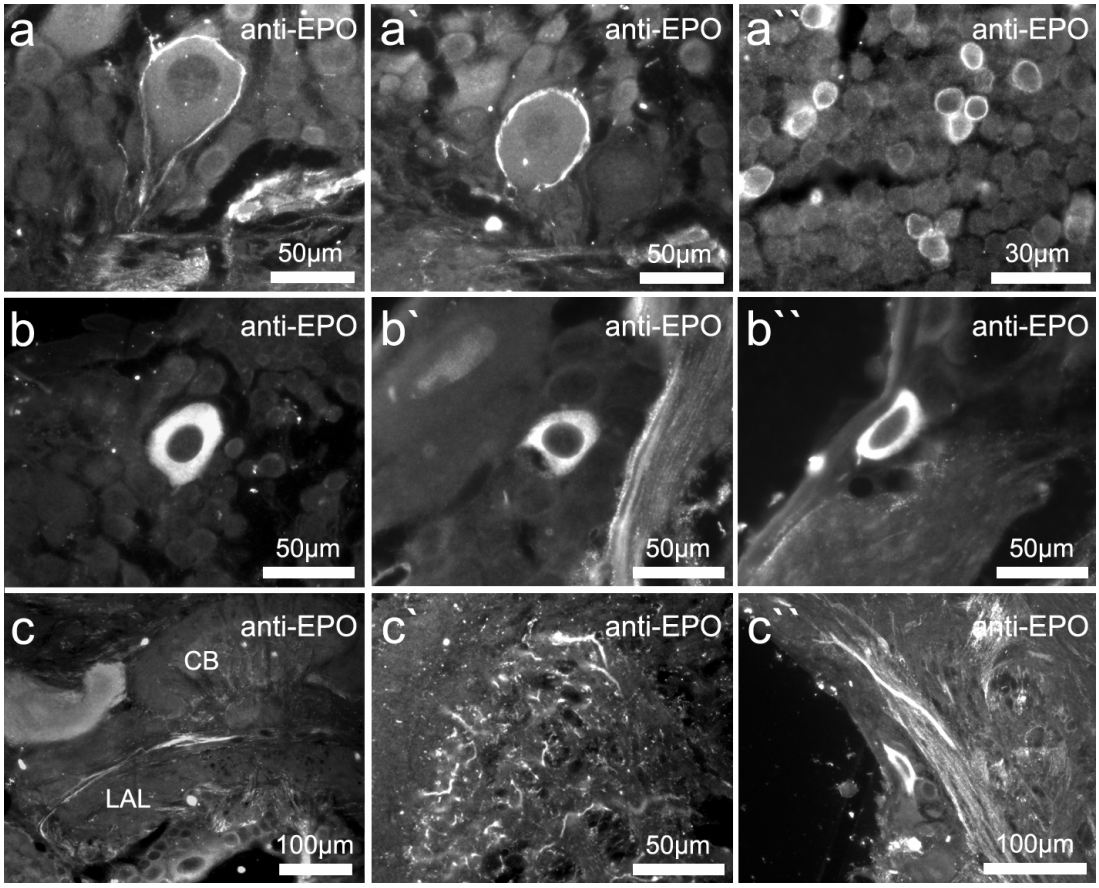


**Figure 7:** Frontal sections through the brain of *Locusta migratoria* labelled with anti-EPO serum. **a-a``:** Cell bodies with *ia*EPO immunolabelling associated with their cytoplasmic membranes were detected in the protocerebrum (a+a`) and in the optic lobes (a``). **b-b``:** Other cell bodies contained homogeneous *ia*EPO immunoreactivity throughout their cytoplasm. **c-c``:** *ia*EPO-immunopositive fibres were detected posterior to the central body (c), in the optical lobes (c`), and in the neuropil of the lateral horn (c``).
CB: central body, LAL: lateral accessory lobe

In some cells *ia*EPO immunolabelling was restricted to membrane associated regions of cell bodies and neurites (Figure 7a-a``). While the protocerebrum contained a number of immunolabelled cells with large cell bodies (50-70µm; Figure 7a-a`) surrounded by smaller

unlabelled cells, *ia*EPO-positive cell bodies in the optic lobes were generally smaller (10-15 µm) and of similar size as their neighbours (Figure 7a``).
Other types of *ia*EPO-immunopositive cells were homogeneously stained throughout the cytoplasm of their somata (Figure 7b-b``). Similarly, homogeneously labelled cell bodies were located in various regions of the grasshopper brain cortex. Furthermore, many *ia*EPO-immunopositive fibres were detected in various regions of the brain. Figure 7c shows a bundle of fibres posterior to the central body that projects into the lateral accessory lobe. In addition fibres with *ia*EPO labelling were also detected in the optic lobe (Figure 7c`) and in the neuropil of the lateral horn (Figure 7c``).

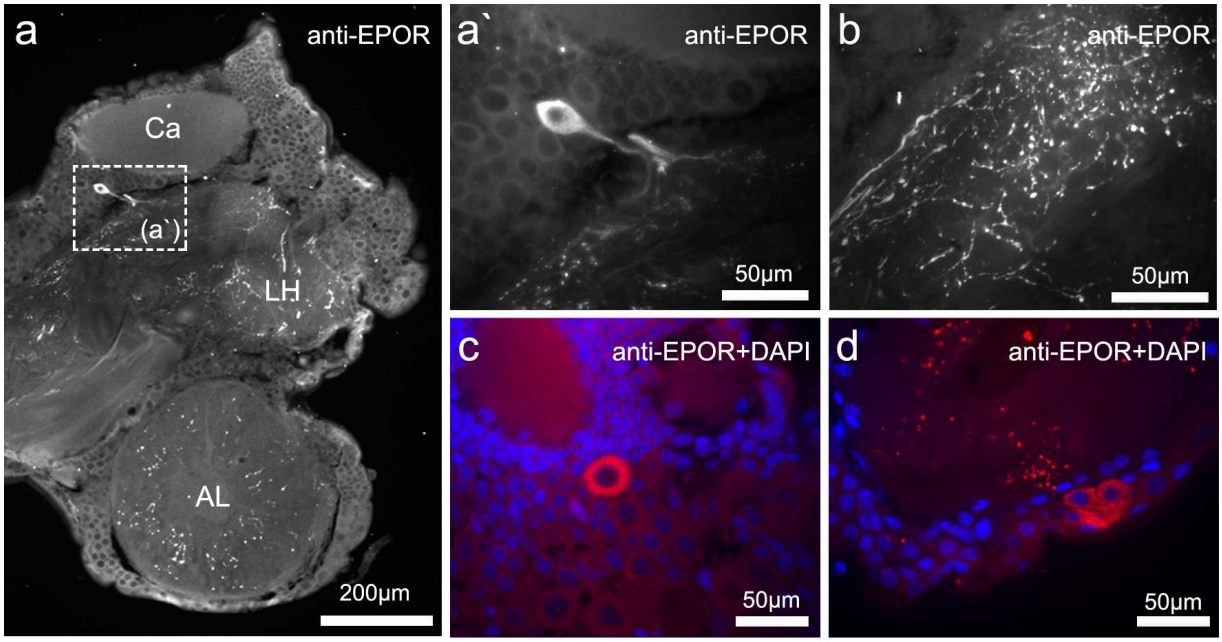


**Figure 8**: Frontal sections through the brain of *Locusta migratoria* labelled with anti-EPOR serum. **a, a`:** Brain section with *ia*EPOR-immunopositive cell body in the anterior protocerebrum (higher magnification in a`) and a multitude of immunopositive fibres in various central neuropil regions except the calyces of the mushroom body. **b:** Detailed view of *ia*EPOR-immunopositive fibres in the deutocerebrum. **c, d:** *ia*EPOR-immunopositive cells located in the protocerebrum (c) and tritocerebrum (d).
Ca: calyx of a mushroom body, LH: lateral horn, AL: antennal lobe

For EPOR immunohistochemistry, brains of *L. migratoria* were sectioned with a vibratome into slices of 50µm thickness and labelled with anti-EPOR serum. The frontal section of a hemibrain displayed in Figure 8a shows a soma of an *ia*EPOR-immunopositive cell body (higher magnification in a`) and several immunoreactive fibres throughout the entire brain except the calyces of the mushroom bodies. A higher magnification of some *ia*EPOR-positive fibres is displayed in Figure 8b. Additional *ia*EPOR-immunopositive cells were located in the protocerebrum (Figure 8c) and tritocerebrum (Figure 8d).

### 2.3.5 Expression of *ia*EPO and *ia*EPOR in the central nervous system of *Drosophila melanogaster*

Brains of *Drosophila melanogaster* were cut with a vibratome into slices of 50µm thickness and labelled with anti-EPO serum. In contrast to the nervous systems of the other invertebrate species, no cell bodies were found to be labelled. Only a few fibres inside neuropil regions seemed to express *ia*EPO immunoreactivity (data not shown).

Brains of *Drosophila* were also labelled with anti-EPOR serum. Figure 9a provides an overview of one section through a *Drosophila* brain with *ia*EPOR-immunopositive cells located in its most posterior part (white asterisk) and several *ia*EPOR-immunopositive fibres in the central body complex (white arrowhead, higher magnification in Figure 9a`). Further examples of *ia*EPOR-immunopositive cells located in various regions of the brain are presented at higher magnification in Figure 9b-d. All cells contained a homogeneous staining in the cytoplasm of cell bodies and their projections (Figure 9b).

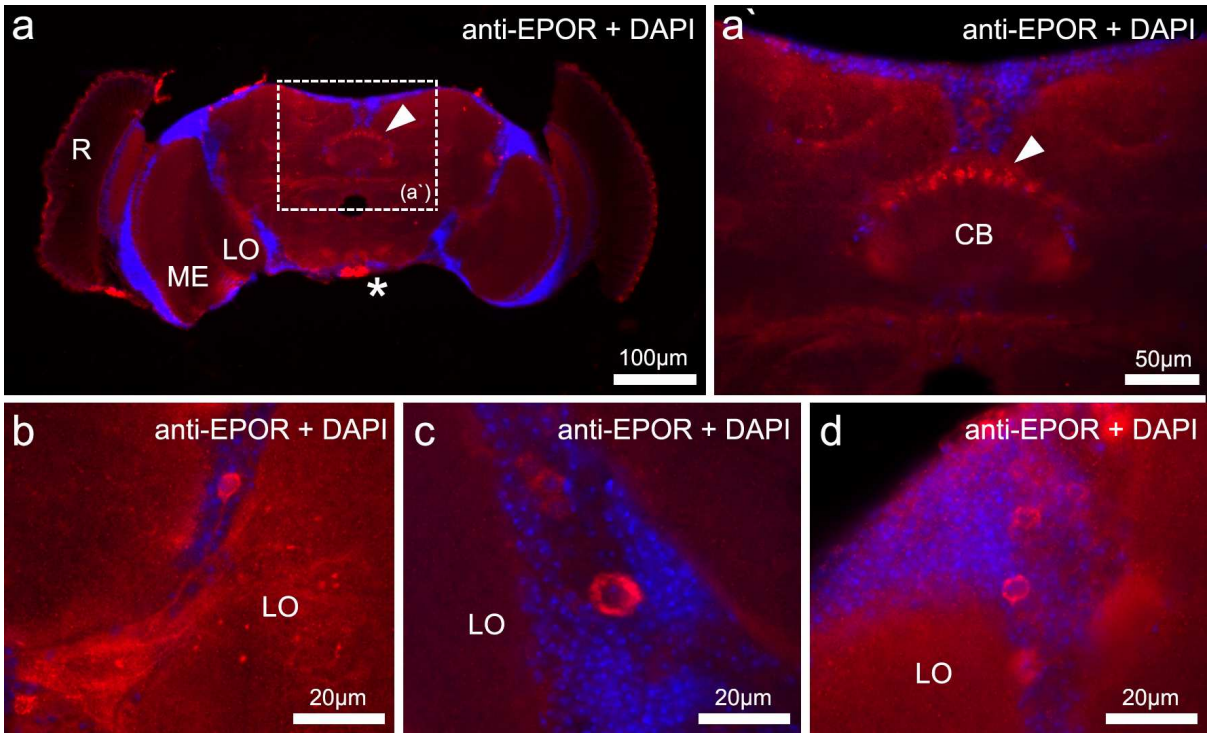


**Figure 9:** Frontal sections through the brain of *Drosophila melanogaster* labelled with anti-EPOR serum (red fluorescence) and the nuclear marker DAPI (blue fluorescence). **a, a`:** Brain section with *ia*EPOR-immunopositive cells (white asterisk) and *ia*EPOR-immunopositive fibres (white arrowhead) in the central body complex (higher magnification in a´). **b-d:** *ia*EPOR-immunopositive cells located in other brain regions contained a homogeneous staining in the cytoplasm and their projections.
R: retina, LO: lobula, ME: medulla, CB: central body

### 2.3.6 Western blot analysis of EPO, its receptor and their invertebrate analogues

For Western blot analysis proteins were extracted from the central nervous systems of mouse, the leech *Hirudo medicinalis*, the crayfish *Procambarus spec.*, the grasshopper *Locusta migratoria* and the fly *Drosophila melanogaster*. Lysates (20µg) were separated by

SDS-PAGE, transferred to a nitrocellulose membrane and incubated with the anti-EPO or anti-EPOR serum. Figure 10 summarises the results of the immunoblot analysis using anti-EPO serum. In lysates of mouse brains an intensive protein band at about 38kDa and several protein bands with less intensive staining at ~27kDa, ~55kDa, ~62kDa, ~70kDa and ~120kDa were detected (Figure 10, first lane). Leech nervous tissue contained no proteins that provided intensively labelled bands with sizes comparable to those of mouse brain tissue (Figure 10, second lane). The most intensively stained protein band was detected at ~68kDa and several protein bands with low staining intensity were detected at ~26kDa, ~38kDa, ~48kDa and ~130kDa. Western blot analysis of the crayfish central nervous system revealed an intensively labelled protein band of ~38kDa and several bands with lower staining intensity at ~23kDa, ~35kDa, ~48kDa, ~70kDa and ~130kDa (Figure 10, third lane). In the CNS of the locust Western blot analysis revealed one main protein band at ~38kDa and several bands at ~26kDa, ~68kDa and ~100kDa (Figure 10, fourth lane). In brains of *Drosophila* no intensively stained protein band was detected by immunoblotting (Figure 10, fifth lane). One protein band at ~43kDa was stained with very low intensity.

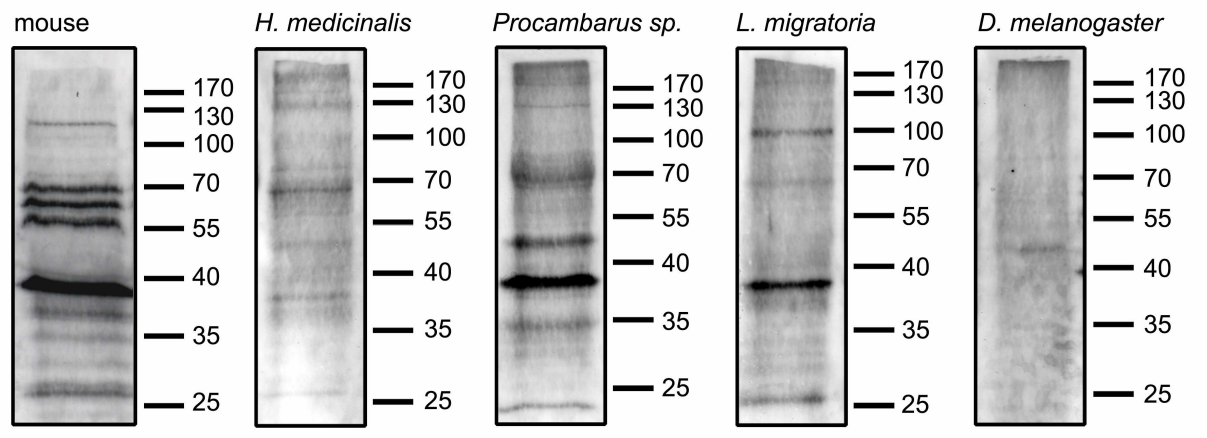


**Figure 10:** Western blot analysis of EPO in lysates of the CNS of mouse, *Hirudo medicinalis*, *Procambarus spec.*, *Locusta migratoria* and *Drosophila melanogaster*. Molecular weight of protein bands are displayed in [kDa]. For further explanations see text.

The results of the Western blot analysis using anti-EPOR serum are summarised in Figure 11. Lysates of mouse brains contained one main ~28kDa protein band and several bands of lower intensity at ~38kDa, ~39kDa and ~53kDa (Figure 11, first lane). In the nervous tissue of the leech two main protein bands (~28kDa,~62kDa) and two protein bands with lower staining intensity at ~35kDa and ~90kDa were detected (Figure 11, second lane). Western blot analysis of the crayfish central nervous system showed protein bands of ~28kDa, ~37-39kDa, ~53kDa and ~68kDa (Figure 11, third lane). In lysates of the locust CNS two main protein bands (~38kDa, ~53kDa) and two bands with lower staining intensity at ~28kDa and~70kDa were detected. In lysed heads of *Drosophila* Western blot analysis revealed five main protein bands at ~28kDa, ~38kDa, ~40kDa, ~53kDa and ~85kDa (Figure 11, fifth lane).

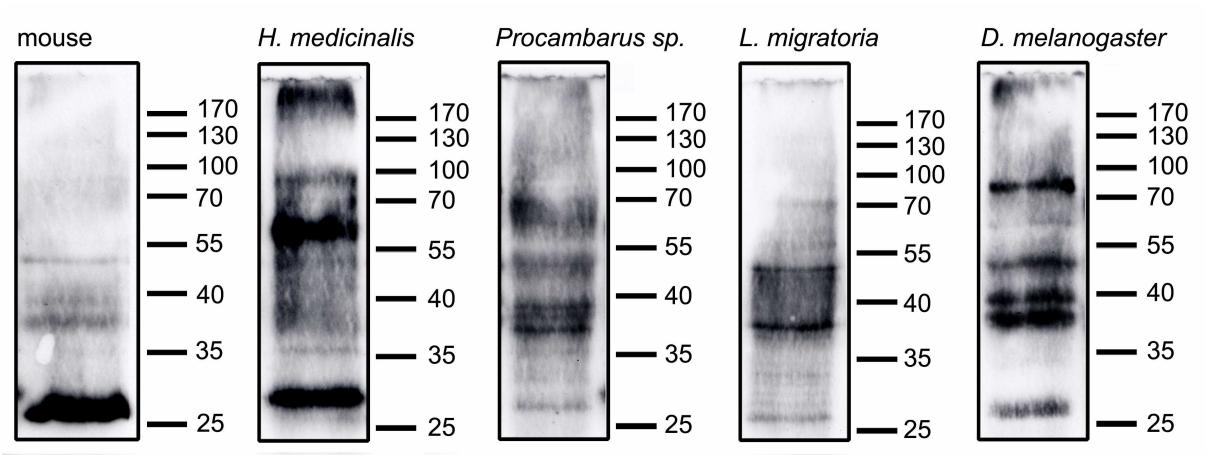


**Figure 11:** Western blot analysis of EPO receptor in CNS lysates of mouse, *Hirudo medicinalis*, *Procambarus spec.*, *Locusta migratoria* and *Drosophila melanogaster*. Molecular weight of protein bands are displayed in [kDa]. For further explanations see text.

## 2.4 Discussion

The expression pattern of EPO and its receptor was analysed in the central nervous system of invertebrates from different phyla using immunohistochemistry and Western blot analysis. The distribution and localisation of proteins within a tissue, or more precisely within a cell compartment, can be analysed by immunohistochemistry and the molecular weight of the immunolabelled proteins can be determined by Western blotting. Both methods have been used for many years to specifically label proteins and characterise their expression pattern (Coons et al. 1945; Towbin et al. 1979). The nervous tissues of the leech *Hirudo medicinalis*, the crayfish *Procambarus spec.*, the grasshopper *Locusta migratoria* and the fly *Drosophila melanogaster* were analysed for endogenous expression of EPO- and EPOR-like proteins using the polyclonal goat anti-EPO antibody (raised against the N-terminus of human EPO) and the polyclonal rabbit anti-EPOR antibody (raised against the C-terminal cytoplasmic domain of EPOR of mouse origin). In addition, mouse brains were immunolabelled for comparison with both results obtained in invertebrate central nervous systems and previous studies on mice and other mammals.

*Immunohistochemistry of EPO*

In the midbrain of mice EPO-like immunoreactivity was detected in cells with morphological characteristics of astrocytes and in cells that appeared to be neurons (Figure 1). Immuno-positive astrocytes showed a homogeneous, cytoplasmic staining indicating that these cells may produce EPO. Various studies identified astrocytes to be the primary source of EPO in the mammalian brain. Marti et al. (1996) showed that cultured murine astrocytes (and not microglia or oligodendrocytes) accumulate EPO mRNA under hypoxic conditions. Likewise, Masuda et al. (1994) demonstrated that astrocytes of rat embryonic brains produce EPO. However, more recent studies indicated that also neurons express and probably release EPO. In embryonic OF1 mice EPO mRNA is constitutively expressed in cultured neocortical neurons and increases from basal levels after 6 hours of hypoxia (Bernaudin et al. 1999, 2000). EPO was immunohistochemically detected in cortical and hippocampal neurons of both normal adult and ischemic human brains (Sirén et al. 2001) and also in the developing brains of humans and mice (Juul et al. 1999; Knabe et al. 2004). The data of this study confirm the presence of EPO immunoreactivity in neuronal cells of mouse brains. But unlike the homogeneous, cytoplasmic staining of EPO in astrocytes EPO-immunoreactive material of neurons appeared granulous and the majority of staining was concentrated in the vicinity of cell membranes of somata and neurites.

In invertebrates *ia*EPO immunoreactivity was found in several cells throughout the whole central nervous system with similar patterns of immunosignal distributions as detected in mouse brains. A glial cell type that is particularly analogous to vertebrate astrocytes has not yet been identified in the CNS of invertebrates and specific astrocyte markers (e.g. antibody against the glial fibrillary acidic protein) (Bignami et al. 1972; Onteniente et al. 1980) fail to label any glial cells in invertebrates (Abbott 1995). Although a specific glia marker is

lacking, a number of studies described glial cells in the CNS of invertebrates that serve the same function as astrocytes in the CNS of vertebrates. This includes metabolic support, forming the blood-brain-barrier, transmitter release/reuptake and regulation of ionic concentrations (reviewed by: Laming et al. 2000; Kretzschmar & Pflugfelder 2002; Villegas et al. 2003; Edenfeld et al. 2005). Therefore, the immunohistochemical results of this study can only determine whether glial cells in general and/or neuronal cells express *ia*EPO immunoreactivity in the CNS of invertebrates.

The immunoreactivity of *ia*EPO in the brains of invertebrates was detected in both cell types with fluorescent labelling restricted to submembranous regions of cell bodies and processes or as homogeneous staining throughout the cytoplasm of entire somata. In contrast to the mouse brain no glial cells in the CNS of the leech and the locust were found to express *ia*EPO. Immunolabelled sections of the leech were compared with a detailed morphological description of leech ganglia from Coggeshall & Fawcett (1964). They described three types of glia: small glial cells lying directly beneath the outer capsule, packet glial cells enclosing somata of neurons and neuropil glia that are associated with small axons. None of the *ia*EPO-immunopositive cells in the leech ganglia resembled one of the three types of glia. In the locust brain the size and morphology of *ia*EPO-immunopositive cells is different, but all labelled cells share the morphological characteristics of neurons. Similary, labelled fibres in the locust brain most likely belong to neuronal cells since processes of glial cells are generally shorter than those of neurons (Hoyle 1986). Only in the CNS of the crayfish one cell type that expressed *ia*EPO immunoreactivity is propably a glial cell. A study of Hoyle (1986) described a satellite glia cell ensheathing neuronal somata in ganglia of the locust (Figure 12).

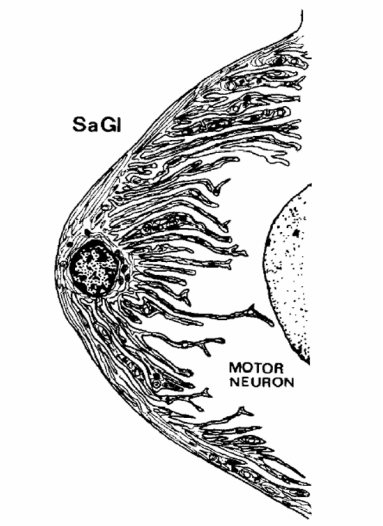


**Figure 12:** Schematic drawing of a satellite glial cell in the metathoracic ganglion of *Schistocerca americana americana* (from Hoyle 1986). Satellite glial cells enclose large motor neurons with fingerlike processes to isolate them from other surrounding cells. SaGl satellite glia

Since crayfish and locusts are arthropods that exhibit many similarities in the organisation of their nervous systems similar types of neuron-enclosing glia may exist in crayfish. Satellite glia enclose individual, large motor neurons with fingerlike processes. Thereby, one glial cell is associated with one motor neuron only. The size of the nucleus of a satellite glia ranges from 3µm to 20µm. The morphological similarities of satellite glia in the locust nervous

system and the *ia*EPO-immunopositive cells in the brain of the crayfish suggest that *ia*EPO is also expressed by glial cells of the crayfish.

Brain slices of *Drosophila melanogaster* were also stained with the anti-EPO serum but in contrast to the nervous systems of the other invertebrate species, no cell bodies were found to be labelled. Only a few fibres inside neuropil regions seemed to express *ia*EPO immunoreactivity (data not shown).

*Western blot analysis using anti-EPO serum*

The amino acid sequence of human EPO contains 166 residues and has a calculated molecular weight of 18.4kDa for the protein moiety. But due to three N-linked and one C-linked carbohydrate chains the overall molecular weight of EPO is 30.4kDa (Lai et al. 1986). The detected protein size of purified human urinary EPO using Western blot analysis ranges from 32-39kDa (Miyake et al. 1977; Yanagawa et al. 1984; Krystal et al., 1986). The heterogeneity of the EPO protein size is due to its variable amount of sialic acid attached to the protein. Goldwasser (1974) reported 16-18 sialic acid residues per molecule of native EPO. The removal of terminal sialic acids from EPO abolishes its *in vivo* activity (Lukowsky & Painter 1972; Goldwasser et al. 1974; Goto et al. 1975), but *in vitro* activity of EPO increases with desialylation, which is probably due to increased affinity to the receptor (Goldwasser et al. 1974; Sasaki et al. 1987; Takeuchi et al. 1990; Tsuda et al. 1990).

In lysates of cortical tissues of mice the EPO-like proteins had sizes of 33kDa and 18kDa (Bernaudin et al. 1998) and of 35kDa and 19kDa in embryonic midbrains of mice (Knabe et al. 2004). In this study a main ~38kDa protein was detected in lysates of mice brains (Figure 10). The variance in the reported EPO protein sizes can be due to the different experimental procedures. The molecular weight can slightly vary depending on the percentage of acrylamide in the SDS gels. For example, purified human EPO has a protein size of 39kDa on an 8% gel and 37kDa on a 12% gel (Krystal et al. 1986). The same EPO antibody used under the same experimental conditions detects the major protein band of ~38kDa in mouse, crayfish, locust and (though weaker) in leech. Since 38kDa is within the range of molecular weights described for EPO in mammals and close to the expected size of mouse EPO, the antibody may have detected similar proteins in the central nervous systems of mouse and invertebrates from three different phylogenetic groups. In *Drosophila* no distinct protein band was detectable, which is consistent with a lack of immunostaining in the brains of this species.

The antibody used for Western blot analysis in this study also labels protein bands of non-expected sizes in all analysed nervous tissues, including mice. Additional protein bands in lysates of mice brains were detected at sizes of ~55kDa, ~62kDa, ~70kDa and ~120kDa (Figure 10, first lane). Most previously published Western blots that analysed the expression of EPO in nervous tissues of mice exclude the range of 120-55kDa protein size (Figure 13a, b lower blot). One Western blot analysis of purified EPO of cultured rat astrocytes described additional protein bands of 55kDa and 67kDa (Masuda et al. 2004; Figure 13c). According to the authors, these protein bands are caused by the BSA component of the solvent used to store EPO.

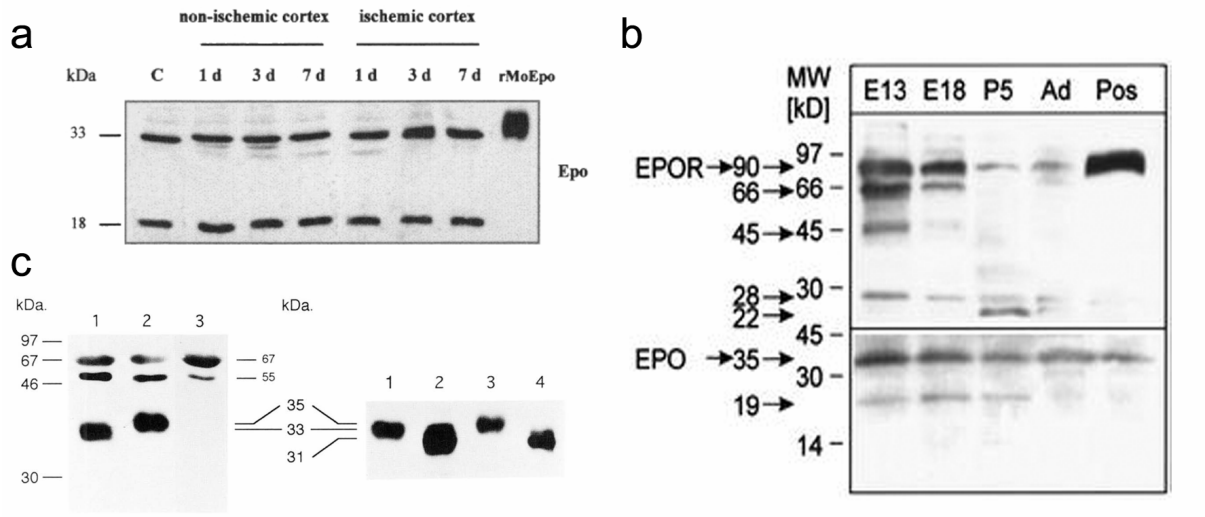


**Figure 13:** Western blot analysis of EPO. **a:** Western blot analysis in lysates from nonischemic and ischemic cortex from adult mice (from Bernaudin et al. 1998). **b:** Western blot analysis for EPOR (upper blot) and EPO (lower blot) in brains of embryonic mice at day 13 (E13), day 18 (E18), postnatal mice of day 5 (P5) and adult mice (Ad) (from Knabe et al. 2004). **c:** Western blot analysis of brain and serum EPO of cultured, cerebral cells from fetal rats (from Masuda et al. 1994).

One explanation for additional protein bands is a cross reactivity of the antibody with other proteins that contain similar epitops. However, intensively stained additional protein bands of non-expected sizes were mainly detected in lysates of mouse brains and much less in lysates of the invertebrate CNS. Particularly, the analysed nervous tissue of locusts and crayfish contained only one intensively labelled protein band, suggesting that no other proteins in these species display cross-reactivity. Therefore immunolabelling of *ia*EPO in nervous tissues may have resulted from exclusive labelling of the 38kDa sized protein. The similar expression patterns of EPO-like immunoreactivity and the detected protein of the same molecular weight in the brains of animals analysed in this study indicate that a homologue of EPO may be exsist in the CNS of invertebrates. Further studies remain to determine the molecular identity of the detected *ia*EPO.

*Sequence homology analysis of EPO*

The amino acid sequence of EPO is described for various vertebrates, ranging from human to fish (Jacobs et al. 1985; Shoemaker et al. 1986; Chou et al. 2004; Chu et al. 2007; Figure 14). An alignment of the human EPO amino acid sequence with those from mouse, fugu and zebrafish (zebrafish has three EPO-related transcripts caused by alternative splicing) exhibits an overall identity of 80%, 32% and 32% (Figure 14). There are four cysteine residues that form internal disulfide bonds and are conserved in all species exept C59 in mouse (Figure 14, black arrows). The mammalian EPO protein has three N-linked (N24, N38, N83) and one O-linked (S126) glycolysation site (Figure 14, white arrowheads), whereas the putative mature form of the zebrafish EPO only contains two N-linked (N38, N81) and one O-linked (S114) glycolysation site. The fugu EPO has no N-linked glycolysation

site, but one O-linked glycolysation site, which is homologue to those of human EPO. The EPO protein has not been characterised in any invertebrate species yet. Therefore the nucleotide sequence of the human *epo* gene was compared to the sequenced *Drosophila melanogaster* genom using a Basic Local Alignment Search Tool (BLAST, National Center for Biotechnology Information - NCBI). No significant similarities were found, which indicates that there is no nucleotide sequence in the *Drosophila* genome coding a protein that is homologue to the human EPO protein. Since there was also no immunohistochemical detection of an EPO protein in the *Drosophila* brain (chapter 2.3.5) and no distinct protein band in the western blot analysis using *Drosophila* brain lysates (Figure 10), it is most likely that *Dosophila melanogaster* has no endogenous EPO-like protein.

The genome sequences of all other invertebrate species analysed in this study (*Hirudo medicinalis*, *Procambarus spec.*, *Locusta migratoria*) have not been characterised so far and therefore cannot be used for further alignment studies. Although the western blot analysis and immunohistochemical studies may suppose the expression of EPO-like proteins in the brain of invertebrates it is thitherto unknown whether the detected proteins are homologous to the human EPO.

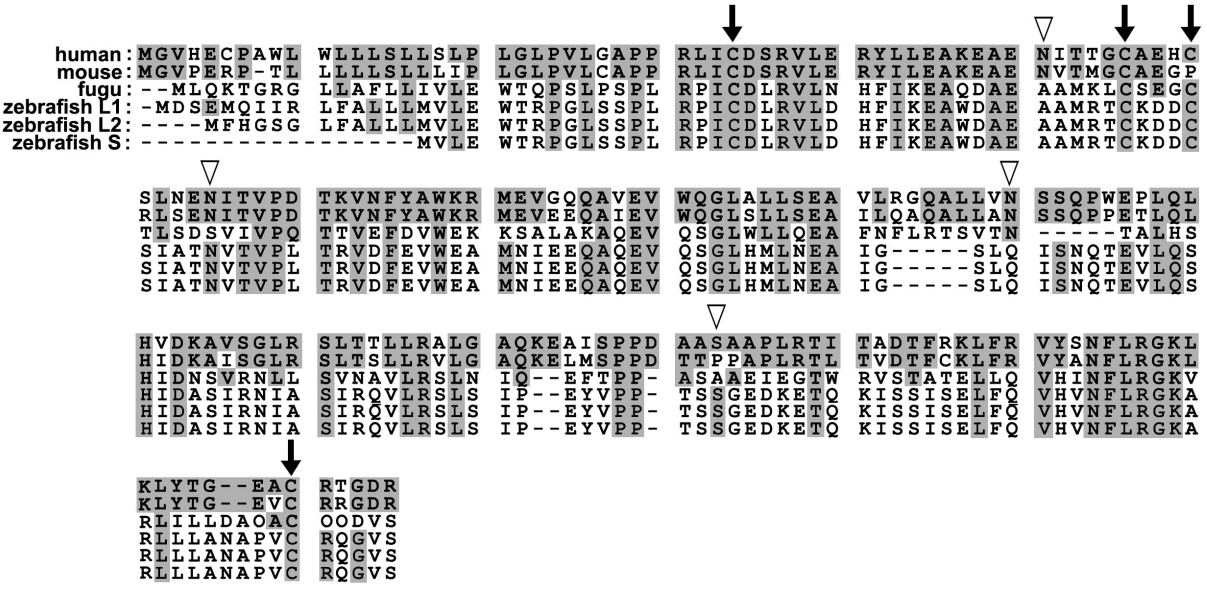


**Figure 14:** Alignment of the human EPO amino acid sequence with those from mouse, fugu (*Takifugu rubripes*) and zebrafish (*Danio rerio*). Identical residues are highlighted in grey. Putative glycolysation sites of human EPO are indicated by white arrowheads and the conserved four cysteine residues are indicated by black arrows.

*Immunohistochemistry of EPO receptor*

Nervous tissues of mice, the leech *H. medicinalis*, the crayfish *Procambarus spec*., the grasshopper *L. migratoria* and the fly *D. melanogaster* were incubated with the anti-EPOR serum to investigate the expression pattern of proteins with the respective epitop. In the midbrains of mice a homogeneous, cytoplasmic immunostaining of EPOR was detected in cells with morphological characteristics of neurons (Figure 2). Previous studies also used anti-EPOR serum to characterise EPOR expressing cells in the CNS of mammals. In the developing midbrain of C57B1 mice EPOR-immunopositive cells were detected in neurons

and at a certain stage of development (from E11 to E12.5) also in radial glial cells (Knabe et al. 2004). Cell cultures of mouse embryonic hippocampus neurons and neuronal progenitor cells were demonstrated to express EPOR (Chen et al. 2007). Furthermore, Bernaudin et al. (1999) showed that cultured astrocytes of embryonic OF1 mice express EPOR. EPOR immunoreactivity was also described in neurons of the rat hippocampus (Morishita et al. 1997; Lewczuk et al. 2000; Weber et al. 2002; Sun et al. 2004), in Schwann cells of rat sciatic nerve and in cultured astrocytes and oligodendrocytes of embryonic rats (Sugawa et al. 2004; Li et al. 2005). In developing and mature brains of humans EPOR immunoreactivity was detected in neuronal cells and astrocytes (Juul et al. 1998, 1999; Sirén et al. 2001). Similar to my studies on invertebrates all authors detected the EPOR immunoreactivity in the cytoplasm.

Immunohistochemical studies on brain slices of the leech, the crayfish, the locust and the fly using anti-EPOR serum revealed similar expression patterns of EPOR. Immunoreactivity of *ia*EPOR was detected in cell bodies and processes of neurons (Figure 4, 6, 8 and 9). No evidence for the expression of *ia*EPOR in glial cells was found in any of the invertebrates studied. Several studies on mammalian nervous systems showed that EPOR is only weakly expressed in normal adult brains but hypoxic conditions can induce EPOR expression in neuronal and glial cells (Lewczuk et al. 2000; Sirén et al. 2001; Knabe et al. 2004). In this study the analysed invertebrate brains were obtained from animals reared under normal conditions. It has not yet been determined whether *ia*EPOR expression in brain tissue of invertebrates may change under hypoxic conditions. However, one experiment performed in the course of my thesis demonstrated that central nervous *ia*EPOR expression can be induced of the grasshopper *Chorthippus biguttulus* following damages to peripheral nerves that contain central nervous projections (see chapter 3 of this doctoral thesis). This indicates that *ia*EPOR expression in the CNS of invertebrates is also modulated by physiological (especially harmful) conditions.

*Western blot analysis using anti-EPOR serum*

The nucleotide sequence of human EPOR isolated from an erythroleukemia line (OC1M1) and fetal liver encodes a 508 amino acid protein with a calculated molecular weight of 55kDa (Jones et al. 1990). Immunoprecipitation and Western blot analysis of erythroid cells revealed protein sizes ranging from 62-66kDa due to posttranslational modification (Li et al. 1990; Yoshimura et al. 1990; Migliaccio et al. 1991; Miura et al. 1991; Quelle & Wojchowski 1991; Quelle et al. 1992). In addition, Sawyer et al. (1993) detected a highly glycosylated form of EPOR at 78kDa in HC-D57 murine erythroleukemia cells, that seemed to be the biologically active form of the receptor.

Immunohistochemical studies and Western blot analysis indicated the expression of EPOR also in brains of mammals. But the results of these studies concerning the molecular weight of EPOR are highly variable. In lysates of nonischemic and ischemic mice cortices protein bands of 68kDa (glycolysated mature receptor form), 62kDa (native intracellular receptor form), 46-43kDa (major proteolytic receptor form), 37kDa (no explanations) and 29kDa (soluble receptor form) were detected (Bernaudin et al. 1999). Similar protein bands

were found in lysates of embryonic C57B1 mice (Knabe et al. 2004, also see Figure 13b). In cortico-hippocampal slice cultures of adult rats an EPOR protein band of 97.4kDa was detected (Weber et al. 2002). In Schwann cells of rats the EPOR protein was detected with a size of 70kDa and 90kDa (Campana & Myers 2001). Furthermore, in the rat retina a 100kDa protein band for EPOR was described (Junk et al. 2000). In addition, several studies demonstrated the expression of EPOR by Western blotting but did not mention the size of the detected protein band (Chen et al. 2007; Spandou et al. 2004; Martínez-Estrada et al. 2003; Digicaylioglu & Lipton 2001). The variability of the detected EPOR protein sizes initiated a debate about the specificity of the used anti-EPOR antibodies. A more recent study analysed the specificity and affinity of different EPOR antibodies (including the M-20 antibody used in this study) and showed that only the M-20 antibody can be used in Western blots to detect the EPOR with a size of 59kDa (Elliott et al. 2009). Various anti-EPOR antibodies showed cross-reactivity with heat shock proteins (HSP70-2, HSP70-5).

The nervous tissues of the animals used in the present study were subjected to Western blot analysis with the anti-EPOR serum and the results are summarised in Figure 11. Although many previous studies revealed different protein sizes for EPOR in neuronal and erythroid cells, the expected size of 59kDa (as indicated by Elliott et al. 2009) was neither detected in mouse brains nor in the invertebrate brain tissues. In lysates of mice brains a main ~28kDa protein band was detected (Figure 11, first lane). A labelled 28kDa protein band using anti-EPOR serum was described for the soluble form of the receptor (sEPOR) (Knabe et al. 2004). In analogy to several other members of the cytokine superfamily type I transmembrane proteins, EPOR is also synthesised in a soluble form that corresponds to the extracellular domain of the complete receptor (Nagao et al. 1992; Harris & Winkelmann 1996; Westphal et al. 2002). The soluble form of the receptor is synthesised by alternative splicing of EPOR mRNA. Following secretion into the extracellular fluid, sEPOR binds EPO thereby limiting its ability to bind the receptor located in the cell membrane (Kuramochi et al. 1990; Baynes et al. 1993). The presence of sEPOR has been reported in plasma, several tissues including liver, spleen, kidney, heart, bone marrow (Fujita et al. 1997) and more recently in mouse brains (Soliz et al. 2007). In the mouse brain sEPOR is constitutively expressed under normoxic conditions and down-regulated during chronic hypoxia (three days of 10% $O_2$). The decrease of sEPOR protein is required for adequate ventilatory acclimatisation of mice to hypoxia (Soliz et al. 2007). This indicates that sEPOR has a biological function in the CNS of mammals. The ~28kDa protein band, that was detected with the same antibody under indentical experimental conditions in mouse brain lysates, was also observed in all invertebrate species analysed in this study, although the intensity of the protein band varied (Figure 11). These results may indicate that in the CNS of the leech, the crayfish, the locust and the fly a soluble EPO receptor is expressed. Whether the expression pattern of sEPOR in the CNS of invertebrates decreases under hypoxic conditions and whether sEPOR also has a biological function have to be confirmed in future studies. Besides the 28kDa protein band, Western blot analysis using anti-EPOR serum revealed additional protein bands of sizes ranging from 37-90kDa (Figure 11). Further studies are needed to determine whether these bands result from cross-reactivity of the antibody as

described by Elliott et al. (2009) or whether these protein bands display different forms of the EPO receptor as described by Knabe et al. (2004) and Bernaudin et al. (1999).

*Sequence homology analysis of EPOR*

The nucleotide and amino acid sequence of the hematopoietic EPO receptor is described for various vertebrates, ranging from human to fish (D`Andrea et al. 1989, Jones et al. 1990, Kuramochi et al. 1990, Youssoufian et al. 1990, Chou et al 2004, Paffett-Lugassy et al. 2007, Chu et al. 2008; Figure 15). An alignment of the human EPOR amino acid sequence with those from mouse, fugu and zebrafish exhibits an overall identity of 80%, 32% and 32% (Figure 15). The four cysteine residues in the extracellular domain (marked with black arrows in Figure 15) that are supposed to be important for EPO binding, homodimerisation of the receptor and transmitting a conformational change through the transmembrane domain are homologue in all analysed vertebrate species. EPOR belongs to the type I superfamily of single-transmembrane cytokine receptors that shares a conserved extracellular Trp-Ser-x-Trp-Ser motif (WSxWS motif, Figure 15 marked in blue) located proximal to the transmembrane domain (TM, Figure 15 marked in black). The WSxWS motif is conserved in all vertebrate species including fishes (except a variation in the zebrafish amino acid sequence: WSxWT). The cytoplasmic domains of the family members are less well conserved, but some short stretches of conserved amino acid residues close to the membrane-spanning region (BOX 1 and BOX 2, Figure 15 marked in green) have been reported. Both of the BOX sequences have been shown to be required for JAK2 activation after EPO treatment (Miura et al. 1993) and are also very similar in all vertebrate species. After JAK2 activation eight tyrosine residues in the distal cytoplasmic domain will be phosphorylated and act as docking sites for downstream signalling molecules including STAT5, PI(3)K and Ras-MAPK. Five of these tyrosine residues (Y-429, Y-431, Y-443, Y-460, Y-464) are conserved in the zebrafish EPOR amino acid sequence and the fugu EPOR has only four of these tyrosine residues conserved (Y-429, Y-431, Y-443, Y-464). Although the nonconserved phosphotyrosines (Y-434, Y-401, Y-479) are supposed to be important for STAT5 and PI(3)K docking, Paffett-Lugassy et al. (2007) demonstrated that STAT5 is also involved in EPO/EPOR signalling during zebrafish development.

The amino acid sequence of the hematopoietic EPOR has not been characterised in any invertebrate species yet. Therefore the nucleotide sequence of the human *epo receptor* gene was compared to the sequenced *Drosophila melanogaster* genom using a Basic Local Alignment Search Tool (BLAST, National Center for Biotechnology Information - NCBI). No significant similarities were found, which indicates that there is no nucleotide sequence in *Drosophila* genome coding a protein that is homologue to the human hematopoietic EPOR. Therefore it is questionable what kind of protein was detected by the EPOR antibody in the immunohistochemical and western blot studies of this work. The genome sequences of all other invertebrate species analysed in this study (*Hirudo medicinalis*, *Procambarus spec.*, *Locusta migratoria*) have not been characterised so far and therefore cannot be used for further alignment studies. Although the western blot analysis and immunohistochemical studies may suppose the expression of EPOR-like proteins in the

brain of invertebrates it is thitherto unknown whether the detected proteins are similar to the human EPOR.

Although a receptor homologue to the mammalian EPOR was not found in the *Drosophila* genome various homologue proteins of the mammalian Jak/STAT pathway have been described for *Drosophila*. The JAK homologue is encoded by *hopscotch* (*hop*) and exhibits an overall identity of 27% to the mammalian JAK2 (Binari & Perrimon 1994). STAT is encoded by *stat92E* and is most similar to the mammalian STAT5 (homology of 37%, Hou et al. 1996, Yan et al. 1996). Other signal molecules that play a role in the mammalian EPO/EPOR signalling pathway were also found in *Drosophila*. A homologue of the PI(3)K (encoded by *Pi3K92E*; 37% homology), Akt (encoded by *dakt1*; 61% homology) and the NF-$_K$B-factor (encoded by *dorsal*, *relish* and *dif*; 41%, 36% and 34% homology) were identified (Franke et al. 1994, Hetru & Hoffmann 2009). Until now only one cytokine receptor of class I has been described for *Drosophila* (encoded by the gene *domeless*), which is most similar to the vertebrate interleukin receptor 6 (Brown et al. 2001). Other types of receptors that induce the JAK/STAT signalling pathway and may be similar to the EPO/EPOR signalling system in mammals have not been identified in *Drosophila* so far.

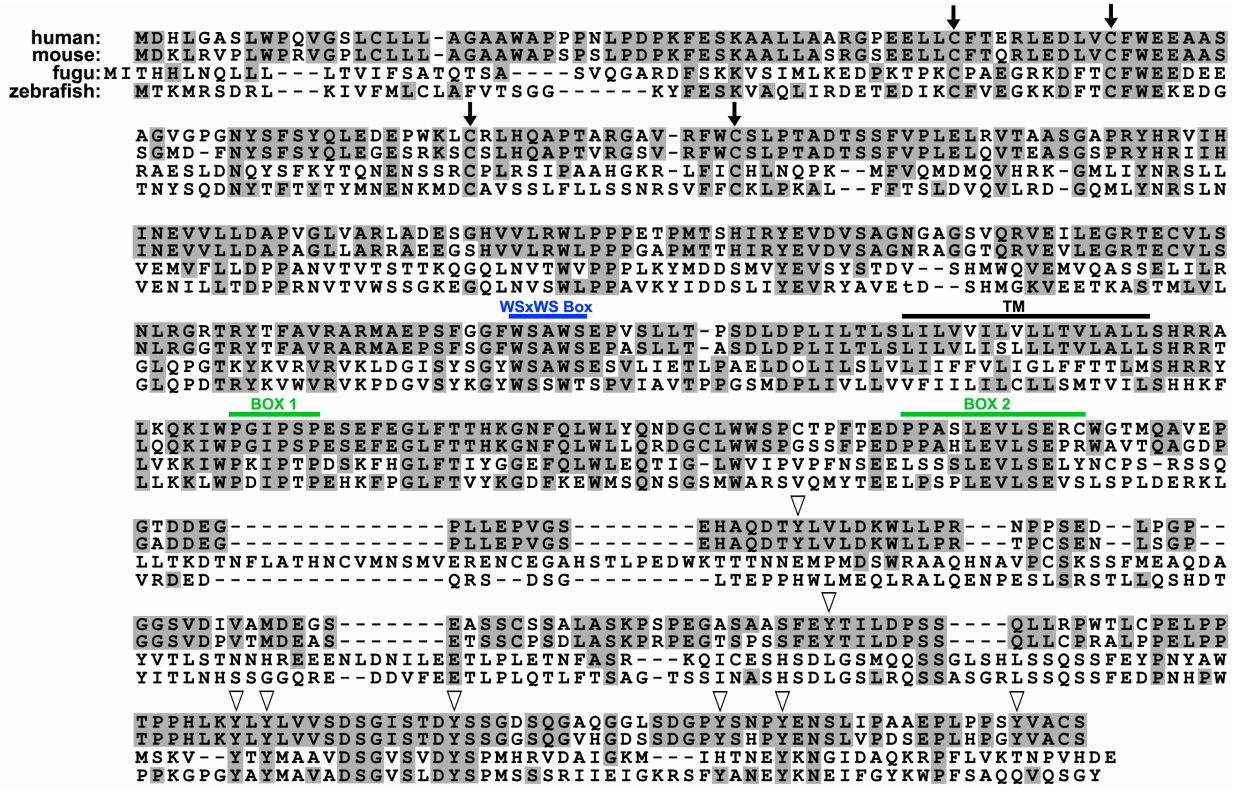


**Figure 15:** Alignment of the human EPOR amino acid sequence with those from mouse, fugu (*Takifugu rubripes*) and zebrafish (*Danio rerio*). Identical residues are highlighted in grey. Putative important cysteine residues for EPO binding are indicated by black arrows. White arrowheads indicate putative tyrosines that will be phosphorylated after receptor dimerisation and activation of janus kinases. The WSxWS box is marked in blue, the transmembran domain in black and the BOX1 and BOX2 motif in green.

# 2.5 References

Abbott NJ (1995) Morphology of nonmammlian glial cells: functional implications. In: Ransom BR, Kettenmann H (eds) Neuroglia. Oxford University Press Inc, USA pp 97-116

Anagnostou A, Liu Z, Steiner M, Chin K, Lee ES, Kessimian N, Noguchi CT (1994) Erythropoietin receptor mRNA expression in human endothelial cells. Proc Natl Acad Sci 91:3974-3978

Arcasoy MO (2008) The non-haematopoetic biological effects of erythropoietin. Bri J of Haematol 141:14-31

Assandri R, Egger M, Gassmann M, Niggli E, Bauer C, Forster I, Görlach A (2004) Erythropoietin modulates intracellular calcium in a human neuroblastoma cell line. J of Physiol 516:343-352

Baynes RD, Reddy GK, Shih YJ, Skikne BS, Cook JD (1993) Serum form of the erythropoietin receptor identified by a sequence-specific peptide antibody. Blood 82:2088–2095

Bernaudin M, Bernaudin M, Marti HH, Roussel S, Divoux D, Nouvelot A, MacKenzie ET, Petit E (1999) A potential role for erythropoietin in focal permanent cerebral ischemia in mice. J Cereb Blood Flow Metab 19:643–651

Bernaudin M, Bellail A, Marti HH, Yvon A, Vivien D, Duchatelle I, Mackenzie ET, Petit E (2000) Neurons and astrocytes express EPO mRNA: Oxygen-sensing mechanisms that involve the redox-state of the brain. Glia 30:271-278

Bignami A, Eye LF, Dahl D, Uyeda CT (1972) Localization of the glial fibrillary acidic protein in astrocytes by immunofluorescence. Brain Res 430:429-35

Binari R, Perrimon N (1994) Stripe-specific regulation of pair-rule genes by hopscotch, a putative Jak family tyrosine kinase in *Drosophila*. *Genes Dev* 8:300-312.

Buemi M, Cavallaro E, Floccari F, Sturiale A, Aloisi C, Trimarchi M, Grasso G, Corica F, Frisina N (2002) Erythropoietin and the brain: from neurodevelopment to neuroprotection. Clin Sci (Lond) 103:275-282

Campana WM & Myers RR (2001) Erythropoietin and erythropoietin receptors in the peripheral nervous system: changes after nerve injury. FASEB J 15:1804–1806

Chandel NS, Maltepe E, Goldwasser E, Mathieu CE, Simon MC, Schumacker PT (1998) Mitochondrial reactive oxygen species trigger hypoxia-induced transcription. Proc Natl Acad Sci USA 95:11715-11720

Chen ZY, Asavaritikrai P, Prchal JT, Noguchi CT (2007) Endogenous erythropoietin signaling is required for normal neural progenitor cell proliferation. J Biol Chem 282:25875–25883

Chen ZY, Warin R, Noguchi CT (2006) Erythropoietin and normal brain development: Receptor expression determines multi-tissue response. Neurodegener Dis 3:68–75

Chikuma M, Masuda S, Kobayashi T, Nagao M, Sasaki R (2000) Tissue-specific regulation of erythropoietin production in the murine kidney, brain, and uterus. Am J Physiol Endocrinol Metab 279:1242-1248

Chou CF, Tohari S, Brenner S, Venkatesh B (2004) Erythropoietin gene from a teleost fish, *Fugu rubripes*. Blood 104:1498-1503

Chu CY, Cheng CH, Chen GD, Chen YC, Hung CC, Huang KY, Huang CJ (2007) The zebrafish erythropoietin: Functional identification and biochemical characterization. FEBS Letters 581:4265-4271

Coggeshall RE, Fawcett DW (1964) The fine structure of the central nervous system of the leech, Hirudo medicinalis. J Neurophysiol 27:229-289

Coons AH, Creech HJ, Jones RN (1945) Immunological properties of an antibody containing a fluorescent group. Proc Soc Exp Biol Med 47:200–202

Dame C, Fahnenstich H, Freitag P, Hofmann D, Abdul-Nour T, Bartmann P, Fandrey J (1998) Erythropoietin mRNA expression in human fetal and neonatal tissue. Blood 92:3218-3225

Dame C, Bartmann P, Wolber EM, Fahnenstrich H, Hofmann D, Fandrey J (2000) Erythropoietin gene expression in different areas of the developing human central nervous system. Develop Brain Res 125:69-74

Dame C, Juul SE, Christensen RD (2001) The biology of erythropoietin in the central nervous system and its neurotrophic and neuroprotective potential. Biol Neonate 79:228-235

Digicaylioglu M & Lipton SA (2001) Erythropoietin-mediated neuroprotection involves cross-talk between Jak2 and $NF_K$- B signalling cascades. Nature 412:641–647

Edenfeld G, Stork T, Klambt C (2005) Neuron-glia interaction in the insect nervous system. Curr Opin Neurobiol 15:34-39

Elliott S, Busse L, Bass MB, Lu H, Sarosi I, Sinclair AM, Spahr C, Um M, Van G, Begley CG (2006) Anti-Epo receptor antibodies do not predict Epo receptor expression. Blood 107:1892–1895 Corrigendum Blood 107:3454, 2006

Erslev A (1953) Humoral regulation of red cell production. Blood 8:349-357

Franke TF, Tartof KD, Tsichlis PN (1994) The SH2-like Akt homology (AH) domain of c-akt is present in multiple copies in the genome of vertebrate and invertebrate eucaryotes. Cloning and characterization of the Drosophila melanogaster c-akt homolog Dakt1. Oncogene 9(1):141-8

Fujita M, Takahashi R, Liang P, Saya H, Ashoori F, Tachi M, Kitazawa S, Maeda S (1997) Role of alternative splicing of the rat erythropoietin receptor gene in normal and erythroleukemia cells. Leukemia 11:444–445

Genc S, Koroglu TF, Genc K (2004) Erythropoietin and the nervous system. Brain Res 1000:19-31

Goldwasser E, Kung C KH, Eliason J (1974) On the mechanism of erythropoietin-induced differentiation; XIII. The role of sialic acid in erythropoietin action. J Biol Chem 249:4202

Goto M, Akai K, Murakami A, Hasimoto C, Tsuda E, Ueda M, Kawanishi G, Takahashi N, Ishimoto A, Chiba H, Saski R (1988) Production of recombinant erythropoietin in mammalian cells: host-cell dependency of the biological activity of the cloned glycoprotein. Bio/Technol 6:67−71

Harris KW & Winkelmann JC (1996) Enzyme-linked immunosorbent assay detects a potential soluble form of the erythropoietin receptor in human plasma. Am J Hematol 52:8–13

Hetru C, Hoffmann JA (2009) NF-kB in the Immune Response of Drosophila. Cold Spring Harb Perspect Biol doi: 10.1101/cshperspect.a000232

Hoyle G (1986) Glial cells of an insect ganglion. J Comp Neurol 246(1):85-103

Hou XS, Melnick MB, Perrimon N (1996) Marelle acts downstream of the Drosophila HOP/JAK kinase and encodes a protein similar to the mammalian STATs. Cell 84:411-419

Jacobs K, Shoemaker C, Rudersdorf R, Neill SD, Kaufman RJ, Mufson A, Seehra J, Jones SS, Hewick R, Fritsch EF, Kawakita M, Shimizu T, Miyake T (1985) Isolation and characterization of genomic cDNA clones of human erythropoietin. Nature 313:806-810

Jelkmann W (1992) Erythropoietin: structure, control of production, and function. Physiol Rev 72:449-489

Jones SS, D'andrea AD, Haines LL, Wong GG (1990) Human erythropoietin receptor: cloning, expression, and biologic characterization. Blood 76 (1):31-35

Junk AK, Mammis A, Savitz SI, Singh M, Roth S, Malhotra S, Rosenbaum PS, Cerami A, Brines M, Rosenbaum DM (2002) Erythropoietin administration protects retinal neurons from acute ischemia-reperfusion injury. Proc Natl Acad Sci USA 99:10659–10664

Juul SE, Anderson DK, Li Y, Christensen RD (1998) Erythropoietin and erythropoietin receptor in the developing human central nervous system. Pediatr Res 43:40-49

Juul SE, Yachnis AT, Rojiani AM, Christensen RD (1999) Immunohistochemical localization of erythropoietin and its receptor in the developing human brain. Pediatr Dev Pathol 2:148-158

Knabe W, Knerlich F, Washausen S, Kietzmann T, Siren AL, Brunnett G, Kuhn HJ, Ehrenreich H (2004) Expression patterns of erythropoietin and its receptor in the developing midbrain. Anat Embryol (Berl) 207:503-512

Kretzschmar D, Pflugfelder GO (2002) Glia in development, function, and neurodegeneration of the adult insect brain. Brain Res Bull 57:121-131

Krystal G, Pankratz HR, Farber NM, Smart JE (1986) Purification of human erythropoietin to homogeneity by a rapid five- step procedure. Blood 67:71-79

Kuramochi S, Ikawa Y, Todokoro K (1990) Characterization of murine erythropoietin receptor genes. J Mol Biol 216:567−575

Lewczuk P, Hasselblatt M, Kamrowski-Kruck H, Heyer A, Unzicker C, Sirén AL, Ehrenreich H (2000) Survival of hippocampal neurons in culture upon hypoxia: effect of erythropoietin. Neuroreport 11:3485-3488

Lai PH, Everett R, Wang FF, Arakawa T, Goldwasser E (1986) Structural characterization of human erythropoietin. J Biol Chem 261:3116

Laming PR, Kimelberg H, Robinson S, Salm A, Hawrylak N, Muller C, Roots B, Ng K (2000) Neuronal-glial interactions and behaviour. Neurosci Biobehav Rev 24:295-340

Li JP, D'Andrea AD, Lodish HF, Baltimore D. (1990) Activation of cell growth by binding of Friend spleen focus-forming virus gp55 glycoprotein to the erythropoietin receptor. Nature 343(6260):762–764

Li X, Gonias S L, Campana WM (2005) Schwann cells express erythropoietin receptor and represent a major target for Epo in peripheral nerve injury. Glia 51:254–265

Liu ZY, Chin K, Noguchi CT (1994) Tissue specific expression of human erythropoietin receptor in transgenic mice. Develop Biol 166:159-169

Lukowsky WA, Painter RH (1972) Studies on the role of sialic acid in the physical and biological properties of erythropoietin. Can J Biochem 50:909-917

Marti HH, Wenger RH, Rivas LA, Straumann U, Digicaylioglu M, Henn V, Yonekawa Y, Bauer C, Gassmann M (1996) Erythropoietin gene expression in human, monkey and murine brain. Eur J Neurosci 8:666-676

Marti HH, Gassmann M, Wenger RH, Kvietikova I, Morganti-Kossmann MC, Kossmann T, Trentz O, Bauer C (1997) Detection of erythropoietin in human liquor: intrinsic erythropoietin production in the brain. Kidney Int 51:416-418

Marti HH (2004) Erythropoietin and the hypoxic brain. J Exp Biol 207:3233-3242

Martínez-Estrada OM, Rodriguez-Millan E, Vicente EG, Reina M, Vilaro S, Fabre M (2003) Erythropoietin protects the *in vitro* blood-brain barrier against VEGF-induced permeability. Eur J Neurosci 18:2538–2544

Masuda S, Nagao M, Takahata K, Konishi Y, Gallyas F, Tabira T, Sasaki R (1993) Functional erythropoietin receptor of the cells with neural characteristics. Comparison with receptor properties of erythroid cells. J Biol Chem 268:11208-11216

Masuda S, Okano M, Yamagishi K, Nagao M, Ueda M, Sasaki R (1994) A novel site of erythropoietin production. Oxygen-dependent production in cultured rat astrocytes. J Biol Chem 269:19488-19493

Masuda S, Chikuma M, Sasaki R (1997) Insulin-like growth factors and insulin stimulate erythropoietin production in primary cultured astrocytes. Brain Res 46:63-70

Migliaccio AR, Migliaccio G, D'Andrea A, Baiocchi M, Crotta S, Nicolis S, Ottolenghi S, Adamson JW. (1991) Response to erythropoietin in erythroid subclones of the factor-dependent cell line 32D is determined by translocation of the erythropoietin receptor to the cell surface. Proc Natl Acad Sci USA 88:11086−11090.

Miura O, Cleveland JL, Ihle JN (1993) Inactivation of erythropoietin receptor function by point mutations in a region having homology with other cytokine receptors. Mol Cell Biol.13(3):1788-1795

Miura O, D`Andrea AD, Kabat D, Ihle JN (1991) Induction of tyrosine phosphorylation by the erythropoietin receptor correlates with mitogenesis. Mol Cell Biol 11:4895-4902

Miyake T, Kung C, Goldwasser E (1977) Purification of human erythropoietin. J Biol Chem 252:5558−5564

Morishita E, Masuda S, Nagao M, Yasuda Y, Sasaki R (1997) Erythropoietin receptor is expressed in rat hippocampal and cerebral cortical neurons and erythropoietin prevents *in vitro* glutamate-induced neuronal death. Neuroscience 76:105-116.

Nagai A, Nakagawa E, Choi HB, Hatori K, Kobayashi S, Kim SU (2001) Erythropoietin and Erythropoietin receptors in human CNS neurons, astrocytes, microglia, and oligodendrocytes grown in culture. J Neuropathol Exp Neurol 60:386-392

Nagao M, Masuda S, Abe S, Ueda M, Sasaki R (1992) Production and ligand-binding characteristics of the soluble form of murine erythropoietin receptor. Biochem Biophys Res Commun 188:888−897

Nicholls JG, Van Essen D (1974) The nervous system of the leech. Scientific American 230: 38-48

Onteniente B, Kimura H, Maeda T (1983) Comparative study of the glial fibrillary acidic protein in vertebrates by PAP immunohistochemistry. J Comp Neurol 215:427–436

Quelle DE, Quelle FW, Wojchowski DM (1992) Mutations in the WSAWSE and cytosolic domains of the erythropoietin receptor affect signal transduction and ligand binding and internalization. Mol Cell Biol 12:4553–4561

Quelle FW, Wojchowski DM (1991) Proliferative action of erythropoietin is associated with rapid protein tyrosine phosphorylation in responsive B6SUt.EP cells. J Biol Chem 266:609-14

Paffett-Lugassy N, Hsia N, Fraenkel PG, Paw B, Leshinsky I, Barut B, Bahary N, Caro J, Handin R, Zon LI (2009) Epo-EpoR signaling not required for cardiovascular or neural development. Blood 110:2718-2726

Paffett-Lugassy N, Hsia N, Fraenkel PG, Paw B, Leshinsky I, Bahary BBN, Caro J, Handin R, Zon LI (2007) Functional conservation of erythropoietin signaling in zebrafish. Blood 110:2718-2726

Ratajczak J, Majka M, Kijowski J, Baj M, Pan ZK, Marquez LA, Janowska-Wieczorek A, Ratajczak MZ (2001) Biological significance of MAPK, AKT and JAK-STAT protein activation by various erythropoietic factors in normal human early erythroid cells. Br J Haematol 115:195-204

Sasaki H, Bothner B, Dell A, Fukuda M (1987) Carbohydrate structure of erythropoietin expressed in Chinese hamster ovary cells by a human erythropoietin cDNA. J Biol Chem 262:12059-12076

Semenza GL (1994) Regulation of erythropoietin production. New insights into molecular mechanisms of oxygen homeostasis. Hematol Oncol Clin North Am 8: 863-84

Shoemaker CB, Mitsock LD (1986) Murine erythropoietin gene: cloning, expression, and human gene homology. Mol Cell Biol 6:849–858

Sirén AL, Knerlich F, Poser W, Gleiter CH, Brück W, Ehrenreich H (2001) Erythropoietin and erythropietin receptor in human ischemic/hypoxic brain. Acta Neuropathol 1001:271-276

Soliz J, Gassmann M, Joseph V (2007) Soluble erythropoietin receptor is present in the mouse brain and is required for the ventilatory acclimatization to hypoxia. J Physiol 583:329–336

Spandou E, Papoutsopoulou S, Soubasi V, Karkavelas GCS, Kremenopoulos G, Guiba-Tziampiri O (2004) Hypoxia-ischemia affects erythropoietin and erythropoietin receptor expression pattern in the neonatal rat brain. Brain Res 102:167–172

Sugawa M, Sakurai Y, Ishikawa-Ieda Y, Suzuki H, Asou H (2002) Effects of erythropoietin on glial cell development; oligodendrocyte maturation and astrocytes proliferation. Neurosci Res 44:391-403

Sun Y, Zhou C, Polk P, Nanda A, Zhang JH (2004) Mechanisms of Erythropoietin induced Brain Protection in Neonatal Hypoxia-Ischemia Rat Model. J Cereb Blood Flow Metab 24:259–270

Takeuchi M, Takasaki S, Shimada M, Kobata A (1990) Role of sugar chains in the in vitro biological activity of human erythropoietin produced in recombinant Chinese hamster ovary cells. J Biol Chem 265:12127-12130

Tan C, Eckardt KU, Firth JD, Ratcliffe PJ (1992) Feedback modulation of renal and hepatic erythropoietin mRNA in response to graded anemia and hypoxia. Am J Physiol Renal Physiol 263:F474-F481

Towbin H, Staehelin T, Gordon J. (1979) Electrophoretic transfer of proteins from polyacrylamide gels to nitrocellulose sheets: procedure and some applications. Proc Natl Acad Sci USA 76(9):4350-4

Tsuda E, Kawanishi G, Ueda M, Masuda S, Sasaki R (1990) The role of carbohydrate in recombinant human erythropoietin. Eur J Biochem 188:405-411

Villegas SN, Poletta FA, Carri NG (2003) GLIA: A reassessment based on novel data on the developing and mature central nervous system. Cell Biol Int 27:599-609

Weber A, Maier R F, Hoffmann U, Grips M, Hoppenz M, Aktas AG, Heinemann U, Obladen M, Schuchmann S (2002) Erythropoietin improves synaptic transmission during and following ischemia in rat hippocampal slice cultures. Brain Res 958:305-311.

Westphal G, Braun K, Debus J (2002) Detection and quantification of the soluble form of the human erythropoietin receptor (sEpoR) in the growth medium of tumor cell lines and in the plasma of blood samples. Clin Exp Med 2:45–52

Yamaji R, Okada T, Moriya M, Naito M, Tsuruo T, Miyatake K, Nakano Y (1996) Brain capillary endothelial cells eypress two forms of erythropoietin receptor mRNA. Eur J Biochem 239:494-500

Yan R, Small S, Desplan C, Dearolf CR, Darnell JE (1996) Identification of a Stat gene that functions in Drosophila development. Cell 84:421-430

Yanagawa S, Hirade K, Ohnota H, Sasaki R, Chiba H, Ueda M, Goto M (1984) Isolation of human erythropoietin with monoclonal antibodies. J Biol Chem 59:2707-2710

Yasuda Y, Nagao M, Okano M, Masuda S, Sasaki R, Konishi H, Tanimura T (1993) Localization of erythropoietin and erythropoietin-receptor in postimplantation mouse embryos. Develop Growth & Differ 35:711-722

Yoshimura A, D'Andrea AD, Lodish HF (1990) Friend spleen focus-forming virus glycoprotein gp55 interacts with the erythropoietin receptor in the endoplasmic reticulum and affects receptor metabolism. Proc Nati Acad Sci USA 87:4139-4143

Yu X, Lin CS, Costantini F, Noguchi CT (2001) The human erythropoietin receptor gene rescues erythropoiesis and developmental defects in the erythropoietin receptor null mouse. Blood 98:475-477

Yu X, Shacka JJ, Eells JB, Suaret-Quian C, Przygodzki RM, Beleslin-Cokic B, Lin CS, Nikodem VM, Hempstead B, Flanders KC, Constantini F, Noguchi CT (2002) Erythropoietin receptor signalling is required for normal brain development. Develop 129:505-516

Zanjani ED, Poster J, Burlington H, Mann LI, Wasserman LR (1977) Liver as the site of Epo formation in the fetus. J Lab Clin Med 89:640-64

# 3 The effect of erythropoietin on the regeneration of auditory receptor fibres in the grasshopper Chorthippus biguttulus

## 3.1 Introduction

Erythropoietin (EPO) is a hematopoietic cytokine with multiple functions that are not exclusively related to erythropoiesis (red cell production) (Jelkmann 1992). EPO has also been detected in the nervous system of vertebrates. Astrocytes (Masuda et al. 1994, 1997; Marti 1996) and to a lesser extend also neurons (Morishita et al. 1997; Bernaudin et al. 1999, 2000) have been identified as central nervous production sites for EPO. In mammals, EPO exerts its biological functions in the CNS via a 66kDa cell-surface receptor (EPOR), which is present on both glial cells and neurons in the cerebral cortex, midbrain and hippocampus (Anagnostou et al. 1994; Digicaylioglu et al. 1995; Yamaji et al. 1996; Morishita et al. 1997; Bernaudin et al. 1999, 2000; Sirén et al. 2001; Sugawa et al. 2002). EPO and EPOR serve important functions during mammalian neurodevelopment and expression patterns of both the ligand and the receptor change characteristically during brain development (Juul et al. 1999; Sirén et al. 2001; Yu et al. 2001, 2002). While EPO and EPOR are only weakly expressed in normal adult brains, a variety of stress factors including hypoxia can induce their enhanced expression via accumulation of the transcription factor hypoxia-inducible factor-1 (HIF-1) (Tan et al. 1992; Masuda et al. 1993; Bernaudin et al. 2000; Lewczuk et al. 2000).

Several *in vitro* and *in vivo* studies demonstrated a neuroprotective function of exogenous EPO during episodes of ischemic, hypoxic, metabolic, neurotoxic and excitotoxic stress (for review see Dame et al. 2001; Buemi et al. 2002; Genc et al. 2004; Marti 2004; Arcasoy 2008). Unlike its neuroprotective function, the potential neuroregenerative effect of EPO on metabolically and/or anatomically compromised nervous cells has not been studied in detail. Some studies indicated an increase of neurite outgrowth rates in rat retinal ganglion cells *in vitro* after EPO treatment (Böcker-Meffert et al. 2002; Kretz et al. 2005; Zhong et al. 2007). In addition, an *in vivo* experimental study by King et al. (2007) revealed that EPO promotes axon regeneration after intraorbital optic nerve transection of adult rats. Recently Berkingali et al. (2008) analysed the neuroprotective and neuroregenerative effects of EPO on spiral ganglion cells (SGC) from isolated cochleae of neonatal rats. While EPO had no effect on the survival of cultivated SGCs, elongation of regenerated neurites was significantly enhanced following EPO treatment. This suggests that EPO rather promotes the regeneration of neurites than supports neuronal survival of rat SGCs, at least under *in vitro* conditions.

After axotomy or crush injury of vertebrate peripheral nerves the distal parts of axons including this nerve undergo Wallerian degeneration, whereas the proximal stump begins to regenerate (Chen et al. 2007). Wallerian degeneration leads to the removal and recycling of axonal- and myelin-derived fragments and generates a permissive environment for axonal regeneration (Waller 1850). The regulatory signals that initiate the regeneration of proximal axonal endings have not been fully understood, but the activated intrinsic growth capacity of the neuronal cell body, in combination with the local permissive environment and axon guidance cues (e.g. extracellular matrix proteins and cell adhesion molecules) permit a successful regeneration of injured axonal projections in the peripheral nervous system (PNS) of vertebrates. Regrowing nerve fibres also require remyelination, otherwise signal conduction in regenerated axons will be insufficient for the reestablishment of previous functions (Höorste et al. 2006). After injury, Schwann cells dedifferentiate and proliferate. They form ´Bünger bands` to guide axonal regrowth and start to remyelinate axons after cell contact (Fawcett & Keynes 1990). Campana & Myers (2001) showed that EPO and its receptor are also expressed in axons and Schwann cells of the PNS of rats, and crushing of the sciatic nerves leads to enhanced expression of both proteins (Li et al. 2005). Application of EPO to injured sciatic nerve stimulates Schwann cell proliferation and reduces the expression of tumor necrosis factor alpha (TNF-α) in Schwann cells (Campana et al. 2006). In addition, EPO protects cultured Schwann cells from TNF-α-mediated cell death (Campana et al. 2006). These results indicate that EPO may facilitate peripheral nerve regeneration in mammals by increasing Schwann cell proliferation and decreasing TNF-α-mediated injury or lethal effects.

So far, potential neuroregenerative effects of EPO have exclusively been studied in mammals or mammalian *in vitro* preparations. But EPO and EPOR protein expression was also detected in the CNS of teleost fishes (Chou et al. 2004; Chu et al. 2007; Paffett-Lugassy et al. 2007) and in various invertebrate species of different phyla (see chapter 2 of this doctoral thesis). The neuroprotective and neurotrophic functions of EPO and EPOR in the mammalian CNS may therefore be mediated by ancient conserved mechanisms that predate the evolution of mammals. Thus, the purpose of this project was to analyse whether EPO also promotes the regeneration of injured nerves in insects. Similar to mammals, distal parts of insect sensory nerve fibres degenerate after nerve crush injury and their proximal parts regrow into the CNS (Murphey et al. 1981, 1984; Chiba et al. 1988; Pallas & Hoy 1988; Kalmring 1991). As documented by various studies in different insect species, regenerating sensory axons can target their original neuropils and re-establish functional synaptic connections with appropriate interneurons (Chiba et al. 1988; Chiba & Murphey 1991). Regeneration experiments in the auditory system of grasshoppers (*Locusta migratoria*, *Schistocerca gregaria* and *Chorthippus biguttulus*) revealed that tympanal receptor fibres regenerate their central projections and synaptic contacts after nerve crush (Lakes & Kalmring 1991; Lakes-Harlan & Pfahlert 1995; Jacobs & Lakes-Harlan 1999). In grasshoppers of the species *Ch. biguttulus* functional regeneration of the auditory system can be monitored by a simple behavioural test. *Chorthippus biguttulus* males perform stereotyped turning reactions towards the direction of singing conspecific females (von

Helversen & von Helversen 1983). Sound localisation depends on the comparison of binaural auditory input resulting from stimulation of the right and left tympanal organs. This comparison and therefore localisation of the sound source is mainly based on intensity differences at both ears. Deafening of one ear by crushing auditory receptor axons causes turning behaviour to the intact side only, even when female songs are presented to the injured side. With the regeneration of auditory receptor fibre central projections, male grasshoppers regain the capability of sound localisation and perform correct turns towards the direction of sound sources (Lakes-Harlan & Pfahlert 1995).

The experiments described in the following use the established ´tympanal nerve crush` preparation in the acoustically communicating grasshopper *Ch. biguttulus*. The aim of this study was to investigate whether crushing of an insect peripheral nerve alters the expression of EPO and EPOR and whether application of EPO promotes the anatomical and functional regeneration of axotomised auditory receptor fibres.

# 3.2 Material and Methods

Unless otherwise mentioned, all chemicals were either purchased from Sigma-Aldrich (Steinheim, Germany) or Merck (Darmstadt, Germany).

### 3.2.1 Animals

Behavioural experiments and anatomical studies were performed with adult male grasshoppers of the species *Chorthippus biguttulus*. Grasshoppers used in the experiments were either caught in the vicinity of Göttingen (during summer) or reared from eggs collected from grasshoppers caught in the previous season.

### 3.2.2 Crushing of the leg nerve N5

The grasshoppers were cooled to 5℃ and fixed with plasticine (Pelikan Nakiplast, Hannover, Germany) and elastic strap to a cooled block of iron. The sternal cuticle of the third thoracic segment was opened and the leg nerve N5 was crushed distal to the ganglion with conventional forceps. After finishing the operation, the excised piece of cuticle was replaced and the wound sealed with wax. Inability of the grasshopper to move the leg that was innervated by the crushed nerve indicated a successful transection of motor axons.

### 3.2.3 Anti-*ia*EPO and anti-*ia*EPOR immunohistochemistry

The central nervous systems of grasshoppers were dissected 24h after crushing the leg nerve N5 (sham operated animals were used for control) and fixed with 4% paraformaldehyde + 7.5% picric acid dissolved in phosphate buffer (PB) for 2h at room temperature (RT). Afterwards, the tissue was dehydrated through an ethanol series, embedded in paraffin and serially cut with a microtome (Reichert-Jung 1130 Biocut, Nußloch, Germany) into 8µm sections. After rehydration and washing several times with PBS-1%Triton, the slices were incubated with blocking buffer (5% rabbit serum for EPO and goat serum for EPOR; 3% BSA in PBS-1%Triton) for 2h at RT. The first antibody (goat anti-EPO or rabbit anti-EPOR; Santa Cruz Biotechnology, Heidelberg, Germany) was dissolved in blocking buffer at a dilution of 1:75 and applied to the sections over night at RT. After three washes with PBS-1%Triton the biotinylated secondary antibody (rabbit α-goat for EPO; goat α-rabbit for EPOR) was added at a dilution of 1:300 for 2h at RT. To visualise the immunoreactivity the sections were washed three times and subsequently incubated with a Cy3-coupled streptavidin (Rockland Immunochemicals, Gilbertsville, USA) at a dilution of 1:400 for 2h at RT. For nuclear staining, tissue sections were incubated for 30 minutes at RT with 100µg/ml 4´-6-diamino-2-phenylindole (DAPI) dissolved in PBS. Finally, the slices were dehydrated in alcohol, cleared in xylene and embedded in Entellan. Immunoreactivity was analysed with a conventional fluorescence microscope (Zeiss Axioskop, Jena, Germany)

equipped with a Spot CCD camera (Invisitron, Sterling Heights, USA). All figures were generated using Adobe Photoshop 7.0.

### 3.2.4 Crushing of the tympanal nerve N6

Adult males of *Ch. biguttulus* were isolated from females for three days. Prior to the operation, their reproductive motivation and their ability to correctly localise a sound source was determined in a behavioural experiment (see below). Grasshoppers that displayed normal behaviour were cooled down to 5℃ and fixed with plasticine and elastic strap to a cooled block of iron. A small window was cut with a piece of razor blade into the ventral cuticle of the third thoracic segment. The tympanal nerve N6 of one side was crushed using very fine forceps. Half of the animals received a single treatment of rhEPO (10µl of 400U/ml) that was directly applied to the haemolymph via the opened thorax. Control animals received a single treatment of 10µl saline. After finishing the operation the excised piece of cuticle was replaced and fixed with wax. In order to confirm the successful transection of auditory receptor fibres, the turning response of operated grasshoppers was determined one day after the operation. Males that made correct turns when female song was presented to the side with the crushed tympanal nerve were excluded from the experiment.

### 3.2.5 Behavioural experiment

Male *Ch. biguttulus* were marked individually by dots of acrylic colours and behavioural tests were performed daily in a sound proof room with a constant temperature of 26-28℃. Animals were transferred to a testing arena equipped with a rotable plate, a white heating light and a loudspeaker placed approximately 15cm away from the plate. After an adjustment period of five minutes, males were acoustically stimulated with the recording of a female song that was played back from a portable CD player. The position of the male was repeatedly adjusted with respect to the position of the loudspeaker to enable lateral presentations of the acoustic stimulus to the intact and the operated side. Turning reactions following ten stimulus presentations to the injured side and ten presentations to the intact side were observed for each male on each of 20 consecutive experimental days. If males generated a response song without turning toward or away from the speaker the reaction was counted as ´no turning behaviour`.

### 3.2.6 Neuroanatomy of the tympanal nerve N6

Central projections of the tympanal nerve N6 into the metathoracic ganglion were labelled by neurobiotin-backfills. Grasshoppers were opened dorsally and the tympanal nerve N6 was cut distal to the ganglion using a pair of fine scissors. The cut end was placed into the tip of a glass microelectrode filled with neurobiotin solution (5% neurobiotin dissolved in aqua dest.) and the preparation was stored in a humid chamber for 12-24h at 4℃. Afterwards the thoracic ganglia were dissected and fixed with 4% paraformaldehyde dissolved in PB for 2h at RT. To permeabilise the tissue, the preparations were dehydrated through an ethanol series and immersed in xylene for five minutes. After rehydration the tissue was treated with collagenase and hyaluronidase (1mg/ml respectively) for 1h at 37℃. After several washes

with phosphate buffer and PBS-0.5% Triton X-100 a Cy3-coupled streptavidin (1:400, Rockland Immunochemicals, Gilbertsville, USA) was added over night at 4℃. The tissue was again dehydrated in alcohol and cleared in methyl salicylate. Fluorescence of labelled structures was analysed as described above.

# 3.3 Results

### 3.3.1 Expression of *ia*EPO and *ia*EPOR in the CNS of *Ch. biguttulus* after crushing the leg nerve N5

Nerve crush injuries in the peripheral nervous system of mammals change the expression pattern of EPO and EPOR both in glial and neuronal cells (Campana & Myers 2001; Li et al. 2005; Toth et al. 2008). The activation of the EPO/EPOR signalling pathway results in an induction of mechanisms that support the injured tissue to survive and regenerate. In this study on the nervous system of the grasshopper *Ch. biguttulus* potential injury-induced changes of *ia*EPO and *ia*EPOR expression were investigated before and after crushing the leg nerve N5.

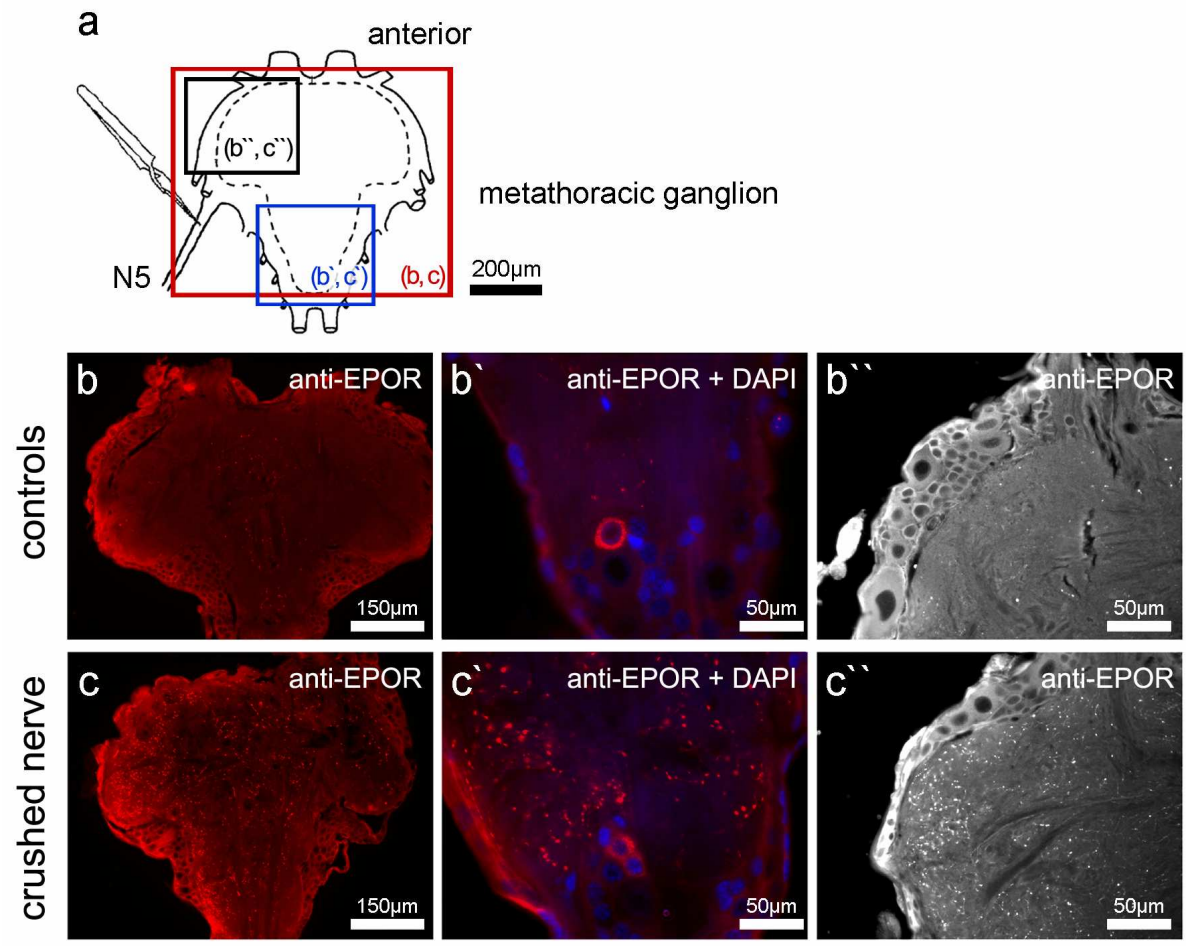


**Figure 1:** Induction of *ia*EPOR expression in the metathoracic ganglion of *Ch. biguttulus* after crushing the leg nerve N5. **a:** schematic drawing of the metathoracic ganglion, the crushed leg nerve N5 and picture frames shown in b-c``. **b-b``:** Horizontal sections of the metathoracic ganglion of sham operated control animals labelled with anti-EPOR serum. **c-c``:** Horizontal sections of the metathoracic ganglion labelled with anti-EPOR serum 24 hours after crushing N5.

The central nervous system of grasshoppers consists of a brain and a set of segmental ganglia, which form the ventral nerve cord. The leg nerve N5 is the thickest nerve that leaves

the metathoracic ganglion laterally and projects into the hindleg of the animal. After 24h following the crushing procedure of the leg nerve, the metathoracic ganglion was labelled with antibodies against EPO and EPOR. Since the antibodies against EPO and EPOR were raised against mammalian proteins, the immunologically labelled proteins in the invertebrate CNS will be termed as *invertebrate analogs* of EPO and EPOR (*ia*EPO and *ia*EPOR).

The immunoreactivity of *ia*EPO in the metathoracic ganglion of the grasshopper *Ch. biguttulus* was not changed 24 hours after crushing the leg nerve N5 (data not shown). In contrast, increased *ia*EPOR immunoreactivity in the metathoracic ganglion was detected (Figure 1). Sham operated animals (marked as ´controls`) contained low *ia*EPOR immunoreactivity within neuropil regions of the metathoracic ganglion (Figure 1b, b``). Only few cells with morphological characteristics of neurons showed intensive cytoplasmic staining (Figure 1b`). Nerve crush increased *ia*EPOR immunoreactivity in all neuropil regions of the metathoracic ganglion (Figure 1c, c``), but no particular labelling was detected inside the crushed nerve itself or in cell bodies of neurons (e.g. motor neurons) that are known to project into the leg nerve. The number of *ia*EPOR-immunopositive somata in the metathoracic ganglion was not increased following nerve crush and there was no evidence that glial cells expressed *ia*EPOR-related immunoreactivity.

### 3.3.2 Human recombinant EPO promotes regeneration of auditory receptor fibres and acoustic orientation in grasshoppers

Various *in vitro* studies revealed a potential regenerative effect of exogenous EPO on the regrowth of axons after nerve crush injury in mammals (Böcker-Meffert et al. 2002; Kretz et al. 2005; Zhong et al. 2007).

The auditory system of the grasshopper *Chorthippus biguttulus* comprises a pair of tympanal organs, that are laterally located in the first abdominal segment (Figure 2a). A tympanal organ consists of a membrane (tympanum) that oscillates in response to acoustic stimulation. These vibrations are detected by auditory receptor neurons located in the Müller´s organ at the inner side of the tympanum (Figure 2b). The auditory receptor cells project through the tympanal nerve N6 into the metathoracic ganglion and arborise in two prominent neuropils, the frontal and caudal auditory neuropil (Figure 2b). Within the two auditory neuropils, the receptor cells contact local and ascending interneurons that process auditory information and relay it to higher auditory neuropils in the brain. The projections of the auditory receptor neurons in the metathoracic ganglion were visualised by backfilling the tympanal nerve with the neuronal tracer neurobiotin (Figure 2c).

If crushed tympanal nerves are backfilled from the periphery (near Müller`s organ) diffusion of the tracer stops at the site of injury (Figure 2d; white arrowhead) suggesting that all axonal connections to the central nervous system have been transected. As a consequence, transmission of auditory information must be impaired and the grasshopper is deaf on the operated side.

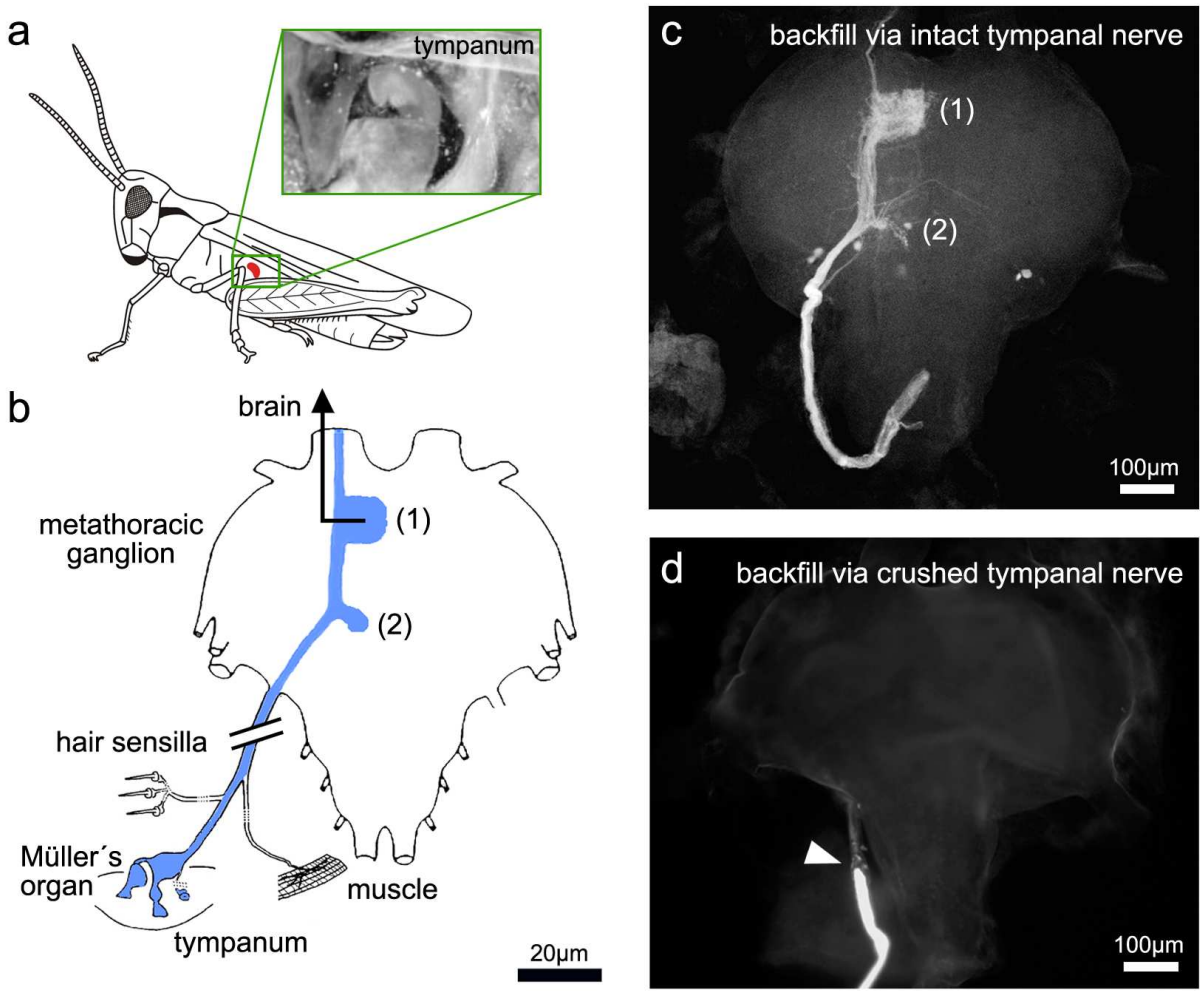


**Figure 2:** Auditory system of the grasshopper *Ch. biguttulus.* **a:** Schematic drawing of *Ch. biguttulus* and the location of the tympanum (coloured in red). The photograph shows a detailed view of the tympanum. **b:** Schematic drawing of the acoustic organ with its central projections into the metathoracic ganglion (coloured in blue). (1) frontal auditory neuropil; (2) caudal auditory neuropil **c:** Backfill of the tympanal nerve. Fluorescence indicates the central projections of the auditory receptor fibres into the frontal (1) and caudal (2) auditory neuropil. **d:** Backfill of a crushed tympanal nerve. All projections of the auditory receptor fibres to the CNS are interrupted.

After nerve crush injury the distal parts of the axons degenerate. Degeneration processes involve disintegration of the axonal skeleton and loss of coherent membranes. Metathoracic tracts that formerly contained the auditory receptor fibre projections appear as granular autofluorescent structures. Figure 3 presents a whole mount preparation of a metathoracic ganglion 3 days after tympanal nerve crush, in which the green fluorescent structures (excitation with 496nm) indicate the previous projections of auditory receptor axons. Whether this autofluorescent material represents debris from degenerating axons or results from some regeneration-related process is not known. The white arrowhead in Figure 3a marks the location of the former frontal auditory neuropil, whose degradation seems to be almost completed. In contrast, the degradation process of injured axons situated closer to the crushed side is still in progress.

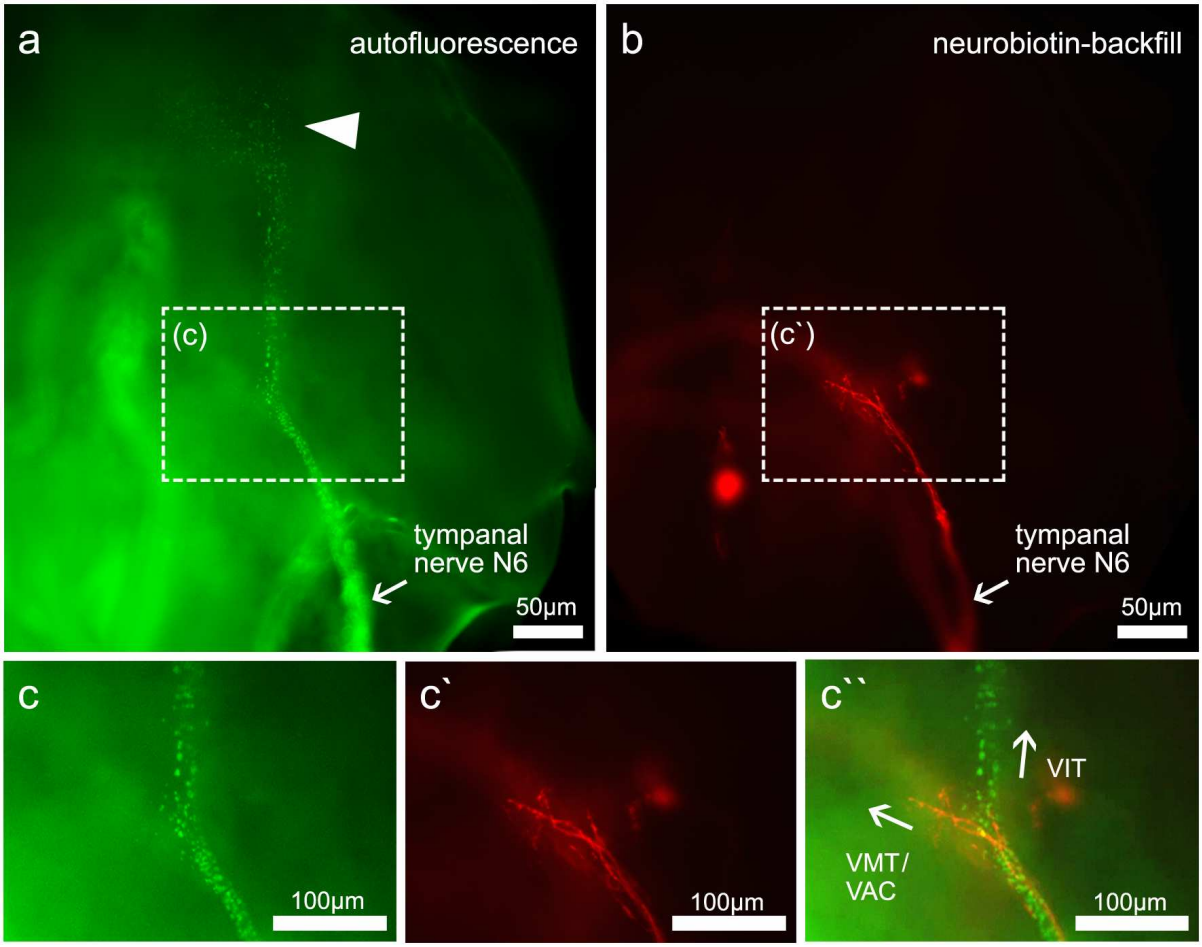


**Figure 3:** Autofluorescence (excitation: 496nm) and neurobiotin-backfill in the metathoracic ganglion of *Ch. biguttulus* 3 days after tympanal nerve crush. The dashed lines in a-b mark regions that are presented at higher magnification in c-c``. **a:** Autofluorescence most likely indicates degeneration products of the distal parts of the crushed auditory receptor axons. White arrowhead marks the former frontal auditory neuropil. **b:** Neurobiotin-backfill of regenerating auditory nerve fibres. **c-c``:** Detailed view of the region were axons of different types separate into different tracts. The overlay in c`` indicates that regenerated axons either regrow into the primary auditory neuropil along the original pathways of the formerly intact axons through the ventral intermediate tract (VIT) or, differently from their original pathway, through the ventral median tract (VMT) and anterior ventral association centre (VAC).

While the distal parts of peripheral axons in the metathoracic ganglion degenerate, the proximal parts, that retain their connections with the cell bodies in the auditory receptor organ, regenerate axonal projections from the side of the crush towards the central nervous system. This process has previously been described by Lakes-Harlan & Pfahlert (1995). Three days after tympanal nerve crush a neurobiotin-backfill of the nerve labelled regenerating fibres that had already reached the metathoracic ganglion (Figure 3b). All regenerating axons, in this and other preparations, entered the metathoracic ganglion via the tympanal nerve N6 (Figure 3a-b, white arrow). Within the CNS the pathways of regenerating auditory receptor axons could deviate from the pathway in the previously intact system. In intact animals all axons of auditory receptors project through the ventral intermediate tract (VIT) to reach the frontal auditory neuropil. Consequently, degeneration products of auditory receptor fibres were only detected within the VIT (Figure 3c``). Regenerating nerve fibres

regrew into the frontal neuropil through their original pathway (the VIT tract) or through the ventral median tract (VMT) and the anterior ventral association centre (VAC) (Figure 3c``; Figure 4a`, b`).

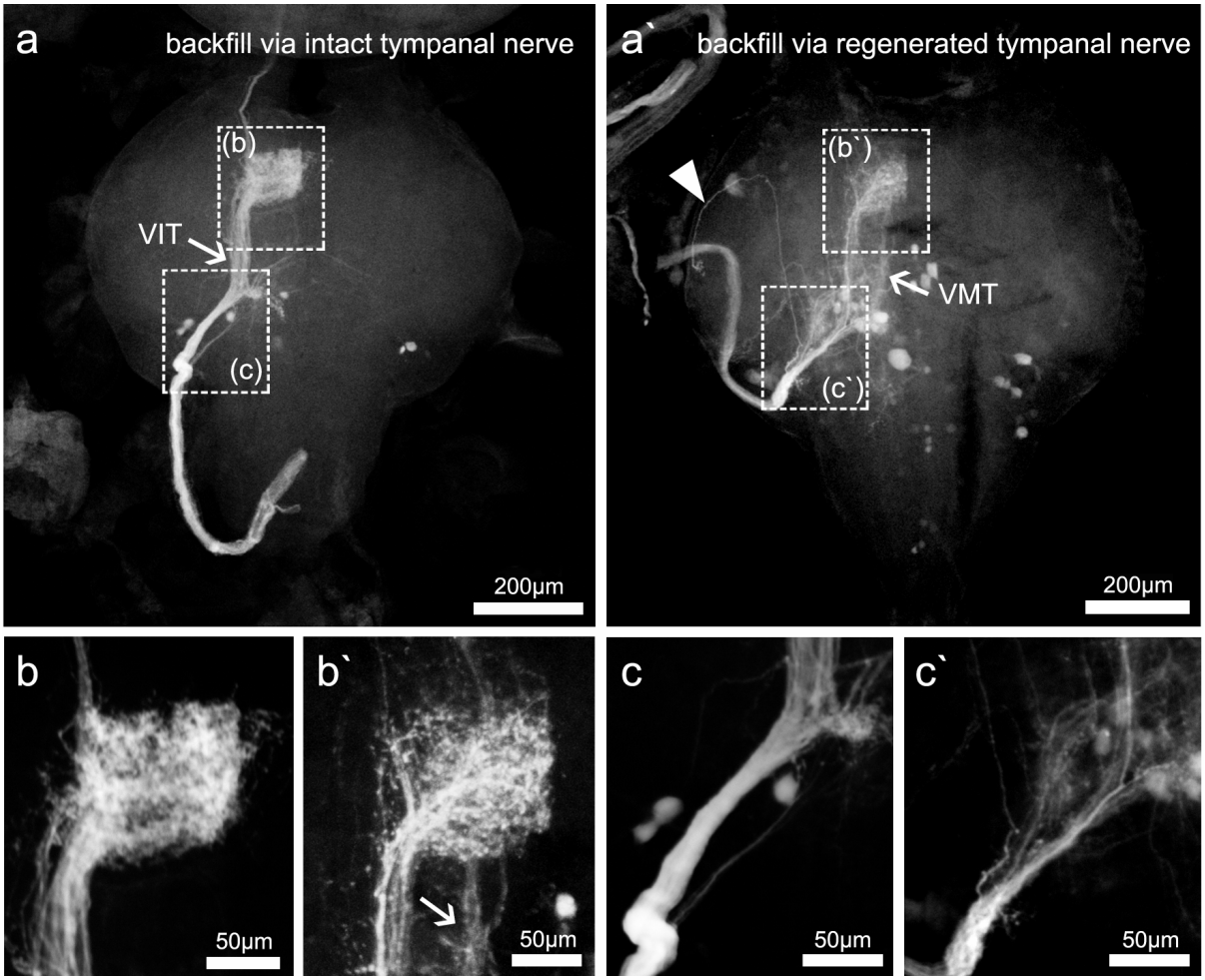


**Figure 4:** Central projections of auditory receptor neurons in an intact control animal (a, b and c) and 20 days after tympanal nerve crush (a`, b` and c`). **a, a`:** Overview of the metathoracic ganglion. The dashed lines in a-a` mark regions that were presented at a higher magnification in b-b` and c-c`. In the intact system, all receptor fibres reach the frontal auditory neuropil via projections through the ventral intermediate tract (VIT; arrow in a). In the regenerated system, some axons reach the frontal auditory neuropil via the ventral median tract (VMT; arrow in a`) and the anterior ventral association centre. Occasionally, fibres project into different neuropils, not related to the processing of auditory information (arrowhead in a`). **b, b`:** Detailed view of the frontal neuropil. The white arrow in b` marks regenerated fibres that project through the ventral median tract and the anterior ventral association centre. **c, c`:** Detailed view of the tympanal nerve basis.

Comparison of backfilled tympanal nerves of control animals and operated animals after 20 days of regeneration suggested that not all transected auditory receptor axons successfully regenerated their central nervous projections and reached their correct destination in the frontal auditory neuropil. Observations at the basis of the tympanal nerve indicated, that the number of regenerated auditory receptor axons was lower than their number in intact preparations (Figure 4c-c`). In addition, the density of terminal arborisations of auditory receptor cells in the frontal auditory neuropil is lower in operated animals than in the control animals (Figure 4b-b`). Although partially using a different pathway within the metathoracic ganglion, the majority of all regenerating tympanal receptor axons that reached

the ganglion also innervated the correct target neuropil (Figure 4a`, b`). As an example, the preparation showed in Figure 4a` contained only one axon that terminated in a far lateral region of the metathoracic ganglion.

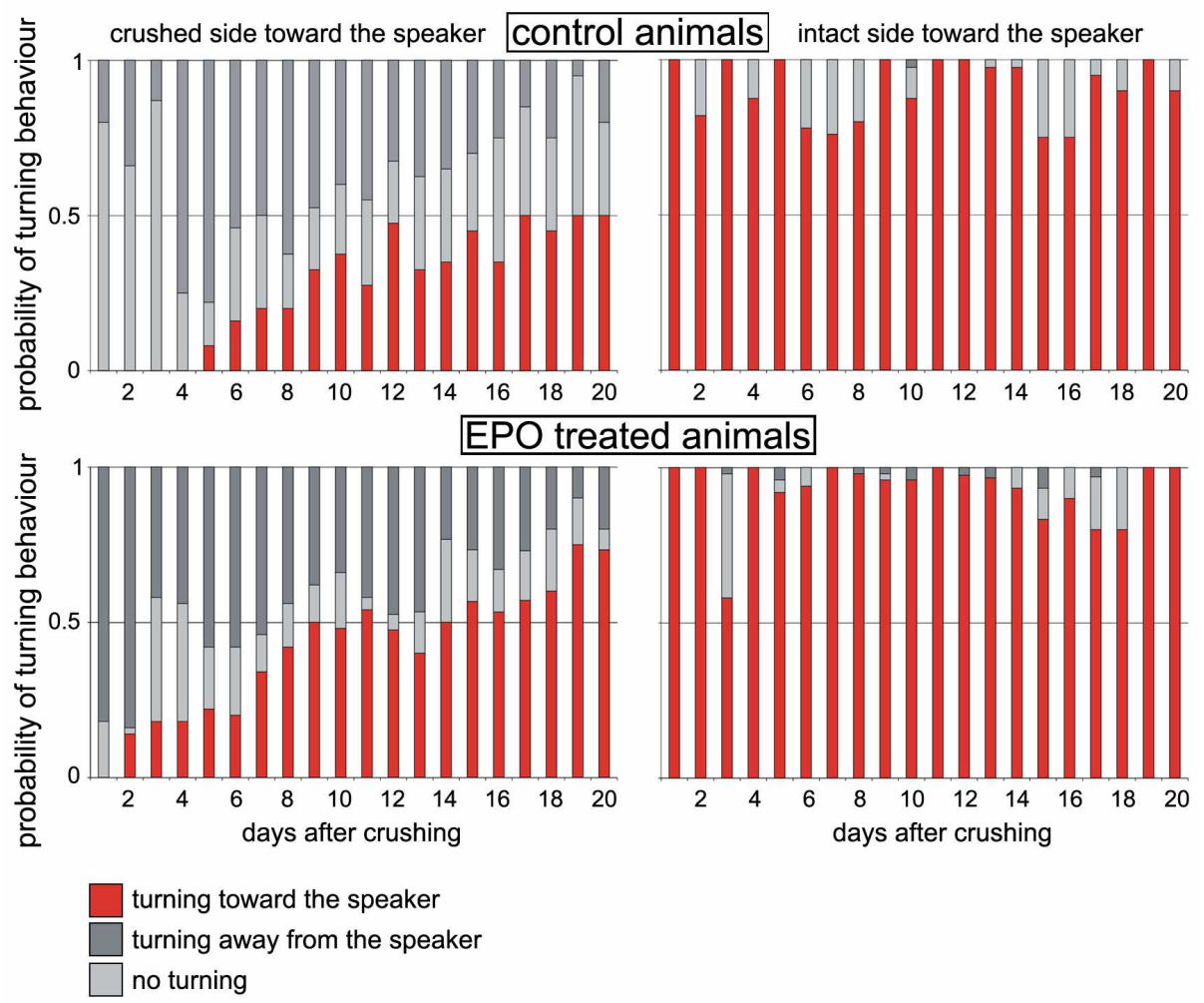


**Figure 5:** Functional regeneration of sound localisation after tympanal nerve crush. Male *Ch. biguttulus* were stimulated with a female song from a laterally placed loudspeaker. On each of 20 consecutive days, each male received 10 stimuli to the operated and 10 stimuli to the intact side. **upper part:** Turning behaviour of non-treated control animals (n=5). **lower part:** Turning behaviour of EPO-treated animals (n=5).

The functional regeneration of the grasshopper auditory system after tympanal nerve crush was determined in a behavioural test. *Chorthippus biguttulus* males perform stereotyped turning reactions toward the direction of singing conspecific females. Sound localisation depends on comparison of binaural auditory input resulting from stimulation of the two tympanal organs. Crushing one tympanal nerve impairs correct sound localisation due to the interruption of the axons of auditory receptor neurons. Monoaural deafness does not impair recognition of the female grasshopper sound pattern since male grasshoppers perform correct turns, when the stimulus is presented to the intact side and also turns to the intact side when the stimulus is presented to the side with the crushed nerve (Figure 5, upper part). With time, correct sound localisation regenerates. After 20 days of regeneration, male

grasshoppers respond with correct turns to approximately 50% of stimulus presentations to the regenerated side (Figure 5, upper part left). In order to investigate whether EPO may promote the functional regeneration of sound localisation following tympanal nerve crush, five EPO-treated male grasshoppers were compared with five control males that received saline instead (Figure 5). EPO-treated and control males were stimulated with female songs via loud speakers to initiate the typical turning reactions. When the signal was presented to the intact side all animals localised the sound source correctly (correct turns: control 91%, EPO 93%; Figure 5, right). In contrast, grasshoppers initially turned away from the speaker when the acoustic signal was presented to the lesioned side. Over time, correct turns to the operated side increased in both groups (Figure 5, left). First correct turns appeared significantly earlier in EPO-treated males (on day $3 \pm 1$ with $^{**}p < 0.01$, Wilcoxon matched paired signed rank test) compared in untreated controls (day $5.4 \pm 0.6$) and the number of correct turns to the regenerated side remained higher in EPO-treated males over the entire period of observation (Figure 5, left).

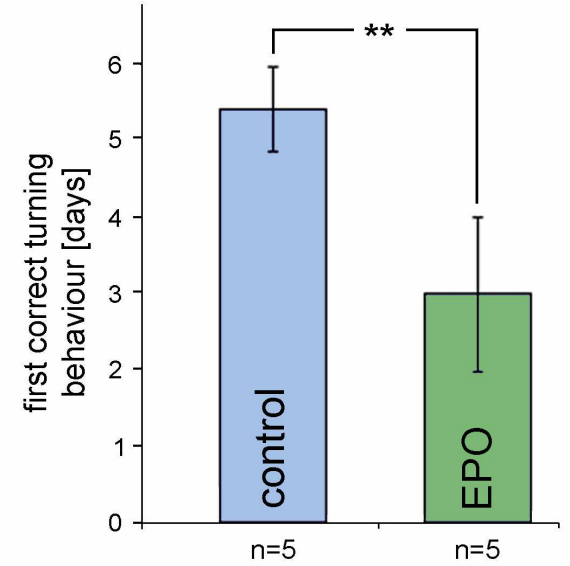


**Figure 6:** First correct turning behaviour of male *Ch. biguttulus* when stimulated with a female song to the operated side. Non-treated animals showed first correct turns on day 5.4±0.6 and EPO-treated animals on day 3±1 (**p<0.01, Wilcoxon matched paired signed rank test).

# 3.4 Discussion

*EPO and EPOR expression after peripheral nerve crush injury*

Peripheral nerve crush injury causes an alteration of EPO and EPOR protein expression in mammals. One of the first studies that analysed the expression changes of both proteins was performed by Campana & Myers (2001) on crushed sciatic nerves and their appendant dorsal root ganglion (DRG) neuron populations of adult rats. They showed that EPO is constitutively expressed in cell bodies and axons of normal DRG neurons and is upregulated in surrounding glial cells (Schwann cells) after nerve crush injury. In contrast, EPOR protein expression in Schwann cells either remained unchanged or was even down-regulated following nerve injury. However, subsequent studies that used the same experimental procedure of sciatic nerve crush injury in adult rats revealed that EPOR is also constitutively expressed in Schwann cells and DRG neurons and becomes upregulated after nerve crush injury (Keswani et al. 2004a; Li et al. 2005; Toth et al. 2008). As illustrated in Figure 6, the authors assume that crushing the sciatic nerve increases EPO production and release from Schwann cells. Keswani et al. (2004a) identified nitric oxide (NO) as the main factor that stimulates EPO production in Schwann cells. Released EPO binds to receptors on axons and cell bodies of DRG neurons and promotes neuroregeneration by decreasing the nuclear factor κB (NFκB) and increasing phosphorylation of the protein kinase Akt and accumulation of the signal transducer and activator of transcription 3 (STAT3) (Toth et al. 2008). Application of exogenous EPO to crushed sciatic nerves potentiates the neuroregenerative effect of endogenous EPO release (Campana & Myers 2003; Keswani et al. 2004a; Li et al. 2004; Toth et al. 2008).

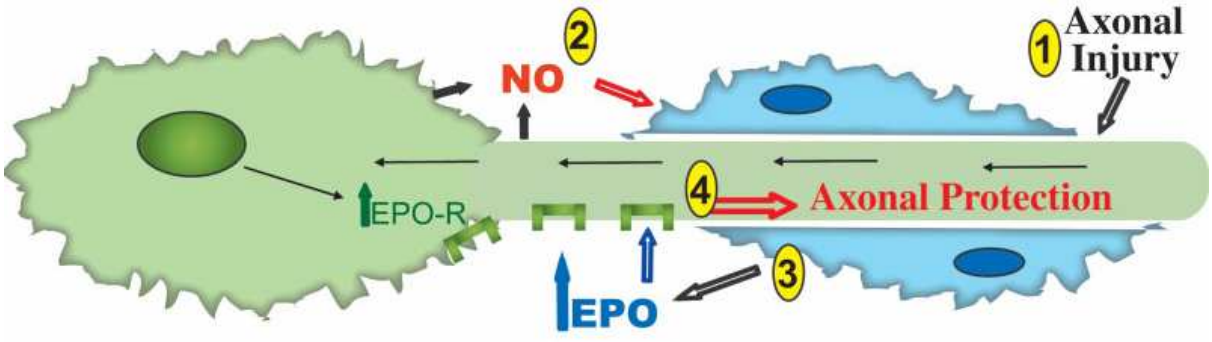


**Figure 6:** Schematic diagram of EPO-mediated intrinsic ´axonoprotective` pathways. Following axonal injury (1) nitric oxide (NO) is released from injured neurons (coloured in green) (2). Neuron-derived NO stimulates EPO production in neighbouring Schwann cells (coloured in blue) (3). EPO released from Schwann cells binds to EPOR and activates an ´axonoprotective` pathway (4). (from Keswani et al. 2004a)

In the present study expression of *ia*EPO and *ia*EPOR within the CNS of the grasshopper *Ch. biguttulus* was analysed after crushing the leg nerve N5. Comparison of *ia*EPO-related immunofluorescence between intact metathoracic nervous structures and following crush injury of the nerve N5 revealed no difference in *ia*EPO expression and no

evidence for *ia*EPO being expressed by glial cells. These results differ from studies on mammalian systems described above, where peripheral Schwann cells constitutively expressed EPO and increased its production after crushing the sciatic nerve of adult rats (Campana & Myers 2001; Keswani et al. 2004a; Li et al. 2005; Toth et al. 2008). Insects also have glial cells associated with peripheral nerves that share similar functions to Schwann cells in vertebrates, but the lack of a reliable marker for insect glial cells makes it difficult to distinguish glia from neurons by immunohistochemistry. Further studies should focus on the distal and proximal part of the crushed nerve, because induction of *ia*EPO expression may be limited to regions in the proximity of site of injury. Electron microscopic studies, similar to Jacobs & Lakes Harlan (1999) provide a useful tool to analyse ultrastructural changes in the tympanal nerve of *Ch. biguttulus.*

Following unilateral crush of the nerve N5 innervating the hind leg *ia*EPOR immunoreactivity increased within all central neuropil regions of the metathoracic ganglion (Figure 1). However neither the crushed nerve nor cell bodies of motor neurons that were known to project into the leg nerve contained obvious *ia*EPOR-like staining. It rather appeared that some interneurons increased *ia*EPOR expression that could not be identified on the basis of the widely distributed immunofluorescence. Whether these interneurons were synaptic partners of those neurons that were injured by nerve crushing and whether increased expression of *ia*EPOR in these neurons serves a beneficial effect on metathoracic neuronal circuits remains to be shown. At this point, it is difficult to assess, whether the consequences of peripheral nerve injury on the expression patterns of *ia*EPO and *ia*EPOR in grasshoppers differ from EPO and EPOR expression induced by mammalian nerve injury, since only few studies dealt with this topic. Expression changes of EPO and EPOR were only analysed after sciatic nerve crush injury in rats and obtained partly contradicting results concerning EPOR expression in Schwann cells and DRG neurons. Whether the hypothesis about the induction of the EPO/EPOR signalling pathway after sciatic nerve crush injury (Figure 6) can serve as a general model for lesioned peripheral nerves needs to be determined by comparative studies on other peripheral nerves. NO was identified as the main signal to increase EPO production after sciatic nerve crush injury (Keswani et al. 2004a). Nitric oxide is also present in the nervous system of insects and plays an essential role in neuronal plasticity of the developing and mature brain (Müller 1997; Bicker 1998, 2001). Whether NO also regulates *ia*EPO- and *ia*EPOR expression in invertebrates is unknown so far. Further studies in mammals, other vertebrates and insects have to reveal the function of the EPO/EPOR signalling pathway in physiological reactions of peripheral nerves to crush injury.

*Effects of exogenous EPO on axonal regeneration after peripheral nerve crush injury*

Neuroprotective effects of EPO in the brain of mammals after ischemic or hypoxic stress have previously been demonstrated in numerous studies (for review see: Dame et al. 2001; Juul 2002; Genc et al. 2004; Ghezzi & Brines 2004; Brines & Cerami 2005; Marti 2004; Arcasoy 2008). Konishi et al. (1993) showed for the first time that experimentally applied

EPO mediates neurotrophic effects on rat cholinergic septal neurons after axotomy (fimbria-fornix transection). Further studies indicated neuroprotective effects of exogenous EPO following sciatic nerve crush (Grasso et al. 2007; Toth et al. 2008), optic nerve transection (King et al. 2007; Zhong et al. 2007), spinal cord injury (Celik et al. 2002; Gorio et al. 2002; Kaptanoglu et al. 2004), cisplatin induced peripheral neurotoxicity (Orhan et al. 2004; Bianchi et al. 2006) and HIV induced sensory neuropathy (Keswani et al. 2004b). One of the first studies that concentrated on the promotive effect of exogenous EPO on neurite outgrowth (neuritogenesis) was conducted by Böckert-Meffert et al. (2002). In cultured retinal explants of rats EPO increased the elongation of retinal ganglion cell (RGC) neurites by up to 169% (controls = 100%) in a dose dependent manner. Subsequent *in vitro* and *in vivo* studies confirmed these results (Kretz et al. 2005; King et al. 2007; Zhong 2007). Similar to these findings, EPO was shown to promote neuritogenesis in spiral ganglion cells of isolated rat cochlea (Berkingali et al. 2008). However, none of these studies analysed whether EPO-promoted regeneration of neurites leads to a faster and eventually more complete regeneration of previous functions of the injured peripheral nerves. Only one recently published study of Zhang et al. (2009) demonstrated that EPO promotes functional recovery of rat facial nerves after crush injury. The facial nerve is the seventh (VII) of twelve paired cranial nerves that emerges from the brainstem between the pons and the medulla and controls the muscles of facial expression (Mattox & Felix 1987; Phillips & Bubash 2002). After crushing the facial nerve at the level of the stylomastoid foramen successful regeneration of the nerve can be measured by the behavioural recovery of the full blink reflex and whisker movements (Ferri et al. 1998; Hadlock et al. 2005). Zhang et al. (2009) showed that animals treated with high doses of EPO (5000-10000 Units/kg body weight) had a shorter recovery time for the blink reflex (~10.5 days instead of ~13 days in control animals) and whisker movements (~13 days instead of ~16 days in control animals). The present study revealed a similar promotive effect of exogenous EPO on axonal regeneration after crushing peripheral nerves in an insect. As in rat facial nerves, EPO treatment accelerated the reestablishment of neural function by two days. Functional regeneration leading to correct sound localisation of grasshoppers included growth of axons from the site of crushing to the CNS, navigating to the primary auditory neuropil in the metathoracic ganglion and re-establishing functional synapses with correct types of auditory interneurons. Whether EPO supports all of these processes or specifically promotes the speed of axonal growth, pathfinding of regrowing fibres or synaptogenesis has to be determined by future studies.

*Degenerative and regenerative processes in insect peripheral nerves after crush injury*

Experimental crush injury or transection of insect axons causes degenerative changes that are analogous to those of mammalian peripheral neurons. Within the first 24h of injury ultrastructural changes manifest at the cut ends of both proximal and distal axons. These include disruption of neurotubules, appearance of amorphous material in the axoplasm and accumulation of large numbers of mitochondria, vesicles of various sizes and quantities of smooth endoplasmatic reticulum (Hess 1960; Boulton 1969; Meiri et al. 1983). Furthermore,

haemocytes accumulate at the site of damage that together with neuroglial cells form the scar tissue (Boulton 1969). Within 2-4 days the distal part of the axons reveals signs of degeneration, including swelling of mitochondria, extensive vacuolisation, appearance of lysosomes and shrinkage of axons (Meiri et al. 1983). In addition, proliferating glial processes separate degenerating axons into smaller compartments. In the grasshopper *Ch. biguttulus* autofluorescent degeneration products of the formerly innervated frontal auditory neuropil and axonal tracts were detected after crushing the tympanal nerve N6 at a far distal position (Figure 3). The distribution of autofluorescent material suggests an incomplete degeneration. Removal of the remainders of the transected axons within the metathoracic ganglion remained in progress 3 days after nerve injury. Degeneration rates of distal segments of transected axons in the CNS of insects are highly variable. Giant axons of the cockroach degenerate within 3-8 days (Hess 1958, 1960; Farley & Milburn 1969), whereas the distal part of transected nerves in the grasshopper *Laplatacris disper* and the locust *Schistocerca gregaria* show only minimal degenerative changes after 10 days of injury (Melamed & Trujillo-Cenóz 1962; Rowell & Doray 1967). The discrepancy of degeneration rates in insects indicates that both the type of injured axons and the environment (e.g. surrounding glial cells) play a critical role for the progress of degeneration of axons after their separation from cell bodies.

Neurons in the CNS and PNS of lower vertebrates and invertebrates, and neurons in the PNS of mammals are capable of extensive axonal regrowth and accurate reestablishment of synaptic connectivity after injury. Regeneration of insect axons was first recognised by Bodenstein (1955, 1957) in the nervous system of the cockroach *Periplaneta americana*. A well studied example for the impressive regenerative capability of insect sensory neurons is the regeneration of abdominal cercal afferents in crickets (Edwards & Palka 1976; Murphey et al. 1984; Kämper & Murphey 1987). After successful regeneration, neurons of transplanted cerci project into the same neuropil regions as the former cercal sensory neurons of the host (Murphey et al. 1984; Kämper & Murphey 1987). Unlike the cercal system, the sensory neurons of the tympanal organ are unable to regenerate effectively in crickets (Ball 1979; Biggin 1981). In contrast, the present work and other studies demonstated that tympanal receptor fibres of grasshoppers can regenerate their central projections after nerve crush injury (Lakes & Kalmring 1991; Lakes-Harlan & Pfahlert 1995; Jacobs & Lakes-Harlan 1999). Although the number of regenerated fibres and the density of axon terminals within the frontal neuropil were still lower in animals after 20 days of regeneration, compared to intact control animals (Figure 4; Lakes-Harlan & Pfahlert 1995), a progressing functional recovery was observed after $3 \pm 1$ days following nerve crush in EPO treated animals and $5.4 \pm 0.6$ days in control animals (Figure 5). Lakes-Harlan & Pfahlert (1995) reported first correct turns of male *Ch. biguttulus* after 6 - 40 days. The long regeneration periods of up to 40 days that they observed in their study results from cutting the tympanal nerve completely, instead of just transecting the axons through crushing but leaving the nerve sheath intact. As a consequence of cutting the tympanal nerve, regenerating axons of auditory receptor cells had a lower probability to reach the CNS and often entered the metathoracic ganglion at sites that were different from their original entry

via the tympanal nerve root. If the auditory receptor axons were transected by crushing and the nerve sheath was left intact, all axons regenerated within the tympanal nerve and entered the metathoracic ganglion at the correct site. In this study the functional recovery of sound localisation in EPO treated *Ch. biguttulus* males was already observed ~3 days after injury. A study of Denburg et al. (1977) revealed an average growing rate of 0.9 mm/day for regrowing motor axons within the metathoracic ganglion of cockroaches. Regenerating auditory receptor fibres have to reach the frontal auditory neuropil for functional recovery (Lakes-Harlan & Pfahlert 1995), which involves axonal growth over a distance of approximately 800µm - 900µm. According to the results of Denburg et al. (1977) and assuming similar conditions as in cockroaches, regrowth of grasshopper auditory receptor fibres from the crush site to the correct neuropil in the CNS can be achieved within one day. Additionally, initiation of neurite outgrowth of the crushed nerve stump and reestablishment of synaptic connectivity with auditory interneurons may take more time. First functional recoveries of sound localisation in untreated male grasshoppers were observed about five days after injury. EPO treatment accelerated this process leading to first correct sound localisations already on the second day after nerve crush. Whether EPO initiates earlier axonal outgrowth, increases the proportion of regenerating fibres, accelerates the speed of regrowing or promotes the reestablishment of synaptic connectivity has to be evaluated by future anatomical and physiological studies.

# 3.5 References

Anagnostou A, Liu Z, Steiner M, Chin K, Lee ES, Kessimian N, Noguchi CT (1994) Erythropoietin receptor mRNA expression in human endothelial cells. Proc Natl Acad Sci USA 91:3974-3978

Arcasoy MO (2008) The non-haematopoetic biological effects of erythropoietin. Bri J of Haematol 141:14-31

Ball EE (1979) Development of the auditory tympana in the cricket *Teleogryllus commodus* (Walker): Experiments on regeneration and transplantation. Experientia 35:324-325

Berkingali N, Warnecke A, Gomes P, Paasche G, Tack J, Lenarz T, Stöver T (2008) Neurite outgrowth on cultured spiral ganglion neurons induced by erythropoietin. Hear Res 243 (1–2):21–6

Bernaudin M, Bernaudin M, Marti HH, Roussel S, Divoux D, Nouvelot A, MacKenzie ET, Petit E (1999) A potential role for erythropoietin in focal permanent cerebral ischemia in mice. J Cereb Blood Flow Metab 19:643–651

Bernaudin M, Bellail A, Marti HH, Yvon A, Vivien D, Duchatelle I, Mackenzie ET, Petit E (2000) Neurons and astrocytes express EPO mRNA: Oxygen-sensing mechanisms that involve the redox-state of the brain. Glia 30:271-278

Bianchi R, Brines M, Lauria G, Savino C, Gilardini A, Nicolini A, Rodriguez-Menendez C, Oggioni N, Canta A, Penza P, Lombardi R, Minoia C, Ronchi A, Cerami A, Ghezzi P, Cavaletti G (2006) Protective Effect of Erythropoietin and Its Carbamylated Derivative in Experimental Cisplatin Peripheral Neurotoxicity. Clin Cancer Res 12(8):2607-2612

Bicker G (1998) NO news from insect brains. Trend Neurosci 21(8):349-355

Bicker G (2001) Sources and targets of nitric oxide signalling in insect nervous systems. Cell Tissue Res 303:137-146

Biggin RJ (1981) Pattern re-establishment - transplantation and regeneration of the leg in the cricket *Teleogryllus commodus* (Walker). J Embryol Exp Morphol 61:87-101

Böcker-Meffert S, Rosenstiel P, Röhl C, Warneke N, Held-Feindt J, Lucius R (2002) Erythropoietin and VEGF promote neural outgrowth from retinal explants in postnatal rats. Invest Ophthalmol Vis Sci 43:2021–2026

Bodenstein D (1955) Contribution to the problem of regeneration in insects. J Exp Zool 129:209-24

Bodenstein D (1957) Studies on nerve regeneration in *Periplaneta americana*. J Exp Zool 136:89-115

Boulton PS (1969) Degeneration and regeneration in the insect central nervous system. Zellforsch Microsk Anat 101:98-119

Brines M, Cerami A (2005) Emerging biological roles for erythropoietin in the nervous system. Nature rev Neurosci 6:484-494

Buemi M, Cavallaro E, Floccari F, Sturiale A, Aloisi C, Trimarchi M, Grasso G, Corica F, Frisina N (2002) Erythropoietin and the brain: from neurodevelopment to neuroprotection. Clin Sci (Lond) 103:275-282

Campana WM, Myers RR (2001) Erythropoietin and erythropoietin receptors in the peripheral nervous system: changes after nerve injury. FASEB J 15:1804–1806

Campana MW & Myers RR (2003) Exogenous erythropoietin protects against dorsal root ganglion apoptosis and pain after following peripheral nerve injury. Eur J Neurosci 18:1497-1506

Campana WM, Li X, Shubayev VI, Angert M, Cai K, Myers RR (2006) Erythropoietin reduces Schwann cell TNF-alpha, Wallerian degeneration and pain-related behaviors after peripheral nerve injury. Eur J Neurosci 23:617–26

Celik M, Gökmen N, Erbayraktar S, Akhisaroglu M, Konakç S, Ulukus C, Genc S, Genc K, Sagiroglu E, Cerami A, Brines M (2002) Erythropoietin prevents motor neuron apoptosis and neurologic disability in experimental spinal cord ischemic injury. Proc Natl Acad Sci USA 99(4):2258-2263

Chen ZL, Yu WM, Strickland S (2007) Peripheral regeneration. Annu Rev Neurosci 30:209–233

Chiba A, Shepherd D, Murphey RK (1988) Synaptic rearrangement during postembryonic development in the cricket. Science 240:901-905

Chiba A, Murphey RK (1991) Connectivity of identified central synapses in the cricket is normal following regeneration and blockade of presynaptic activity. J Neurobiol 22:130-142

Chou CF, Tohari S, Brenner S, Venkatesh B (2004) Erythropoietin gene from a teleost fish, *Fugu rubripes*. Blood 104:1498-1503

Chu CY, Cheng CH, Chen GD, Chen YC, Hung CC, Huang KY, Huang CJ (2007) The zebrafish erythropoietin: Functional identification and biochemical characterization. FEBS Letters 581:4265-4271

Dame C, Juul SE, Christensen RD (2001) The biology of Erythropoietin in the central nervous system and its neurotrophic and neuroprotective potential. Biol Neonate 79:228-235

Denburg JL, Seecof RL, Horridge GA (1977) The path and rate of growth of regenerating motor neurons in the cockroach. Brain Res 125:213-226.

Digicaylioglu M & Lipton SA (2001) Erythropoietin-mediated neuroprotection involves cross-talk between Jak2 and $NF_K$- B signalling cascades. Nature 412:641–647

Edwards JS, Palka J (1976) Neural generation and regeneration in insects. In: Fentress JC (eds) Simpler networks and behavior. Sinauer Ass. Inc., Sunderland, Mass, pp 167-185

Farley RD, Milburn NS (1969) Structure and function of the giant fibre system in the cockroach, *Periplaneta americana.* J Insect Physiol 15:457-476

Fawcett JW, Keynes RJ (1990) Peripheral nerve regeneration. Annu Rev Neurosci 13:43–60

Ferri CC, Moore FA, Bisby MA (1998) Effects of facial nerve injury on mouse motoneurons lacking the p75 low-affinity neurotrophin receptor. J Neurobiol 34:1-9

Genc S, Koroglu TF, Genc K (2004) Erythropoietin and the nervous system. Brain Res 1000:19-31

Ghezzi P, Brines M (2004) Erythropoietin as an antiapoptotic, tissue-protective cytokine. Cell Death and Differentiation. 11:37-44

Gorio A, Gökmen N, Erbayraktar S, Yilmaz O, Madaschi L, Cichetti C, Di Giulio AM, Vardar E, Cerami A, Brines M (2002) Recombinant human erythropoietin counteracts secondary injury and markedly enhances neurological recovery from experimental spinal cord trauma. Proc Natl Acad Sci USA 99(14):9450-9455

Grasso G, Meli F, Fodale V, Calapai G, Buemi M, Iacopino DG (2007) Neuroprotective potential of erythropoietin and darbepoetin alfa in an experimental model of sciatic nerve injury. J Neurosurg Spine 7:645-651

Hadlock TA, Heaton J, Cheney M, Mackinnon SE (2005) Functional recovery after facial and sciatic nerve crush injury in the rat. Arch Facial Plast Sur 7(1):17–20

Helversen von D, Helversen von O (1983) Species recognition and acoustic localization in acridid grasshoppers: a behavioural approach. In: Huber F, Markl H (eds) Neuroethology and behavioural physiology. Springer, Berlin Heidelberg, pp 95-107

Hess A (1958) The fine structure of nerve cells and fibers, neuroglia, and sheaths of the ganglion chain in the cockroach (*Periplaneta americana*). J Biophys Biochem Cytol 4:731-742

Hess A (1960) The fine structure of degenerating nerve fibres, their sheaths, and their terminations in the central nerve cord of the cockroach (*Periplaneta americana*). J Biophys Biochem Cytol 7:339-342

Höorste GM, Prukop T, Nave KA, Sereda MW.(2006) Myelin disorders: causes and perspectives of Charcot-Marie-Tooth neuropathy. J Mol Neurosci 28:77–88

Jacobs K, Lakes-Harlan R (1997) Lectin histochemistry of the metathoracic ganglion of the locust *Schistocerca gregaria* before and after axotomy of the tympanal nerve. J Comp Neurol 387:255-265

Jelkmann W (1992) Erythropoietin: structure, control of production, and function. Physiol Rev 72:449-489

Juul SE, Yachnis AT, Rojiani AM, Christensen RD (1999) Immunohistochemical localization of erythropoietin and its receptor in the developing human brain. Pediatr Dev Pathol 2:148-158

Juul S (2002) Erythropoietin in the central nervous system, and its use to prevent hypoxic-ischemic brain damage. Acta Paediatr Suppl 438:36-42

Kämper G, Murphey RK (1987) Synapse formation by sensory neurons after cross-species transplantation in crickets: The role of positional information. Dev Biol 122: 492-502

Kaptanoglu E, Solaroglu I, Okutan O, Surucu US, Akbiyik F, Beskonakli E (2004) Erythropoietin exerts neuroprotection after acute spinal cord injury in rats: effect on lipid peroxidation and early ultrastructural findings. Neurosurg Rev 27:113-120

Keswani SC, Buldanlioglu U, Fischer A, Reed N, Polley M, Liang H, Zhou C, Jack C, Leitz GJ, Hoke A (2004a) A novel endogenous erythropoietin mediated pathway prevents axonal degeneration. Ann Neurol 56:815-826

Keswani SC, Leitz GJ, Hoke A (2004b) Erythropoietin is neuroprotective in models of HIV sensory neuropathy. Neurosci Let 371:102-105

King CE, Rodger J, Bartlett C, Esmaili T, Dunlop SA, Beazley LD (2007) Erythropoietin is both neuroprotective and neuroregenerative following optic nerve transection. Exp Neurol 205:48–55

Konishi Y, Chui DH, Hirose H, Kunishita T, Tabira T (1993) Trophic effect of erythropoietin and other haematopoietic factors on central cholinergic neurons *in vitro* and *in vivo*. Brain Res 609:29–35

Kretz A, Happold CJ, Marticke JK, Isenmann S (2005) Erythropoietin promotes regeneration of adult CNS neurons via Jak2/Stat3 and PI3K/AKT pathway activation. Mol Cell Neurosci 29:569-79

Lakes R, Kalmring K (1991) Regeneration of the projection and synaptic connections of tympanic receptor fibers of *Locusta migratoria* (Orthoptera) after axotomy. J Neurobio122:169-181

Lakes-Harlan R, Pfahlert C (1995) Regeneration of axotomized tympanal nerve fibres in the adult grasshopper *Chorthippus biguttulus* (L.) (Orthoptera: Acrididae) correlates with regaining the localization ability. J Comp Physiol A 176:797-807

Lewczuk P, Hasselblatt M, Kamrowski-Kruck H, Heyer A, Unzicker C, Sirén AL, Ehrenreich H (2000) Survival of hippocampal neurons in culture upon hypoxia: effect of erythropoietin. Neuroreport 11:3485-3488

Li XQ, Gonias SL, CampanaWM (2005) Schwann cells express erythropoietin receptor and represent a major target for Epo in peripheral nerve injury. Glia 51:254–265

Marti HH, Wenger RH, Rivas LA, Straumann U, Digicaylioglu M, Henn V, Yonekawa Y, Bauer C, Gassmann M (1996) Erythropoietin gene expression in human, monkey and murine brain. Eur J Neurosci 8:666-676

Marti HH (2004) Erythropoietin and the hypoxic brain. J Exp Biol 207:3233-3242

Masuda S, Nagao M, Takahata K, Konishi Y, Gallyas F, Jr., Tabira T, Sasaki R (1993) Functional erythropoietin receptor of the cells with neural characteristics. Comparison with receptor properties of erythroid cells. J Biol Chem 268:11208-11216

Masuda S, Okano M, Yamagishi K, Nagao M, Ueda M, Sasaki R (1994) A novel site of erythropoietin production. Oxygen-dependent production in cultured rat astrocytes. J Biol Chem 269:19488-19493

Masuda S, Chikuma M, Sasaki R (1997) Insulin-like growth factors and insulin stimulate erythropoietin production in primary cultured astrocytes. Brain Res 46:63-70

Mattox DE, Felix H (1987) Surgical anatomy of the rat facial nerve. Am J Otol 8:43-47

Meiri H, Dormann A, Spira ME (1983) Comparison of uttrastructural changes in proximal and distal segments of transected giant fibers of cockroach *Periplaneta americana.* Brain Res 263:1-14

Melamed J, Trujillo-Cenós O (1962) Electron microscope observation on the calyces of the insect brain. J Ultrastruct Res 7:389-398

Morishita E, Masuda S, Nagao M, Yasuda Y, Sasaki R (1997) Erythropoietin receptor is expressed in rat hippocampal and cerebral cortical neurons and erythropoietin prevents in vitro glutamate-induced neuronal death. Neuroscience 76:105-116

Müller U (1997) The nitric oxide system in insects. Prog Neurobiol 51:363–381

Murphey RK, Johnson SE, Walthall WW (1981) The effects of transplantations and regeneration of sensory neurons on a somatotopic map in the cricket CNS. Dev Biol 88:247-258

Murphey RK, Walthall WW, Jacobs GA (1984) Neurospecificity in the cricket cercal system. J Exp Biol 112:7-25

Orhan B, Yalcin S , Nurlu G, Zeybek D, Muftuoglu S (2004) Erythropoietin against cisplatin-induced peripheral neurotoxicity in rats. Med Oncology 21(2):197-203

Paffett-Lugassy N, Hsia N, Fraenkel PG, Paw B, Leshinsky I, Barut B, Bahary N, Caro J, Handin R, Zon LI (2009) Epo-EpoR signaling is not required for cardiovascular or neural development. Blood 110:2718-2726

Pallas SL, Hoy RR (1988) Regeneration of normal afferent input does not eliminate aberrant synaptic connections of an identified interneuron in the cricket *Teleogryllus oceanicus.* J Comp Neurol 248:348-359

Philips CD, Bubash LA (2002) The facial nerve: anatomy and common pathology. Semin Ultrasound CT MR 23(3):202–217

Rowell CHF, Dorey AE (1967) The number and size of axons in the thoracic connectives of the desert locust, *Schistocerca gregaria* Forsk Z Zellforsch 83:288-294

Sirén AL, Knerlich F, Poser W, Gleiter CH, Brück W, Ehrenreich H (2001) Erythropoietin and erythropietin receptor in human ischemic/hypoxic brain. Acta Neuropathol 1001:271-276

Sugawa M, Sakurai Y, Ishikawa-Ieda Y, Suzuki H, Asou H (2002) Effects of erythropoietin on glial cell development; oligodendrocyte maturation and astrocytes proliferation. Neurosci Res 44:391-403

Tan C, Eckardt KU, Firth JD, Ratcliffe PJ (1992) Feedback modulation of renal and hepatic erythropoietin mRNA in response to graded anemia and hypoxia. Am J Physiol 263: F474-F481

Toth C, Martinez JA, Liu WQ, Diggle J, Guo GF, Ramji N, Mi R, Hoke A, Zochodne DW (2008) Local erythropoietin signaling enhances regeneration in peripheral axons. J Neurosci 154(2):767-783

Waller A (1850) Experiments on the section of the glossopharyngeal and hypoglossal nerves of the frog and observations of the alterations produced thereby in the structure of their primitive fibers. Phil Trans R Soc Lond (Biol) 140:423-429

Yamaji R, Okada T, Moriya M, Naito M, Tsuruo T, Miyatake K, Nakano Y (1996) Brain capillary endothelial cells eypress two forms of erythropoietin receptor mRNA. Eur J Biochem 239:494-500

Yu X, Lin CS, Costantini F, Noguchi CT (2001) The human erythropoietin receptor gene rescues erythropoesis and developmental defects in the erythropoietin receptor null mouse. Blood 98:475-477

Yu X, Shacka JJ, Eells JB, Suaret-Quian C, Przygodzki RM, Beleslin-Cokic B, Lin CS, Nikodem VM, Hempstead B, Flanders KC, Constantini F, Noguchi CT (2002) Erythropoietin receptor signalling is required for normal brain development. Develop 129:505-516

Zhang W, Sun B, Yu Z, An J, Liu Q, Ren T (2009) High dose erythropoietin promotes functional recovery of rats following facial nerve crush. J of Clinic Neurosci 16(4):554-556

Zhong Y, Yao H, Deng L, Cheng Y, Zhou X (2007) Promotion of neurite outgrowth and protective effect of erythropoietin on the retinal neurons of rats. Graefes Arch Clin Exp Ophthalmol 245:1859–1867

# 4 Effects of erythropoietin on cultured insect brain cells

## 4.1 Introduction

The detection of EPO in the nervous system of vertebrates lead to the identification of previously unknown functions of EPO signalling beyond its role in the production of red bood cells (erythropoiesis). In monkey and mouse brains as well as in primary cell cultures of mammalian neurons and astrocytes EPO gene expression is upregulated under hypoxic conditions (Digicaylioglu et al. 1995; Marti et al. 1996; Bernaudin et al. 2000; Sirén et al. 2001b; Liu et al. 2006). In monkey brains EPO mRNA increases 3-fold after 2 hours of reduced $O_2$ and studies on an established mouse model for hypoxia (4 hours of 0.1% $CO_2$) revealed a 20-fold increase of EPO gene expression in the brain compared to a 200-fold increase in the kidney. In addition to neurons, hypoxia (1% $O_2$) also increased EPO mRNA levels in primary cultured astrocytes to 100-fold of basal expression. Upregulation of EPO gene transcription during hypoxia is mediated by the activation of the transcription factor HIF-1 (hypoxia-inducible factor-1), which consists of two subunits: HIF-1α (120kDa) and HIF-1β (91-94kDa, also called ARNT) (Semenza & Wang 1992; Wenger 2002). Under normal oxygen conditions HIF-1α is constantly expressed but rapidly degraded by a series of reactions: The presence of oxygen, iron and 2-oxoglutarate causes the hydroxylation of proline and asparagine residues in the oxygen-dependent degradation domain (ODD) and the C-terminal transactivation domain (C-TAD) of HIF-1α (Metzen et al. 2003; Metzen & Ratcliff 2004). Due to these hydroxylations the conformation of HIF-1α changes and allows the binding of the von Hippel Lindau protein (VHL). Other factors (elongin B, elongin C, Cullin and RBX1) additionally bind to the VHL and act as ubiquitin ligase. Finally, HIF-1α is ubiquitylated which induces its degradation by proteasomes (Maxwell et al. 1999; Ivan et al. 2001). Under hypoxic conditions the prolyl- and asparaginyl-hydroxylases are inhibited, tagging for degradation is prevented and HIF-1α can rapidly accumulate in the cell (Maxwell et al. 1999; Jaakkola et al. 2001). Accumulating HIF-1α is phosphorylated, dimerises with HIF-1β and binds to p300/CBP (CREB (cyclic-AMP-response element-binding protein) binding protein). This complex activates hypoxia-responsive elements (HREs) in HIF target genes to modulate their transcription (Semenza 2001a, 2001b).

Brain derived EPO is thought to function as endogenous protectant of neurons against mild hypoxia and ischemia. Sakanaka et al. (1998) demonstrated that neutralisation of endogenous EPO (by infusion of a soluble EPO receptor) resulted in neuronal cell death in gerbil brains subjected to mild ischemia. Similar results were obtained following transient global ischemia of the rat retina. Loss of functional endogenous EPO impaired the survival and recovery of retinal neurons (Junk et al. 2002). In contrast, the application of recombinant human EPO (rhEPO) in various mouse, rat, gerbil and rabbit hypoxia/ischemia models

demonstrated that EPO can restrict the extension of anatomical destruction and improve physiological functions and performance of neurons that survive in compromised tissues (for review see Dame et al. 2001; Buemi et al. 2002; Genc et al. 2004; Marti 2004; Arcasoy 2008). Cellular damage from hypoxic/ischemic periods results from different mechanisms in both acute phase of oxygen and glucose depletion and the following period of reperfusion. During the acute phase cells are damaged by excitotoxicity. The lack of oxygen disrupts oxidative phosphorylation in mitochondria resulting in energy depletion and depolarisation of neuronal membrane potentials. As a consequence, enhanced release of glutamate overstimulates neuronal glutamate receptors and causes a massive influx of calcium, sodium and water. This in turn leads to the production of free radicals, impairment of mitochondrial functions, cell swelling and subsequent neuronal cell death (Choi 1992, 1995, 1996; Zipfel et al. 2000). During the reperfusion period a second wave of neuronal damage occurs that is thought to be caused by postischemic release of oxygen radicals, synthesis of nitric oxide (NO), inflammatory reactions and an imbalance between excitatory and inhibitory neurotransmitter systems (Volpe 2001). These processes and conditions ultimately induce apoptosis (Northington et al. 2001a, 2001b). EPO intervenes at multiple sites in the nervous system to prevent neuronal damage after episodes of hypoxia/ischemia. These include the decrease of glutamate toxicity (Morishita et al. 1997; Kawakami et al. 2001), induction of anti-apoptotic factor generation (such as bcl-2 and bcl-xL - Silva et al. 1996; Renzi et al. 2002), reduction of inflammation (Brines et al. 2000), decrease of NO mediated injury (Digicaylioglu & Lipton 2001) and stimulation of angiogenesis (Yamaji 1996; Sirén et al. 2001). Furthermore, Chattopadhya et al. (2000) showed that EPO mediates antioxidant effects.

The signalling pathways that mediate neuroprotective effects of EPO in the nervous system of vertebrates are not fully understood. Various studies identified an EPO receptor in both glial and neuronal cells, which is similar to the hematopoietic receptor expressed in erythroid progenitor cells (Anagnostou et al. 1994; Digicaylioglu et al. 1995; Yamaji et al. 1996; Morishita et al. 1997; Bernaudin et al. 1999, 2000; Sirén et al. 2001; Sugawa et al. 2002). Binding of EPO causes dimerisation of the receptor and subsequent autophosphorylation of constitutively associated Janus-tyrosine kinases-2 (JAK-2). JAK-2 activation initiates several downstream signalling pathways including Ras mitogen-activated protein kinase (Ras-MAPK), phosphatidylinositol-3-kinase (PI(3)K) and signal transducers and activators of transcritption (STAT-5) (for review see Lacombe & Mayeux 1999). Distinct intracellular signalling cascades that have been characterised in hematopoietic cell lines are also functional in neurons (Yoshimura et al. 1998; Digicaylioglu & Lipton 2001; Kilic et al. 2005; Wu et al. 2007). EPO mediated neuroprotection against hypoxia-induced cell death is completely abolished in the presence of specific inhibitors of MAPK and PI(3)K (Siren et al. 2001a). Furthermore, phosphorylation dependent activation of STAT5 after hypoxic episodes was demonstrated in mouse neuronal cultures and cultured rat hippocampal cells (Sirén et al. 2001a; Liu et al. 2005). More recently, the important role of the nuclear factor-$_K$B (NF-$_K$B) for neuroprotection in rat cerebrocortical cultures and mouse neuronal cultures has been reported (Digicaylioglu & Lipton 2001; Liu et al. 2005). By current knowledge, this signalling pathway is not involved in EPO mediated effects in the hematopoietic system. In addition, Brines et al. (2004) demonstrated that the protective effect of EPO in the mammalian spinal

cord requires the binding of a second receptor component to EPOR (βcR subunit of the IL-3, IL-5 and granulocyte-macrophage colony stimulating factor receptor). Though still limited, the presently available information suggests that the EPO initiated molecular mechanisms that mediate neuroprotective effects may be more diverse and complex than the processes that regulate erythropoiesis.

*In vitro* studies provide a useful tool to identify the molecular mechanisms underlying neuroprotective effects of EPO. The controlled environment of primary cell cultures or neuronal cell lines outside organisms simplifies the manipulation of signalling cascades and the interpretation of resulting effects. All previous studies were performed on cultured neuronal or glial cells of mammals. But EPO protein expression was also detected in the CNS of teleost fish (Chou et al. 2004; Chu et al. 2007; Paffett-Lugassy et al. 2007) and EPO-like immunoreactivity was found in various invertebrate species of different phyla (see chapter 2 of this doctoral study). Furthermore, EPO promotes the regeneration of peripheral nerves in the grasshopper *Ch. biguttulus* after crush injury (chapter 3 of this doctoral study). These results indicate that the neuroprotective function of EPO described in the mammalian CNS may be mediated by ancient conserved mechanisms that predate the evolution of mammals. Thus, primary cultured insect neurons and insect cell lines provide a new approach to analyse the molecular mechanisms initiated by EPO. Since none of the previous *in vitro* studies used insect or any other invertebrate cells, the purpose of this project was to investigate for the first time a potential neuroprotective effect of EPO on cultured insect brain cells. Therefore, cell cultures of locust brain cells were used to determine the effect of EPO on cell viability both under normoxic and hypoxic conditions. In addition, the promotive effect of EPO on neurite outgrowth of cultured locust neurons was analysed. Furthermore, initial comparative studies on a neuronal cell line from *Drosophila melanogaster* were conducted.

# 4.2 Material and Methods

Unless otherwise mentioned, all chemicals were either purchased from Sigma-Aldrich (Steinheim, Germany) or Merck (Darmstadt, Germany).

### 4.2.1 Animals

Locusts, *Locusta migratoria* (L.), were purchased from a commercial animal breeder (Schätzle Terraristik, Karlsruhe, Germany) and maintained in colonies at 18-21℃ on a 12h/12h day/night cycle. All experiments were carried out with fourth-instar nymphs of *L. migratoria*.

### 4.2.2 Preparation of primary cultures of locust brain cells

Brains without optic lobes were dissected and transferred into sterile culture medium (Leibowitz L-15, Gibco, Invitrogen, Karlsruhe, Germany) containing 0.5% gentamicin (GM). To exclude hemocytes from cell cultures, brains were washed three times with fresh L15-0.5% GM. To ease the dissociation of cells, brains were treated with a collagenase/dispase (Gibco, Invitrogen, Karlsruhe, Germany) solution (1mg/ml in L15-0.5% GM) for 15-20 minutes at 29℃. The reaction was stopped by washin g twice with 250µl/brain of Hanks' balanced salt solution (HBBS, Gibco, Invitrogen, Karlsruhe, Germany). Afterwards, the tissue was gently titurated by repeated passage (~15-20 times) through the tip of a 100µl Eppendorf pipette (Eppendorf, Wesselin-Berzdorf, Germany). After brief spinning (3000 x g) in a bench-top centrifuge (Quick Spin 7000, Süd-Laborbedarf, Gauting, Germany) the supernatant containing cellular debris was discarded while the pellet of dispersed cells was resuspended in 200µl/brain of L15-0.5% GM. The cell suspension was plated on concavalin-coated (1µg/ml) cover slips (100µl/coverslip, Hartenstein, Würzburg, Germany), which were placed in sterile plastic culture dishes (35 x 10mm, Corning Inc., Sigma-Aldrich, Steinheim, Germany). Cells were allowed to adhere to the bottom of the cover slip for 90 minutes. Afterwards the culture dishes were filled up with 2ml L15-0.5% GM containing 5% fetal calf serum (FCSG, PAA laboratories, Cölbe, Germany) and placed in a humidified culture chamber at 29℃ (Heraeus, Hanau, Germany). The medi um was replaced every four days.

### 4.2.3 Cell viability tests

Brains of *L. migratoria* were taken into primary cell culture as described above. Viability of cells was either determined by counting DAPI stained nuclei or by MTT-assay.

*Counting of DAPI stained nuclei.* Cultured cells were fixed for 15 minutes in 4% paraformaldehyde dissolved in phosphate buffer (PB), rinsed three times with phosphate buffered saline (PBS) and two times with PBS-0.1% Triton. DAPI (100µg/ml) was dissolved in PBS and incubated either for 30 minutes at RT or over night at 4℃. Following several washes in PBS and transfer to PBS with glycerol (1:1), DAPI fluorescence was analysed with a conventional fluorescence microscope (Zeiss Axioskop) and photographed with a Spot

CCD camera (Intas or Invisitron). The overall area that was analysed consisted of two continuous rows of pictures passing to the right and to the left of the centre of the cover slip. This procedure assured the inclusion of both densely and sparsely overgrown regions in the analysis. Nuclei of living cells were identified by a discontinuous patchy distribution of DAPI fluorescence while nuclei of dead cells were usually smaller and uniformly labelled by DAPI (Gocht et al. 2009; also see 1.3.3 of this doctoral thesis). The data of cell counts were transferred to a spreadsheet (Microsoft Excel) to generate initial diagrams. The diagrams were reformatted and labeled with Photoshop 7.0 (Adobe).

*MTT-Assay.* MTT (3-(4,5-dimethylthiazol-2-yl)2,5-diphenyl tetrazolium bromide) was dissolved at a concentration of 1mg/ml in PBS and added to the cultured cells (MTT : medium = 1:5). Culture dishes were incubated for 4h at 37℃. Subsequently, MTT solution was removed and cells were lysed in 200µl of ethanol/DMSO (1:1). Prior spectrophotometric messurements, lysates of cell cultures were transferred to a 96 well plate (100µl in each well). Their optical density was measured with an automatic microplate reader (MRX Microplate Reader, Dynatex Laboratories, Issy-les-Moulineaux, France) with 670nm reference wavelength and 570nm test wavelength.

### 4.2.4 Hypoxia in cultured locust brain cells

For each experiment the brains of 12 locusts were prepared for primary cell culture as described above, pooled and equally allocated into 6 culture dishes. For the first five days brain cells were cultured with full medium (L15-medium + 0.5% GM + 5% FCSG) under normoxic conditions. Afterwards, full medium was replaced with deficient medium (L15-medium + 0.5% Gentamicin) with or without EPO (4 Units/ml EPO). After 12h of preincubation cell cultures were exposed to hypoxia (≤1% $O_2$) for 24 hours. For this procedure culture dishes were transferred to an airproof exsiccator, oxygen ($O_2$) was replaced by nitric oxid ($N_2$) and concentration of $O_2$ was controlled by an oxygen analyser (Greisinger GOX 100, Conrad, Hirschau, Germany). Subsequently, cells were cultured for another 12 hours in normal air conditions, then fixed with 4% paraformaldehyde dissolved in PB for 15 minutes and stained with DAPI (100µg/ml) for 30 minutes at RT. Following several washes in PBS and transfer to PBS with glycerol (1:1), fluorescence was analysed with a fluorescence microscope (Zeiss Axioskop) equipped with a Spot CCD camera (Intas). Cell viability of cultured cells was analysed as described above. Statistical analysis of data (EPO-treated cell cultures compared to non-treated cultures under hypoxic conditions) was performed with the program SPSS (13.0 for Windows) using a nonparametric paired sample test (Wilcoxon matched paired singed rank test).

### 4.2.5 Neurite outgrowth of cultured locust brain neurons

Brains of locusts were prepared for primary cell culture as described above. Culture dishes were incubated for five days with full medium (L15-medium + 0.5% GM + 5% FCSG), deficient medium (L15-medium + 0.5% Gentamicin), or deficient medium + 4 Units/ml EPO. Afterwards, cultured cells were fixed with 4% paraformaldehyde for 15 minutes and permeabilised in PBS containing 1% Triton X-100 for 1h at RT. Nonspecific binding of the

antibody was reduced by blocking with 5% normal goat serum (GE Healthcare, Munich, Germany) and 0.25% bovine serum albumin (MPI Biomedical, Heidelberg, Germany) dissolved in PBS with 1% Triton for 1h at RT. To visualise fine neurites of cultured cells anti-HRP serum was used. The antibody (rabbit α-HRP) was applied at a dilution of 1:500 at 8°C over night. After washing several times with PBS, a Cy3-coupled secondary antibody (Cy3 goat α-rabbit IgG, Rockland, Gilbertsville, USA) at a dilution of 1:300 at RT was used to visualise immunoreactivity. Following several washes in PBS and transfer to PBS with glycerol (1:1), fluorescence was analysed with a fluorescence microscope (Zeiss Axioskop) and cells were photographed with a Spot CCD camera (Invisitron). The overall area that was analysed in this way consisted of two continuous rows of pictures passing to the right and to the left of the centre of the cover slip. The diameter of the cell somata and the distance between the centre of the soma and the most distantly located neurite was measured with the program Image Tool 2.00 (Texas Health Science Center, San Antonio, USA). Data were transferred to a spreadsheet (Microsoft Excel or SPSS 13.0) to generate initial diagrams. These diagrams were reformatted and labeled with Photoshop 7.0 (Adobe). Statistical analysis of data was performed with the program SPSS (13.0 for Windows) using a non-parametric test for independent samples (Mann-Whitney U-test). Both the length of neurite outgrowth and the diameter of the somata were compared between non-treated, EPO-treated and FCS-treated locust brain cell cultures that were cultivated for five days under normoxic conditions.

### 4.2.6 Glial cell count *in vitro*

To determine the percentage of glial cells in primary cell cultures, dissociated brain cells of 12 *L. migratoria* were pooled (as described above) and allocated in similar portions to eight culture dishes. Cells were cultured for three days in deficient medium (minus FCS) with or without EPO (4 Units/ml) or in full medium (plus FCS) with or without EPO (4 Units/ml). Cell cultures were stained with anti-HRP and DAPI (as described above) and analysed with a conventional fluorescence microscope (Zeiss Axioskop) equipped with a Spot CCD camera (Intas or Invisitron). DAPI- and anti-HRP immunofluorescence were individually photographed and subsequently merged. Glial cells were identified by a discontinuous, patchy DAPI fluorescence pattern of their nuclei and the absence of neuron-specific anti-HRP fluorescence. Cell counts were performed on 40 photographs per culture dish. The numbers of cells were transferred to a spreadsheet (Microsoft Excel) to generate initial diagrams. All values were expressed as means ± SD (standard deviation). The diagram was reformatted and labeled with Photoshop 7.0 (Adobe).

### 4.2.7 Cell line ML-DmBG2-c2

*Drosophila* BG2 cells initially derived from larval central nervous systems (Ui-Tei et al. 2000). They are maintained in Schneider's cell medium (Gibco, Invitrogen, Karlsruhe, Germany) supplemented with 1% penicillin/streptamycin solution, 10% heat-inactivated FBS (Biochrom AG, Berlin, Germany) and 10 g/ml insulin. Cells were cultured at a density of $10^6$ cells/ml at 27°C in a humidified culture chamber.

### 4.2.8 Anti-HRP immunocytochemistry of cultured ML-DmBG2-c2 cells

For immunostaining against HRP, DmBG2-c2 cells were plated on concavalin-coated (1µg/ml) cover slips (100µl/coverslip, Hartenstein, Würzburg, Germany). Cells were allowed to adhere to the bottom of the cover slip for at least one hour. Afterwards, cell cultures were fixed for 15 minutes with 4% paraformaldehyde dissolved in PB, rinsed three times with PBS and two times with PBS-0.1% Triton. To reduce nonspecific binding of the anti-HRP antibody, cells were treated with blocking buffer (3% BSA, 2% NGS in PBS-0.1% Triton) for 1h at RT. Cultures were incubated over night at 8℃ with the anti-HRP serum (rabbit α-HRP) at a dilution of 1:500. After several washing steps with PBS a Cy3-coupled second antibody (Cy3 goat α-rabbit IgG, Rockland, Gilbertsville, USA) was added at a dilution of 1:1000 for 1h at RT. For nuclear staining the cells were incubated with DAPI (100µg/ml) for 30 minutes at RT. Following several washes in PBS and transfer to PBS with glycerol (1:1), fluorescence was analysed with a fluorescence microscope (Zeiss Axioskop) equipped with a Spot CCD camera (Intas or Invisitron).

### 4.2.9 MTT assay on cultured ML-DmBG2-c2 cells

DmBG2-c2 cells were plated on 36-well culture dishes and each well was filled up with 500µl medium. MTT (3-(4,5-dimethylthiazol-2-yl)2,5-diphenyl tetrazolium bromide) was dissolved in a concentration of 1mg/ml in PBS and 100µl was added to the cultured cells. Culture dishes were incubated for 4h at 37 ℃. Subsequently, MTT s olution was removed and the cells were lysed in 300µl or 400µl (depending on the cell density) of ethanol/DMSO (1:1). Prior to spectrophotometric measurements, the solutions of each well were transferred to a 96 well plate (100µl in each well). The optical density was measured using an automatic microplate reader (MRX Microplate Reader, Dynatex Laboratories, Issy-les-Moulineaux, France) with 670nm reference wavelength and 570nm test wavelength.

### 4.2.10 Hypoxia in cultured ML-DmBG2-c2 cells

For each experiment the DmBG2-c2 cells were equally allocated to 36-well culture dishes. Cells were allowed to adhere to the bottom of the culture dishes for 12 hours. Afterwards, full medium was replaced with deficient medium (Schneider's cell medium with 1% penicillin/streptamycin solution) with or without EPO (4 Units/ml EPO). After 12h of preincubation, cell cultures were exposed to hypoxia (≤1% $O_2$) for 24 hours, as described above. Additional studies were performed with repeated series (three times) of hypoxic/normoxic intervals (6h/18h; 15h/9h). Subsequently, cells were cultured for another 12 hours in normal air conditions and cell viability was analysed using the MTT assay.

# 4.3 Results

### 4.3.1 Effects of recombinant human EPO (rhEPO) on primary cultured locust brain cells under normoxic conditions

To analyse the potential neuroprotective effect of rhEPO on cultured insect brain cells, *L. migratoria* brains were prepared for cell culture and incubated with different concentrations of EPO (ranging from 0 to 40 Units/ml, dissolved in L-15 medium without FCS). Cell vitality was either analysed after 24h (Figure 1a) or after three days of cultivation (Figure 1b). In cultured locust brain cells incubated for 24h cell viability was analysed by counting DAPI-stained nuclei. DAPI is a fluorescent stain that binds strongly to A/T-rich sequences in the minor groove of the DNA (Kapuscinski & Szer 1979). Since viable and dead cells differ in their chromatin structure (patchy structure in viable cells, condensed structure in dead cells) the DAPI fluorescence can be used to distinguish between dead and living cells (Gocht et al. 2009; also see 1.3.3, 1.3.4 of this doctoral thesis). The portion of living cells in dependence of the EPO concentration is presented in Figure 1a. EPO treatment increased the number of viable cells up to a dosis of 0.4 Units/ml. With higher EPO concentrations, the average number of viable cells decreased while variability between the tested cultures increased. The maximal supportive effect on neuronal survival was detected at a concentration of 0.4 Units/ml. Compared to cultures that were incubated without EPO (n = 3, normalised to 1.0) the portion of living cells increased to 1.05 ± 0.024 (a plus of approximately 5%) in culture dishes treated with 0.4 Unit/ml EPO.

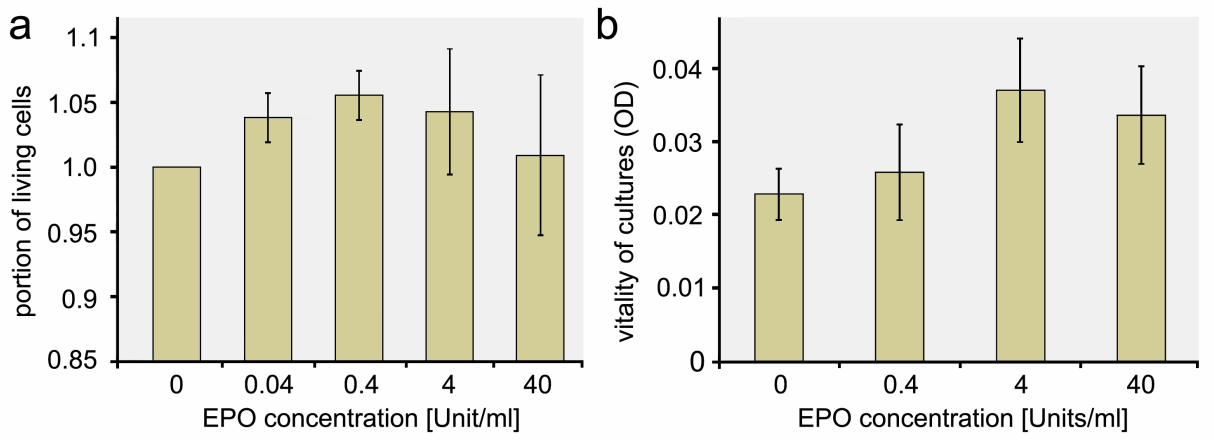


**Figure 1:** Dose-response effect of EPO on the survival of primary cultured locust brain cells. **a:** Cultivation of locust brain cells for 24 hours with different concentrations of EPO (0, 0.04, 0.4, 4, 40 Units/ml). Cell viability was determined by DAPI-staining (number of living cells/total number of counted cells) (n = 3). **b:** Cultivation of locust brain cells for 3 days with different concentrations of EPO (0, 0.4, 4, 40 Units/ml). Cell vitality was determined by MTT assay (n = 2). OD: optical density

To confirm these results the vitality of locust brain cells in dependence of different EPO concentrations (0, 0.4, 4, 40 Units/ml) was analysed after 3 days of cultivation using the MTT assay. The tetrazolium salt MTT is cleaved by mitochondrial enzymes within viable cells into

a blue coloured product (formazan) (Mosmann 1983). The measured optical density (OD) depends on both the number of viable cells within a culture dish and the physiological state of the cells. A dose-response curve of different concentrations of EPO is presented in Figure 1b. Similar to cultures that were incubated for 24 hours high doses of EPO (40 Units/ml) caused a reduced protective effect in comparison to lower doses of EPO (4 Unit/ml). The maximal neuroprotective effect of EPO was found at a concentration of 4 Units/ml. The optical density of culture dishes incubated without EPO was 0.022 ± 0.003 and increased to 0.037 ± 0.007 in cell cultures treated with 4 Units/ml (Figure 1b).

Optimal conditions for cultured locust brain cells comprehend their incubation in L15-medium with the addition of several growth factors and other additives that enhance the vitality of cells (referred as full medium = L15-medium + 5% FCS). However, due to the procedure of cultivation (e.g. enzymatic treatment and mechanical dissociation of the brain tissue) approximately half of the cells (50.9% ± 6.1%) died within the first 24 hours of cultivation (Figure 2, +FCS/-EPO). Application of EPO (0.4 Units/ml) to full medium increased the percentage of surviving cells by 2.7% to 53.6% ± 5.8%. Cultivation of cells in L15-medium without FCS decreased the number of living cells by 5% (45.8% ± 7.1%) in comparison to cells treated with FCS. Addition of 0.4 Units/ml EPO to the deficient medium increased the average survival of locust brain cells by 9.4% to 55.2% ± 0.7%.

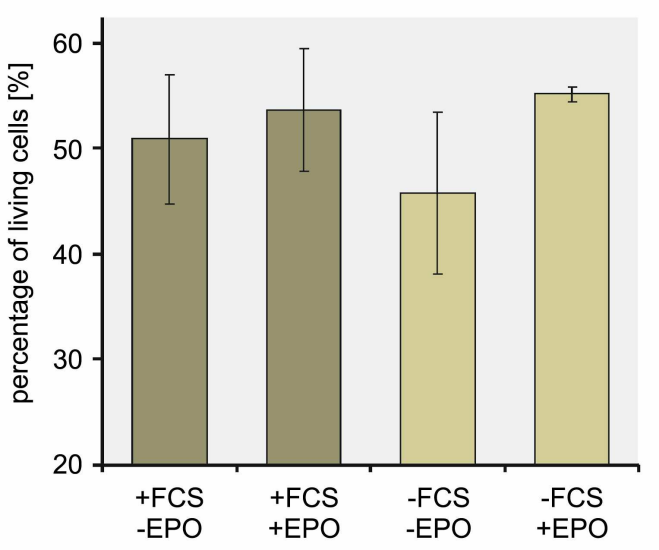


**Figure 2:** Percentage of living cells in primary cell cultures from locust brains after 24h of cultivation under different conditions. Cell cultures were either incubated in deficient medium (-FCS) with or without EPO (0.4 Units/ml) or in full medium (+FCS) with or without EPO (0.4 Units/ml) (n = 4). Dead and alive cells were distinguished by the pattern of nucleic DAPI staining.

### 4.3.2 Effects of recombinant human EPO (rhEPO) on primary cultured locust brain cells under hypoxic conditions

Previous studies revealed the neuroprotective effect of EPO after episodes of hypoxia on cultured hippocampal and cortical neurons of rats, P19 cells and primary rat motorneurons (Lewczuk et al. 2000; Sinor & Greenberg 2000; Sirén et al. 2001; Wen et al. 2002).

Locust brain cells were incubated for five days in full medium under normoxic conditions. During this period, neurons that were irreversibly damaged during the procedure of cultivation died and disintegrated while surviving neurons stabilised their conditions and

started to regenerate neurites. In addition, most of the glial cells died within the first days of cultivation (Gocht et al. 2009, also see 1.3.4 of this doctoral thesis) leaving relatively pure neuronal cultures for the hypoxia experiments. Eliminating glial cells from cell cultures abolishes a possible modulating effect of glial cell derived factors on surrounding neurons. After five days, full medium was exchanged for deficient culture medium (with or without EPO) to exclude neuroprotective effects mediated by factors contained in the FCS. The experimental procedure of the hypoxic study is illustrated in Figure 3a.

The neuroprotective effect of EPO (4 Units/ml) on primary cultured locust brain cells during and after hypoxic episodes of 11 individual experiments is summarised in Figure 3. A hypoxic period of 36 hours is a severe and harmful stimulus that causes neuronal death. In comparison to cell cultures incubated under normoxic conditions (normalised to 100%) half of the cultured cells died during or after exposure to hypoxia (Figure 3b; median of surviving cells = 49.9%). In the presence of EPO, hypoxia-induced neuronal cell death was reduced to approximately 40% (median of surviving cells = 60.3%). EPO significantly increased the survival of primary cultured locust brain neurons under hypoxic conditions. The graphical presentation of all 11 individual experiments in Figure 3c revealed that the neuroprotective effect of EPO ranged from 1.93% to 20.59% compared to non-treated cultures. Only one experiment failed to show a neuroprotective effect of EPO (-3.12%) on cultured insect cells under hypoxic conditions (Figure 3c).

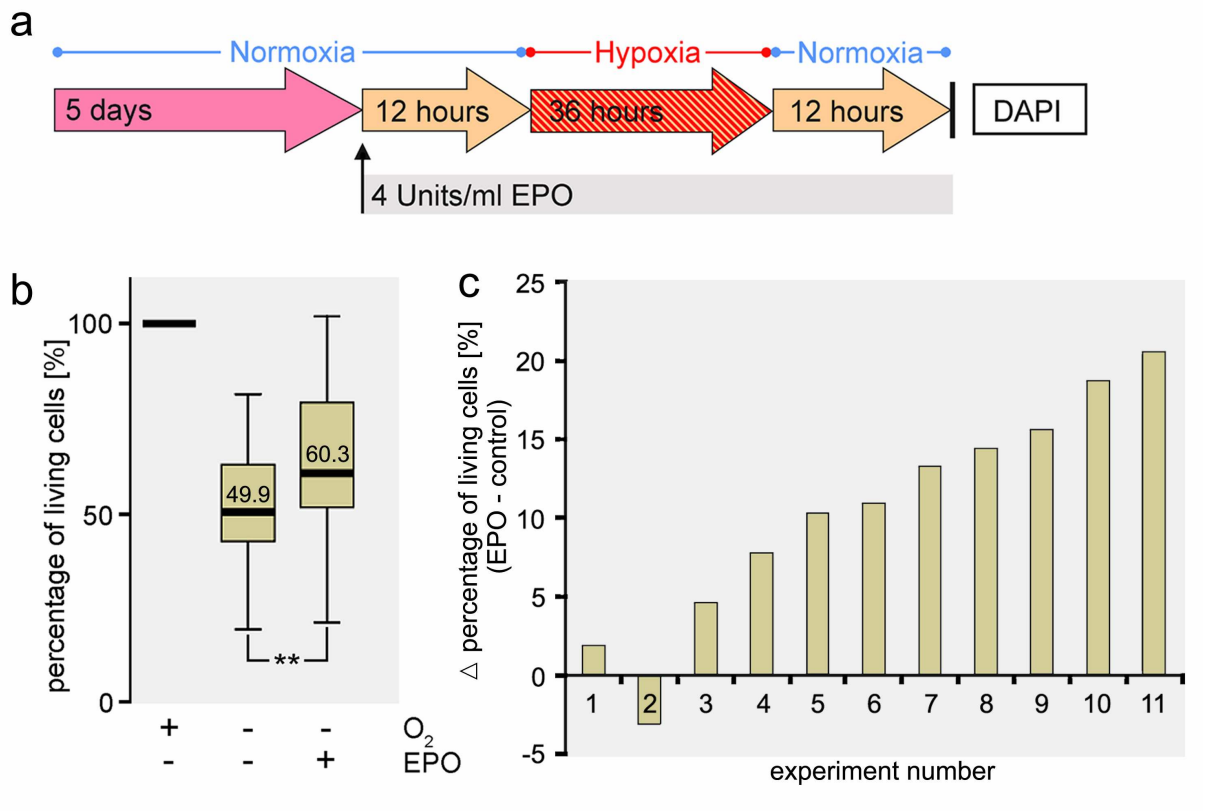


**Figure 3:** Neuroprotective effect of EPO on primary cultured locust brain cells under hypoxic conditions. **a:** Schematic drawing of the experimental procedure. **b:** Percentage of living cells cultured under normoxic conditions (normalised to 100%), hypoxic conditions (median = 49.9%) and hypoxic conditions treated with 4 Units/ml EPO (median = 60.3%) (n = 11, Wilcoxon matched paired signed rank test, **p < 0.01) **c:** Individual experiments sorted and plotted as differences of percentage of living cells of EPO treated cultures and control cultures.

To exclude that the allocation of dissociated locust brain cells and the density of primary cultured cells influenced the vitality of neurons in particular culture dishes, a control experiment was performed (Figure 4). The experimental procedure was similar to that described in Figure 3a (without EPO treatment) and the percentage of living cells was determined in two different areas of the cover slips of each culture dish. Only small variances between both analysed areas within each culture dish and between different culture dishes were detected (Figure 4a). The red line in Figure 4a illustrates the average protective effect of EPO on cultured locust brain cells calculated from previously described exposures to hypoxia (Figure 3)). The results demonstrate that individual cultures, derived from the allocation of cells from 12 locust brains to individual dishes, react similarly to exposure of hypoxia. Small variations in the proportions of living cells after exposure to hypoxia cannot account for the enhanced cellular survival in the presence of EPO.

Furthermore, due to the procedure of cultivation the density of cultured cells can highly vary. High cell densities were usually found in the centre of the cover slips and lower densities in the periphery. The cell cultures used in the control experiment were also evaluated concerning their cell density to exclude a possible influence of cell density on the survival of cultured neurons (Figure 4b). Each dot in the diagram represents the average percentage of living cells in one analysed area (35 - 40 pictures per analysed area) and dots of the same colour indicate data from the same culture dish. The density of analysed cells varied from 10.9 to 26.4 cells/picture. Culture dish number 1 (violet dots) had the lowest density of cultured cells in both analysed areas and contained the lowest percentage of living cells. Culture dish 2 (green dots) contained the highest percentage of living cells but a relatively low density of cultured cells. The lack of a consistent association of cell density and cell survival during hypoxia suggests that small differences in cell densities between different culture dishes have only minor impact (if at all) on cell survival.

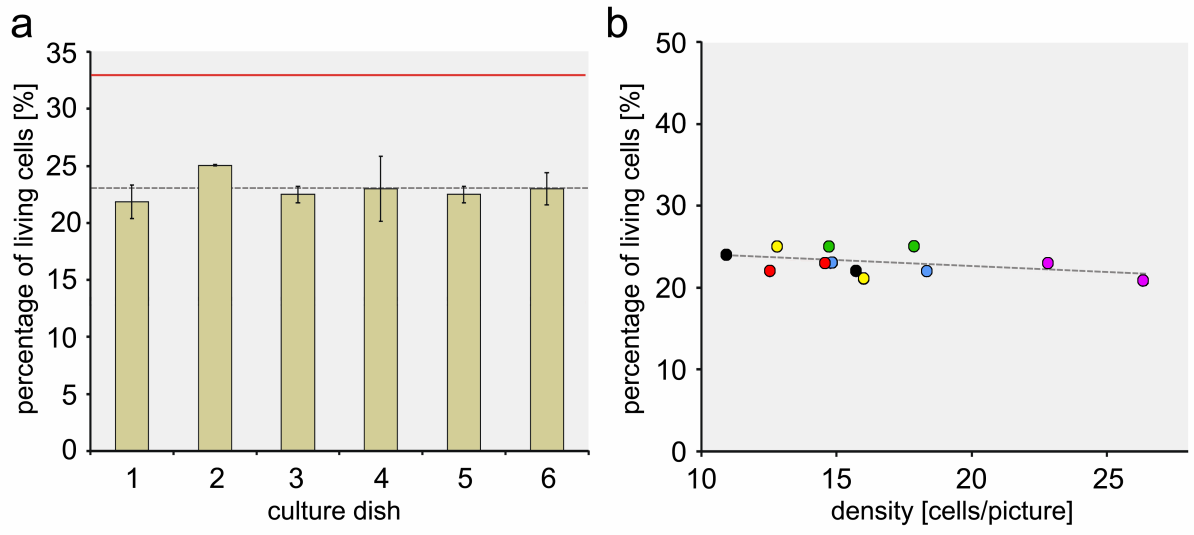


**Figure 4:** Percentage of living locust brain cells cultivated under equal conditions in different culture dishes. **a:** Dissociated brain cells of 12 animals were allocated to six culture dishes and incubated under hypoxic conditions as described in Figure 3a (without EPO treatment). The red line represents the average percentage of surviving cells in the presence of 4 Units/ml EPO, based on the results shown in Figure 3. The dashed line indicates the average percentage of surviving neurons in all six dishes. **b:** Percentage of surviving cells in relation to their density in individual cultures. Dots of the same colour indicate analysed areas of the same culture dish. Experiment numer: 1 (violet dots); 2 (green dots); 3 (blue dots); 4 (yellow dots); 5 (red dots); 6 (black dots)

### 4.3.3 Effects of recombinant human EPO (rhEPO) on the neurite outgrowth of primary cultured locust brain neurons

The brain of locusts is divided into three major regions (Proto-, Deuto- and Tritocerebrum) and each of these divisions consists of a cortex of cell bodies surrounding a core of tracts, commissures and neuropils (see Figure 2a in chapter one of this doctoral thesis). The locust brain contains approximately 360,000 neurons (Burrows, 1996) and various other cells (e.g. glial cells and tracheal cells). After dissociation of a locust brain approximately 200,000 cells adhere to the bottom of the culture dish. Since whole brains of locusts were used for primary cell culture a multitude of neuronal and other cell types were co-cultured in one dish. As expected, the morphology of cultured cells was highly variable (Figure 5). Cultured cells differed greatly in the diameters of their somata that ranged from 9µm to 50µm. Due to the procedure of cultivation most neurites were disrupted from neuronal cell bodies. During the first six hours in culture neurons began to regenerate neurites of variable numbers and shapes. Most of the cultured cells regenerated multiple neurites (Figure 5b-c), but also monopolar (Figure 5d) and bipolar cells (Figure 5d) were observed. In contrast to neuronal cells, cultured glia had a flat shape without a particular partitioning into cell somata and processes (Figure 5f, also see 1.3.3). Since almost all glial cells died within the first 4-6 days (Gocht et al. 2009, also see 1.3.4) this type of cells was only detected fresh primary cultures.

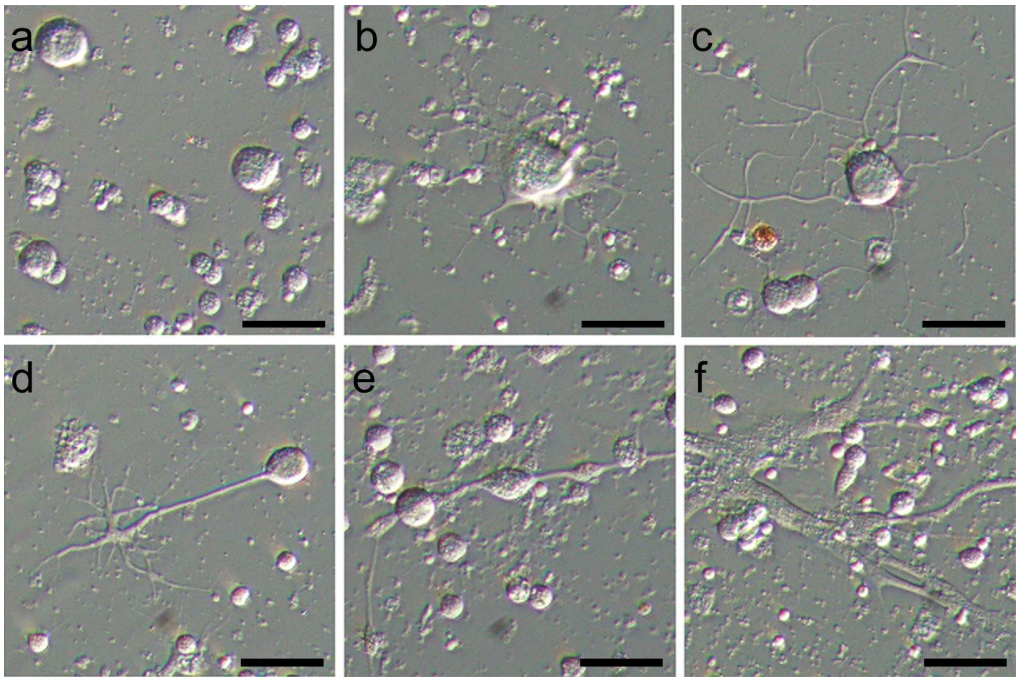


**Figure 5a-f:** Phase contrast pictures of cultured locust brain cells showing various morphological characteristics. Cultured cells differ in the size of their somata (a) and the shape of their regenerated neurites (b-e). Glial cells had a very flat shape with an absent partitioning into cell somata and neurites (f). scale = 50µm

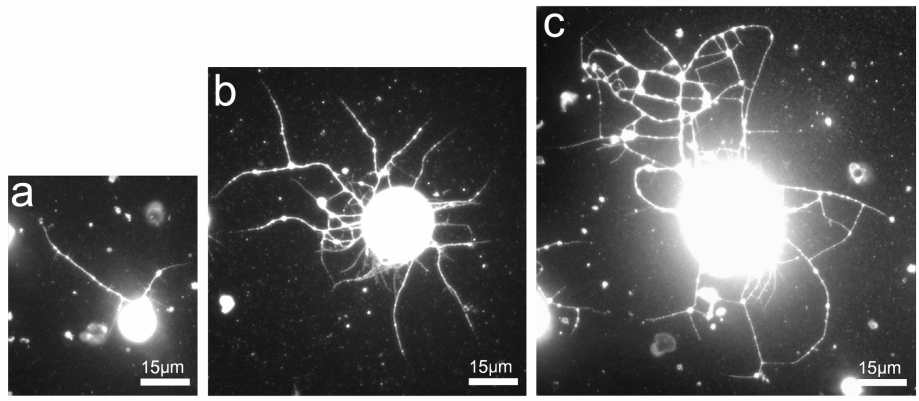


**Figure 6:** Neurite outgrowth from cultured locust brain neurons after five days of cultivation in full medium. **a-c:** Three cultured neurons with different sizes of cell bodies and different numbers and extensions of regenerated neurites.

To quantify the length of regenerated neurites cultured locust brain cells were labelled with anti-HRP serum to visualise even fine neurites. Figure 6 exemplarily shows three different locust brain neurons from the same culture dish that were incubated for five days in full medium. The cells vary in the size of their cell bodies and the length and complexity of regenerated neurites. The diameters of the cells were 12.3µm (Figure 6a), 22.6µm (Figure 6b) and 34.8µm (Figure 6c). The maximal neurite extension (distance between the centre of the soma and the most distantly located part of a neurite) was 44.8µm in the smallest cell, 61µm in the medium cell and 72.2µm in the largest cell suggesting that large neuronal cell bodies may regenerate longer and more complex neurites within certain periods of culturing. Though the extension of regenerated neurites was positively correlated with soma size in the majority of cultured neurons, some cell bodies from the same culture dishes deviated from this general trend. Figure 7 shows four different cells with similar cell body size of approximately 23.7µm diameter whose regenerated neurites extended over largely variable distances (from 21.7µm to 97.3µm). In addition, neurons with the longest extensions of neurites also had the largest number of neurites and the highest complexity of branching patterns.

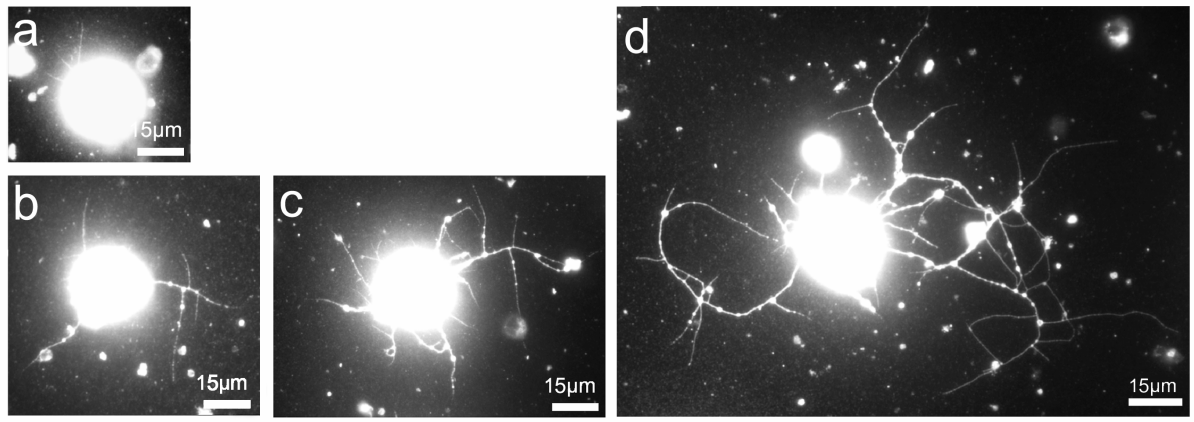


**Figure 7:** Neurite outgrowth of cultured locust brain cells after five days of cultivation in full medium. **a-d:** Maximal distance of neurite extension was 21.7µm in (a), 40.3µm in (b), 50.6µm in (c) and 97.3µm in (d) though all neurons had cell bodies with similar diameters of ~23.7µm.

To analyse the effect of EPO on the regeneration of cultured insect neurons, locust brain cells were cultivated for five days either in deficient medium (control), deficient medium with 4 Units/ml EPO (EPO) or in full medium (FCS). Two experiments were performed and analysed. One aspect of this evaluation was the question, whether EPO may promote the initiation of neurite regeneration, leading to smaller fractions of viable neuronal cell bodies that do not regenerate any neurites. Therefore, the number of viable cells without neurites was counted and related to the overall count of living cells. The results of the two experiments are summarised in Figure 8. In control cultures about 14.4% ± 1.3% of viable cells contained no neurite. Application of EPO did not alter the percentage of viable cells without neurites (13.8% ± 2.7%). Likewise, incubation of cultured cells with FCS also did not decrease or increase the portion of cells without neurites (13.2% ± 2.5%). The results of these experiments indicated that neither EPO nor FCS influenced the initiation of neurite formation.

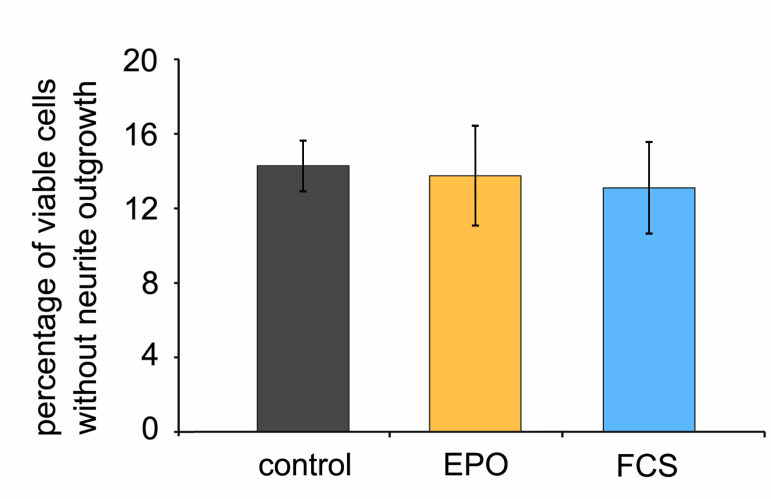


**Figure 8:** Percentage of viable cells without at least one neurite outgrowth in primary cell cultures of locust brains incubated in deficient medium (control, black bar), deficient medium with 4 Units/ml EPO (EPO, yellow bar) and full medium (FCS, blue bar). Each column presents the mean and standard deviation of two individual experiments.

To evaluate whether EPO may promote the extension of neurites in comparison to untreated controls or FCS-treated cultures, two experiments were performed. The diameters of 782 neuronal cell bodies and the distance between the centre of their somata and the most distant neurite (neurite outgrowth) were determined (control: $n_1 = 138$, $n_2 = 98$; EPO: $n_1 = 153$, $n_2 = 109$; FCS: $n_1 = 170$, $n_2 = 114$). The data on neurite elongation of cultured insect cells in dependency of the diameter of their somata are presented in Figure 9. The dot diagram (Figure 9a-a`) displays individual values of all analysed cells. Data of controls are illustrated as black triangles, data of EPO-treated cells are marked as yellow quadrangles and data of cells incubated with FCS are marked as blue diamonds. In general, larger somata generated longer neurites under all three culture conditions in both runs of the experiment which is reflected by the positive slopes of all regression lines (Figure 9a, a`). Data from individual cells from both runs of the experiments are summarised in Figure 9b and 9b` that display the arithmetic mean of soma sizes and maximal neurite extensions and standard deviations of the respective values.

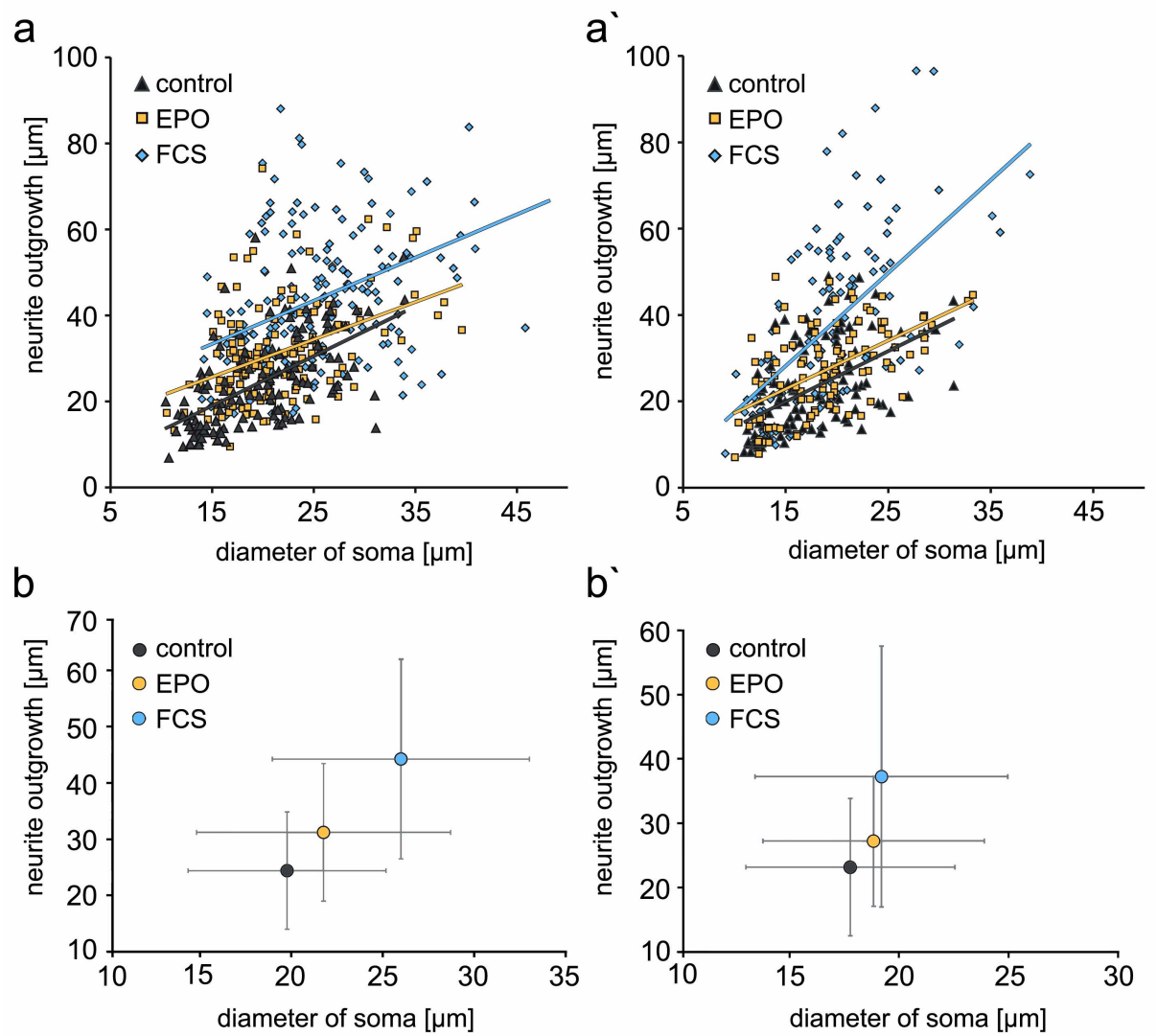


**Figure 9:** Neurite outgrowth of locust brain cells cultured for five days in deficient medium (control), deficient medium with 4 Units/ml EPO (EPO) or full medium (FCS) (For statistical analysis see Figure 10). **a, a`:** Dot diagrams represent individual values of analysed neurons of the control group (black triangle), EPO-treated group (yellow quadrangle) and FCS-treated group (blue diamond). Lines indicate the linear regression of all values from differently treated cultures. **b, b`:** Neurite outgrowth in relation to the diameter of the somata represented as arithmetic mean and standard deviation of controls (black circle), EPO-treated cells (yellow circle) and FCS-treated cells (blue circle).

Cells incubated with deficient medium (controls) had an average neurite extension of 24.2µm ± 10.4µm and an average cell body size of 19.8µm ± 5.4µm (Figure 9b). EPO treatment increased both the neurite outgrowth (31.2µm ± 12.2µm) and the diameter of neurons (21.8µm ± 6.9µm) (Figure 9b). Cells that were incubated with FCS had the largest diameter of cell bodies (25.9µm ± 7.0µm) and the most extended neurites with an average length of 44.3µm ± 17.8µm (Figure 9b). Similar results were found in a second, identically conducted, experiment illustrated in Figure 8b`. The average neurite outgrowth of neurons in control cultures was 23.2µm ± 10.7µm, 27.3µm ± 10.1µm in EPO-treated cultures and 37.3µm ± 20.3µm in FCS-treated cultures. The average diameter of the cell bodies was 17.7µm ± 4.8µm in control cultures, 18.8µm ± 5.1µm in EPO-treated cultures and 19.2µm ± 5.8µm in cultures incubated with FCS.

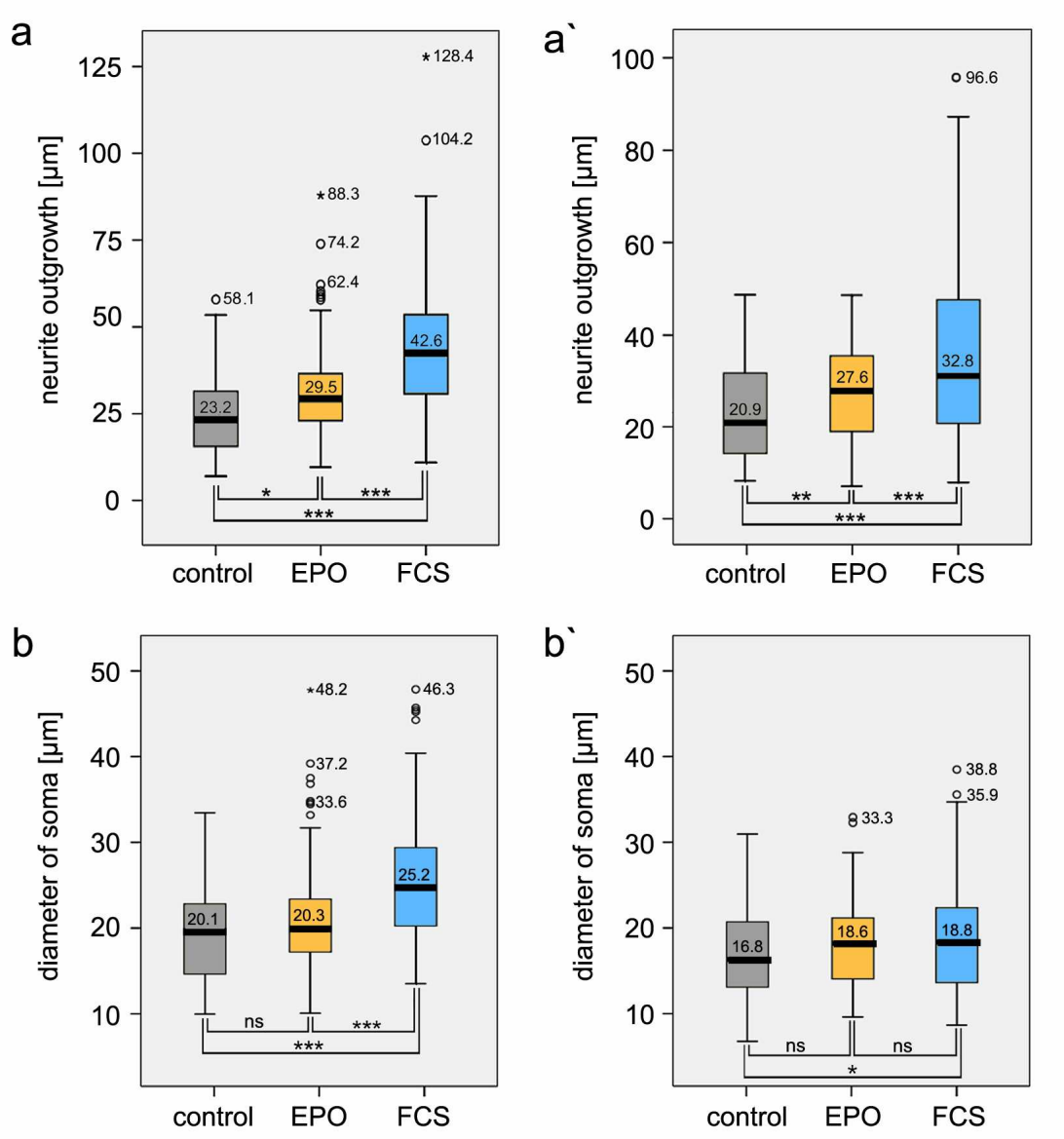


**Figure 10a, a`:** Boxplot diagram of the neurite outgrowth of cultured locust brain cells incubated in deficient medium (control), deficient medium with 4 Units/ml EPO (EPO) and full medium (FCS). Statistical analysis was performed using the Mann-Whitney U-test (*p < 0.05, **p < 0.01, ***p < 0.001). **b, b`:** Boxplot diagram of the cell body diameter of cultured locust brain cells incubated in deficient medium (control), deficient medium with 4 Units/ml EPO (EPO) and full medium (FCS). Statistical analysis was performed using the Mann-Whitney U-test (*p < 0.05, ***p < 0.001).

For statistical analysis data of neurite extensions and diameters of the cell bodies were also presented in boxplot diagrams (Figure 10). A boxplot diagram is a useful tool to compare a set of data of different groups concerning the smallest value (lower whisker), the lower quartile (lower box), the median (black bar), the upper quartile (upper box), the maximum value (upper whisker) and values, which might be considered as outliers (circles and asterisks). Since the data had no normal distribution (tested with the Kolmogorov-Smirnov test) a non-parametric test for independent samples (two-tailed Mann-Whitney U-test) was used to analyse significant differences between controls, EPO-treated and FCS-treated cultures. Concerning the neurite outgrowth, EPO treatment significantly enhanced the regeneration of neurites in comparison to control cultures (Figure 10a with *p < 0.05,

Figure 10a` with **p < 0.01). The treatment with FCS caused a highly significant increase of the neurite outgrowth in comparison to control and EPO-treated cultures of both experiments (Figure 10a, a` with ***p < 0.001). Concerning the cell body diameters of cultured cells, a significant differences were only detected between FCS-treated cultures and both EPO-treated and control cultures in the first experiment (Figure 10b) and between FCS-treated cultures compared to control cultures in the second experiment (Figure 10b`). EPO treatment had no effect on the diameter of cultured neurons compared to non-treated cells.

### 4.3.4 Effects of EPO on the survival of glial cells in primary cell cultures from locust brains

Locust brain cells were prepared for primary cell culture and incubated for three days either in full medium with or without EPO (4 Units/ml) or in deficient medium with or without EPO. The portion of glial cells among all viable cells in the culture was counted in three independent experiments (Figure 11a, each column represents the data of two analysed culture dishes).

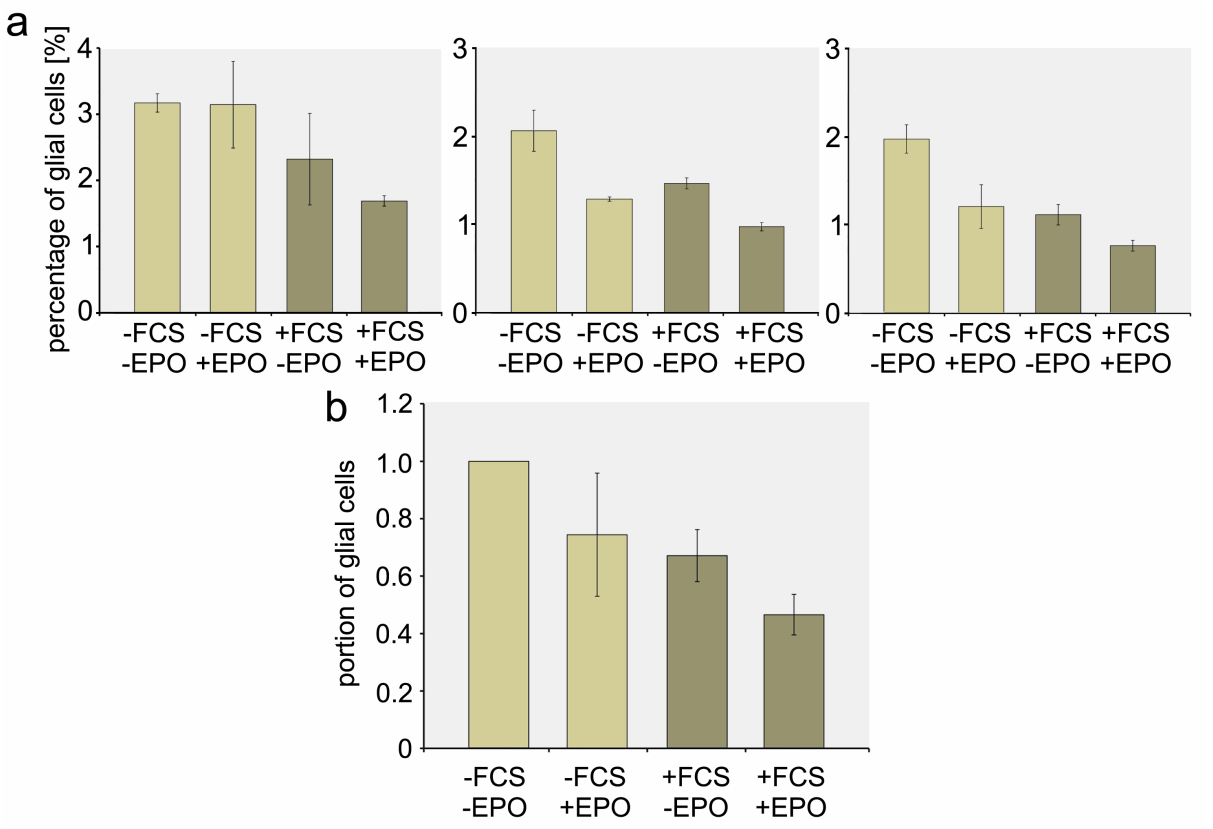


**Figure 11a, b:** Portion of viable cells in primary cultures from locust brains after three days of cultivation in deficient medium (-FCS, bright bars) with and without EPO (4 Units/ml) and in full medium (+FCS, dark bars) with or without EPO. Three individual experiments (a) (each column represents the data of two analysed culture dishes) are combined in b. The proportion of glial cells in -FCS/-EPO cultures was normalised to 1.0.

Primary cultures incubated with deficient medium contained the highest proportions of viable glial cells in all experimental runs (Figure 11a, -FCS / -EPO). EPO treatment with 4 Units/ml

either had no effect on glial cell abundance (Figure 11a, first experiment) or decreased the portion of glial cells (Figure 11a, second and third experiment). FCS treatment decreased the portion of glial cells in all three series (Figure 11a). The combination of EPO and FCS treatment reduced the proportion of glia more than each substance alone. In Figure 11b the data of the three independent experiments are combined and the portion of glial cells incubated in deficient medium was normalised to 1.0. The incubation of primary cultured insect cells with EPO caused an average decrease of viable glial cells to 0.7 ± 0.3. The average portion of viable glial cells in FCS-treated cultures was 0.63 ± 0.1 and additional application of EPO reduced the average portion of glial cells to 0.43 ± 0.1. These results indicate that both EPO- and FCS-treatment mediate unfavourable culture conditions, which decrease the survival of locust brain glial cells in primary cultures.

### 4.3.5 Effects of recombinant human EPO (rhEPO) on the neuronal *Drosophila* cell line ML-DmBG2-c2

The use of primary cell cultures from locust brains to study the potential of EPO to mediate neuroprotection and to support neuronal regeneration revealed some disadvantages such as the relatively small number of cells obtained from individual brains, the heterogeneity of neurons and other cells from different regions of the brain and limited lifespan of primary cultured neurons. Therefore, the usefulness of a stable neuronal cell line for further studies on EPO/EPOR signalling in insect nervous systems was explored in a series of initial experiments. The ML-DmBG2-c2 cell line was cloned from the nervous system of an embryonic *Drosophila melanogaster* male (Ui-Tei et al. 2000).

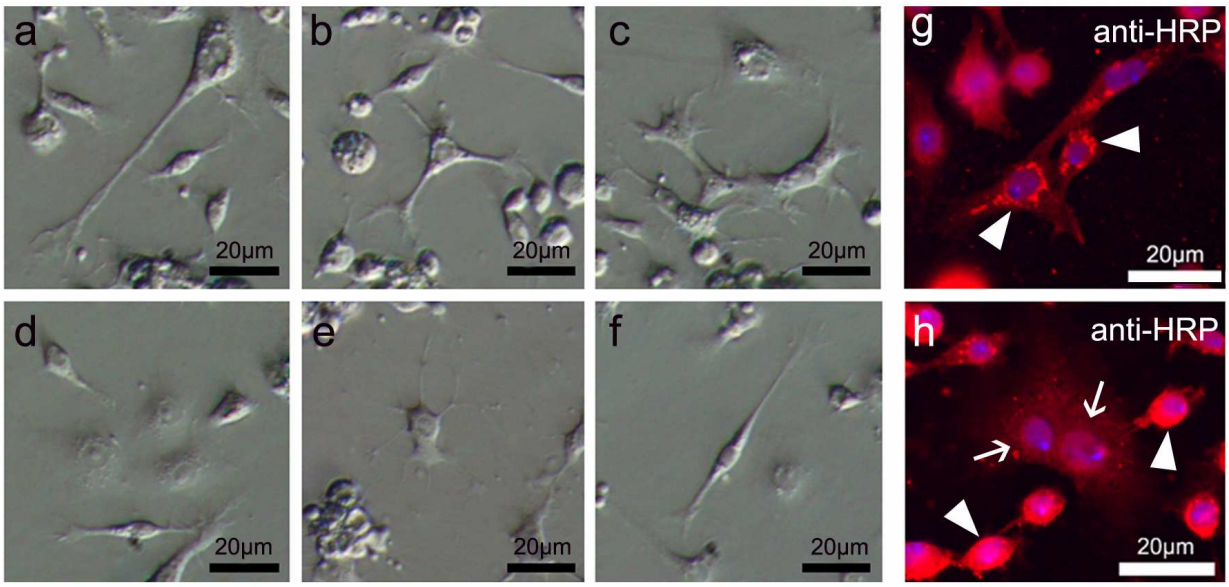


**Figure 12a-f:** Phase contrast pictures of cultured ML-DmBG2-c2 cells showing different morphological characteristics. **g, h:** ML-DmBG2-c2 cells labelled with the neuronal marker anti-HRP (red fluorescence) and the nuclear marker DAPI (blue fluorescence). Cultured cells contain a granular (g, white arrowheads), homogeneous (h, white arrowheads) or no anti-HRP staining (h, white arrows).

An overview of the different morphological characteristics of these permanently cultured cells is presented in Figure 12a-f. The neurons generate monopolar (Figure 12a), bipolar (Figure 12f) or multipolar (Figure 12b, c, e) neurites that establish intimate contact to the bottom of the culture dish. Some of the cells had a flat shape with rather diffuse borders (Figure 12d, centre). In order to evaluate whether the *Drosophila* cell cultures were pure neuronal cultures or also contained glial cells, cultures were labelled with the neuronal marker anti-HRP. Figure 12g-h displays cultured ML-DmBG2-c2 cells that were labelled with the nuclear marker DAPI (blue fluorescence) and anti-HRP serum (red fluorescence). In most of the HRP-labelled cells, fluorescence was homogeneously distributed over the entire cells (Figure 12h, white arrowheads). Some cells contained accumulations of immunoreactive material in the cytosol of their cell bodies (Figure 12g, white arrowheads). Only few cells with large cytoplasmic regions surrounding the nucleus lacked a distinct immunoreactivity for the neuronal marker (Figure 12h, white arrows). Therefore, neurons represent the vast majority of cells in ML-DmBG2-c2 permanent cell cultures but few cells of other types are also present.

To investigate a potential neuroprotective effect of EPO on cultured ML-DmBG2-c2 cells, cell cultures were initially treated with different concentrations of EPO (ranging from 0.1 to 200 Units/ml) to generate a dose-response curve. Cells were plated at a density of $10^6$ cells/ml and incubated for three days in deficient medium with different concentrations of EPO. The cell vitality was determined using the MTT assay and the results are presented inFigure 13. Low concentrations of EPO (0.1 - 5 Units/ml) had no effect on the vitality of cultured cells. The application of 10 Units/ml EPO increased the vitaility of cell cultures to 118% ± 6%. The maximal effect of EPO was found for 40 Units/ml (120% ± 7%). Positive effects on culture vitality were reduced in the presence of 50 Unit/ml and 100 Units/ml EPO. Doses of 200 Units/ml EPO reduced the vitality to 93% ± 8% of control levels without EPO.

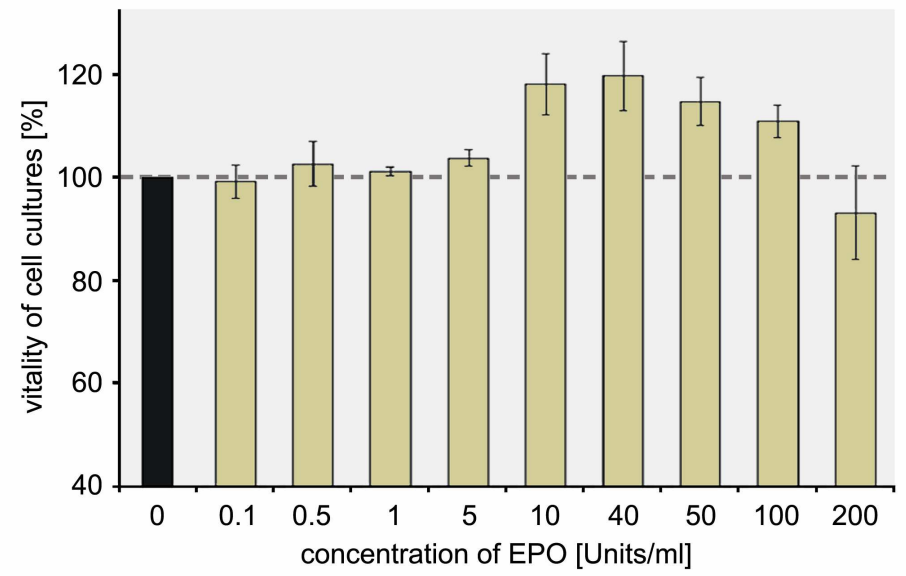


**Figure 13:** Effect of EPO on the vitality of cultured ML-DmBG2-c2 cells. Vitality of cell cultures was determined by MTT assay.

For comparison with the studies carried out with primary cell cultures of locust brain cells, the potential neuroprotective effect of EPO on cultured ML-DmBG2-c2 cells under hypoxic conditions was investigated. First experiments were performed with hypoxic episodes of 24

hours and analysis of cell vitality with the MTT assay was determined after 12 hours following the end of the hypoxic stimulus. Hypoxia for 24 hours reduced the vitality of the cultured cells (compared to cells cultured in normoxia) to 79.8% (Figure 14a), 74.8% (Figure 14d), 60.8% (Figure 14c) and 41.8% (Figure 14b). Application of EPO at concentrations of 0.4, 4 and 10 Units/ml had no effect on the vitality of cultured cells following hypoxic conditions. A slight increase of the average cell vitality by 11.3% was only detected in cultures treated with 40 Units/ml EPO (Figure 14d).

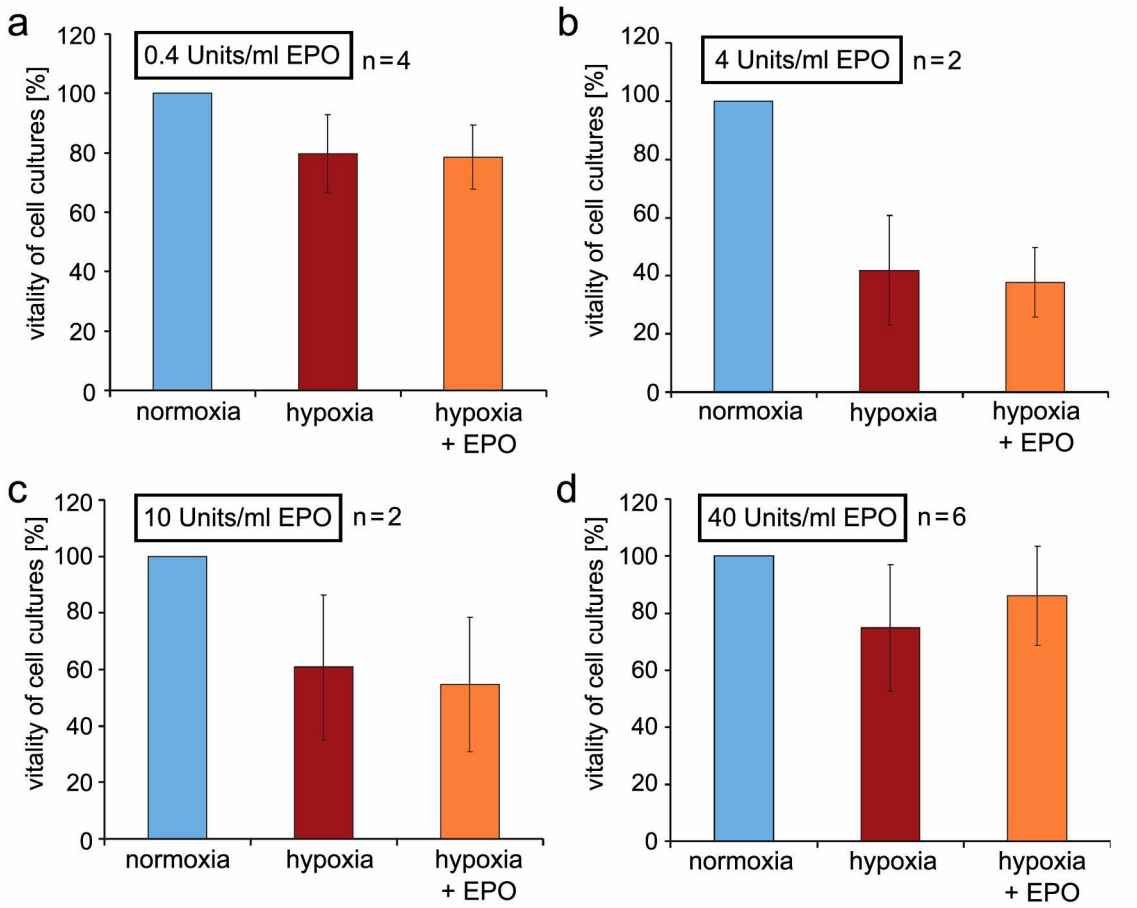


**Figure 14a-d:** Neuroprotective effect of EPO on cultured ML-DmBG2-c2 cells during and after 24 hours of hypoxia. Analysis was performed after 12 hours following the end of the hypoxic period.

Since it appeared that the cell line was more robust to hypoxia than previously studied primary cultured locust brain neurons, ML-DmBG2-c2 cell cultures were exposed to repeated episodes of hypoxia (Figure 15a, b). Hypoxic periods of either 6 or 15 hours were repeated for three times with normoxic intervals of 18 (for 6h of hypoxia) or 9 hours (for 15h of hypoxia). A three times repeated hypoxic/normoxic episode of 6h/18h decreased culture vitality to 71.7% ± 8.8% compared to cultures incubated for the same overall duration under normoxic conditions (normalised to 100%). Application of 40 Units/ml of EPO increased the vitality of hypoxia-exposed cells to 98.8% ± 18.6% (Figure 15a). Repeated hypoxic/normoxic intervals of 15h/9h decreased the average cell vitality to 47.3% ± 8.2% compared to cultures

incubated under constant normoxia (normalised to 100%). Application of 40 Units/ml of EPO increased the vitality of cultured cells to 75.9% ± 8.4% (Figure 15b).

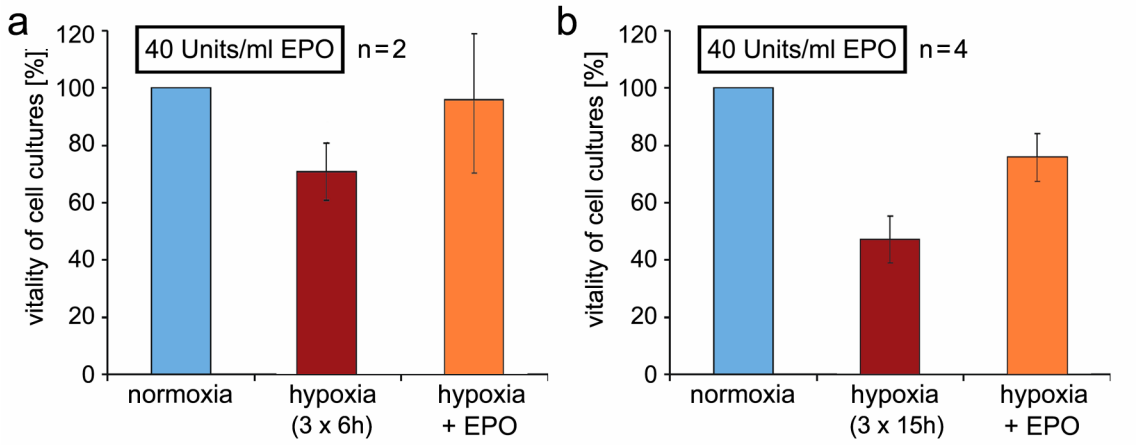


**Figure 15a, b:** Neuroprotective effect of EPO on cultured ML-DmBG2-c2 cells after hypoxic episodes of 3 x 6 hours (a) or 3 x 15 hours (b). Analysis was performed after 12 hours following the end of the hypoxic period.

# 4.4 Discussion

*Neuroprotective effects of exogenous EPO*

Numerous studies investigated the neuroprotective effect of EPO on neuronal cells of mammals. In these studies the most effective concentrations of EPO varied with respect to the species studied, the nervous region investigated and the type of experimentally applied injury. Nevertheless, all studies reported a range of optimal concentrations of EPO that mediate the maximal neuroprotective effect, therewith both lower and higher concentrations being less effective. Axonal degeneration of cultured dorsal root ganglia neurons was maximally reduced in the presence of 1-10pM EPO while higher doses (>100pM) mediated no protective effect (Keswani et al. 2004). Weishaupt et al. (2004) reported a bell-shaped dose-response curve of EPO on the survival rate of cultured retinal ganglion cells (RGCs) of rats. RGCs were cultured without neurothrophic support and EPO was applied in concentrations ranging from 0.1 to 1 Units/ml. The maximal neuroprotective effect of EPO was found at a concentration of 0.6 Units/ml. In undifferentiated P19 teratoma cells EPO prevents apoptosis (induced by 24h serum withdrawal) in a dose-dependent manner (Sirén et al. 2001). The optimal protective effect of EPO was found at concentrations of 1 Unit/ml and both higher and lower doses of EPO (10/0.1 Units/ml) reduced the beneficial effect. The dose-dependent effect on the proliferation of mice cultured embryonic neuronal progenitor cells (NPCs) was demonstrated by Chen et al. (2007). Maximal proliferation of NPCs was induced by EPO concentrations of 10 Units/ml, while 5, 20 and 40 Units/ml stimulated proliferation less effectively and even lower concentrations of EPO had no effect. Treatment with different concentrations of EPO protected cultured cortical neurons of rats against chemical hypoxia-induced damage (Wen et al. 2002). The most effective concentration range was $10^{-4}$ – $10^{-2}$ Units/ml, while higher and lower EPO concentrations were ineffective. EPO-treatment of cultured cortical neurons of embryonic rats under hypoxic conditions (2% $O_2$; 5% $CO_2$; 93% $N_2$) enhanced neuronal survival with an optimum effect of EPO at concentrations of 0.1 Units/ml (Liu et al. 2006). Higher concentrations of EPO (1, 10 Units/ml) were ineffective to increase neuronal survival compared to non-treated cultures. Shang et al. (2007) showed that EPO mediated dose-dependent neuroprotective effects on cultured cortical rat neurons during ketamine-induced cytotoxicity. All EPO concentrations used in that study (0.3, 1, 3, 10 Units/ml) reduced neuronal death and maximal protection was mediated by a concentration of 1 Unit/ml EPO. In addition, an *in vivo* study of Sakanaka et al. (1998) showed that EPO rescued hippocampal CA1 neurons from lethal ischemic damage and prevented ischemia-induced learning disability. The infusion of EPO was most effective at concentrations of 2.5, 5 and 25 Units/day but ineffective at higher doses of 50 and 500 Units/ml EPO.

Several authors discussed the dose-dependency of EPO`s neuroprotective effects of EPO. Sakanaka et al. (1998) assumed that the *in vivo* injection of high doses of EPO may cause a down-regulation of EPOR leading to subsequent loss of responsiveness to EPO. In

primary hippocampal neuronal cultures of newborn rats the bell-shaped dose-response curve of EPO may be explained by cross-binding of EPO to the thrombopoietin receptor (TPOR) whose ligand binding domain is similar to that of EPOR (Ehrenreich et al. 2005). Since TPO induces pro-apoptotic signalling cascades in cells of the nervous system the gradual loss of the protective effect of EPO with increasing concentrations can be explained by increased binding of EPO to TPOR. Other substances that mediate neurotrophic actions (e.g. basic fibroblast growth factor, interleukins, tumor necrosis factor, prosaposin and immunophilin ligands) were also reported to act most potently in a particular range of concentrations (Morrison et al. 1986; Rousselet et al. 1988; Araujo & Cotman 1991; Araujo & Cotman 1993; Kotani et al. 1996; Keswani et al. 2003). Similar to the neuroprotective effects of EPO, the mechanisms underlying this phenomenon are largely unknown.

This study investigated a dose-response effect of EPO on neuroprotection of primary cultured insect neurons and an insect neuronal cell line. Similar to the studies on mammalian nervous systems described above, EPO mediated its protective effects most effectively at a particular concentration. In primary cultured locust brain cells the optimal effect of EPO emerged at concentrations of 0.4 and 4 Units/ml, which is similar to the average optimum concentrations of EPO that mediates neuroprotection in cultured mammalian neurons (as described above). In contrast to primary cultured neurons from locust brains the *Drosophila*-derived neuronal cell line ML-DmBG2-c2 required a concentration of 40 Units/ml EPO for optimal effects on the vitality of cells. Whether this difference simply results from higher densities of cultured Drosophila neurons (1,000,000 cells/$cm^2$) compared with the densities of locust brain primary cultures (65,000 cells/$cm^2$) or whether differences of EPO signalling components (e.g. affinity of EPO to *ia*EPOR, level of *ia*EPOR expression) between insect species or types of neurons exist, remains to be investigated. The results of this study suggested a harmful effect of high doses of EPO (200 Units/ml) on ML-DmBG2-c2 cells. Similar observations were made by Weber and coworkers (Weber et al. 2005) who demonstrated toxic effects of high EPO concentrations (≥10 Units/ml) on cultured rat cortical neurons exposed to hypoxia. The authors proposed that hypoxia induced enhanced EPOR expression in cultured neurons and subsequent overstimulation by high doses of EPO evoked apoptosis. Whether overstimulation of EPO-responsive neurons leading to apoptosis may be the reason for decreased vitality of the *Drosophila*-derived neuronal cell line is presently unknown. Respective studies could be initiated by the identification of the receptor that mediates EPO effects in the nervous system of insects. Whether this receptor is a homologue of the EPOR involved in vertebrate erythropoiesis or a different receptor with an EPO binding domain remains to be evaluated.

*Effects of exogenous EPO on cultured cells under hypoxic conditions*

Various studies revealed neuroprotective effects of exogenous EPO on cultured cells of mammalian nervous tissue during and after episodes of hypoxia. Sirén et al. (2001) demonstrated that EPO-treatment (0.3 Units/ml) of cultured rat hippocampal neurons under hypoxic conditions (for 15 hours) decreased the amount of cell death from 55% to 30% of

cultured neurons. In cultured cortical neurons of adult rats episodes of chemically induced hypoxia (induced by rotenone + 2-DG) for 1 hour reduced the intensity of anti-MAP2 stained protein bands (neuronal marker) to ~50% compared with cultures that were not exposed to hypoxia (Wen et al. 2002). Application of 0.01 Units/ml EPO increased the protein band intensity to ~95%. The incubation of cultured rat neurons with 30pM EPO protected the cells against hypoxia/glucose deprivation-induced cell death (Sinor & Greenberg 2000). EPO-treatment increased cell viability (assayed by Almar blue fluorescence) to 96.9% compared to 78.6% in non-treated cultures. Lewczuk et al. (2000) revealed a protective effect of 100pM EPO on primary cultured rat hippocampal neurons after a hypoxic period of 120min (8% $O_2$). The neuronal death decreased from 56.75% (without EPO-treatment) to 33.0% (with EPO-treatment). Furthermore, Ruscher et al. (2002) demonstrated a 75% increase of neuronal viability in EPO-treated (0.1 Units/ml) primary cultured rat cortical cells after oxygen/glucose deprivation compared to control cultures.

The present study investigated the neuroprotective effect of EPO on cultured insect neurons under hypoxic conditions. After a hypoxic episode of 36 hours the increased percentage of living cells in EPO-treated locust brain cultures (compared to non-treated cells) ranged from 1.93% to 20.59% in 11 individual experiments. This variability of the neuroprotective effect of EPO may be due to the variance of cell types cultivated in primary cell cultures. All previous studies that analysed the neuroprotective effect of EPO in mammals used neuronal cell lines of the same cell type or primary cultured cells of one specific region of the mammalian brain (e.g. hippocampus). The primary cell cultures used in this study consisted of mixtures of all locust brain cells. It is unlikely that all cultured brain cells express the *ia*EPOR that mediates the effects of EPO in the same fashion. Since EPO can only mediate a neuroprotective effect via *ia*EPOR, the range of the protective effect depends on the portion of *ia*EPOR-expressing cells in a particular culture. Additional studies have to be performed to analyse the number of *ia*EPOR-expressing cells in primary cultures of locust brain cells and the changes of *ia*EPOR expression after episodes of hypoxia. Sinor and Greenberg (2000) demonstrated that EPO protects primary cultured rat neurons, but not astrocytes, from hypoxia. This indicates that EPO mediates its neuroprotective effect not on all brain cell types, especially not on glial cells. In a locust brain about one third of all cells are of glial type (Gocht et al. 2009; also see 1.3.2 of this doctoral thesis). Primary cultures of freshly dissociated brain cells contained 25.1% glia, but during the first six days of cultivation almost all glial cells died (Gocht et al. 2009; also see 1.3.4 of this doctoral thesis). Application of EPO and/or FCS to cultured locust brains cells further decreased the portion of glial cells in primary cultures of locust brains (Figure 11). Since all cell cultures were subjected to hypoxia after five days of cultivation in culture medium with FCS the portion of glial cells at the time of evaluation should be insignificant. Although the neuroprotective effect of exogenous EPO on primary cultured locust brain cells is variable the results of this study indicate that the signalling cascades by which EPO mediates its neuroprotective effect in the nervous systems of mammals may also be present in insect nervous cells.

The protective effect of exogenous EPO against hypoxia-induced damage of cultured neurons is not only dose-dependent as described above, but also time-dependent. The time

of EPO application is important for its neuroprotective effect on neuronal cells. In cultured cortical neurons of embryonic rats transient oxygen/glucose deprivation reduced neuronal viability to 26% (compared to control cultures = 100%) (Meloni et al. 2006). The incubation of EPO (0.5 Units/ml) increased cell viability to a range of 61% - 89% in dependency of the period of EPO preincubation. Preincubation of ´only` eight hours prior to oxygen/glucose deprivation had a lower protective effect (61% cell viability) than EPO preincubation for a longer period (12 and 24 hours up to 89% viability). The authors assumed that prolonged periods of EPO preincubation caused a higher expression of EPO receptor controlled target genes leading to enhanced accumulation of proteins that mediate anti-apoptotic effects. Ruscher et al. (2002) demonstrated on primary cultured rat cortical cells that preincubation of EPO (0.1 Units/ml) in the period of 5min to 72 hours before oxygen/glucose deprivation mediated some neuroprotection, but the optimal effect appeared following preincubation for 48 hours. In contrast to these results, Liu et al. (2006) demonstrated that 24 hours of EPO preincubation of cultured cortical neurons of embryonic rats had no effect on neuronal survival after hypoxic episodes. Only preincubation of 0.1 Units/ml EPO for relatively short periods prior to the hypoxic period (6, 3, 1 or 0 hours) increased neuronal survival to 63.9%, compared to 34.4% in non-treated cultures. Although the above mentioned studies were conducted on similar cell culture preparations and used similar concentrations of EPO, preincubation periods that mediates maximal neuroprotectionto subsequent hypoxia were clearly different. In this study the neuroprotective effect of EPO on primary locust brains cells and a neuronal *Drosophila* cell line was demonstrated (Figure 3b, 14e-f). EPO was preincubated in all experiments for 12 hours prior hypoxia. Since the neuroprotective effect of EPO is time-dependent in neuonal cultures of mammals, future studies have to analyse whether neuroprotective effects of EPO on cultured insect neurons are altered with different periods of EPO pre-exposure.

*Effects of exogenous EPO on neurite outgrowth of primary cultured locust brain neurons*

One of the first studies that analysed the neurite outgrowth of mammalian neuronal cells *in vitro* was performed by Böcker-Meffert et al. (2002). In rat retinal explants EPO-treatment enhanced neurite elongation after three days of cultivation to 169% (compared to non-treated explants = 100%). The promotive effect of EPO on the regeneration of neurites was dose-dependent, with a half-maximum concentration ($EC_{50}$) of $7.8 \times 10^{-15}$M. Another study of Kretz et al. (2005) analysed the neurite outgrowth of cultured retinal ganglion cells (RGC) after five days of cultivation. They demonstrated that EPO-treatment both induces and enhances neurite outgrowth of RGCs. The number of ganglion cells that regenerated neurites was increased by a factor of 2.66 in the presence of EPO (10 Units/ml EPO) compared to non-treated cultures and the neurite length increased to 8.31 fold at EPO concentrations of 1000 Units/ml. In a similar study, the application of 6 Units/ml EPO on cultured retinal neurons enhanced neurite outgrowth to 162% compared to control cultures (Zhong et al. 2007).

In this study potential effects of EPO on the initiation and elongation of regrowing neurites were investigated in primary cultures from locust brains. In contrast to the study of Kretz et al. (2005) on rat retinal ganglion cells, EPO treatment had no effect on the proportion

of locust brain cells that regenerated at least one neurite (Figure 8). Whether higher concentrations of EPO may initiate the reestablishment of neurites is presently unknown. However, EPO treatment promoted the elongation and complexity of neurites of cultured locust neurons to approximately 129% compared to untreated control cultures (=100%). Enhancement of neurite outgrowth in primary cultured insect neurons is smaller compared with that of cultured rat retinal cells (129% versus ~165%). But in studies of mammalian retinal neurons the EPO concentrations were very high (up to 1000 Units/ml, Kretz et al. 2005). In contrast to the loss of the neuroprotective effect of EPO using high concentrations, increasing EPO concentrations did not impair the promotion of neurite outgrowth. One interpretation could be, that EPO-mediated promotion of neurite extension may depend on different signalling pathways than EPO-mediated neuroprotection. The promotive effect of EPO on neurite outgrowth on cultured locust brain cells was performed with concentrations (4 Units/ml) that mediated optimal neuroprotective effects on freshly dissociated and hypoxia-treated locust neurons. It may be quite possible that the applied dose of EPO, though optimal for neuroprotection, may have been too low to mediate full support of neurite regeneration. That locust neurons can grow faster into more complex arborisation patterns has been demonstrated by FCS-treatment, which increased neurite extensions to ~170% compared to cultured neurons without FCS.

In summary, first *in vitro* approaches to study the effects of EPO on cultured insect neurons revealed similar results as demonstrated in *in vitro* studies of mammalian neurons. The results of this study indicated both a protective effect mediated by EPO on primary cultured locust brain cells and a neuronal *Drosophila* cell line (under normoxic and hypoxic conditions), and a promotive effect of EPO on the regeneration of neurite extensions of locust brain cultures.

# 4.5 References


Anagnostou A, Liu ZY, Steiner M, Chin K, Lee ES, Kessimian N, Noguchi CT (1994) Erythropoietin-receptor mRNA expression in human endothelial cells. Proc Natl Acad Sci USA 91:3974 -3978

Araujo DM & Cotman CW (1991) Effects of lymphokines on glial and neuronal cells *in vitro*: a role for lymphokines as modulators of neural-glial interactions. Soc Neurosci Abstr 17/1199

Araujo DM, Cotman CW (1993) Trophic effects of interleukin-4, -7 and -8 on hippocampal neuronal cultures: potential involvement of glial-derived factors. Brain Res 600*:*49–55

Arcasoy MO (2008) The non-haematopoetic biological effects of erythropoietin. Bri J of Haematol 141:14-31

Bernaudin M, Bellail A, Marti HH, Yvon A, Vivien D, Duchatelle I, Mackenzie ET, Petit E (2000) Neurons and astrocytes express EPO mRNA: Oxygen-sensing mechanisms that involve the redox-state of the brain. Glia 30:271-278

Bernaudin M, Bernaudin M, Marti HH, Roussel S, Divoux D, Nouvelot A, MacKenzie ET, Petit E (1999) A potential role for erythropoietin in focal permanent cerebral ischemia in mice. J Cereb Blood Flow Metab 19:643–651

Böcker-Meffert S, Rosenstiel P, Röhl C, Warneke N, Held-Feindt J, Lucius R (2002) Erythropoietin and VEGF promote neural outgrowth from retinal explants in postnatal rats. Invest Ophthalmol Vis Sci 43:2021–2026

Brines ML, Ghezzi P, Keenan S, Agnello D, de Lanerolle NC, Cerami C, Itri LM, Cerami A (2000) Erythropoietin crosses the blood–brain barrier to protect against experimental brain injury. Proc Natl Acad Sci USA 97:10526-10531

Brines A, Grasso G, Fiordaliso F, Sfacteria A, Ghezzi P, Fratelli M, Latini R, Xie QW, Smart J, Su-Rick C, Pobre E, Diaz D, Gomez D, Hand C, Coleman T, Cerami A (2004) Erythropoietin mediates tissue protection through an erythropoietin and common β-subunit heteroreceptor. Proc Natl Acad Sci USA 101(41):14907-14912

Buemi M, Cavallaro E, Floccari F, Sturiale A, Aloisi C, Trimarchi M, Grasso G, Corica F, Frisina N (2002) Erythropoietin and the brain: from neurodevelopment to neuroprotection. Clin Sci (Lond) 103:275-282

Burrows M (1996) The neurobiology of an insect brain. Oxford: Oxford UP

Chattopadhyay A, Choudhury TD, Bandyopadhyay D, Datta AG (2000) Protective effect of erythropoietin on the oxidative damage of erythrocyte membrane by hydroxyl radical. Biochem Pharmacol 59:419–425

Chen ZY, Asavaritikrai P, Prchal JT, Noguchi CT (2007) Endogenous Erythropoietin Signaling Is Required for Normal Neural Progenitor Cell Proliferation. J Biol Chem 282:25875-25883

Choi DW (1992) Excitotoxic cell death. J Neurobiol 23:1261–1276

Choi DW (1995) Calcium: still center-stage in hypoxic-ischemic neuronal death. Trends Neurosci 18:58–60

Choi DW (1996) Ischemia-induced neuronal apoptosis. Curr Opin Neurobiol 6:667–72.

Chou CF, Tohari S, Brenner S, Venkatesh B (2004) Erythropoietin gene from a teleost fish, *Fugu rubripes*. Blood 104:1498-1503

Chu CY, Cheng CH, Chen GD, Chen YC, Hung CC, Huang KY, Huang CJ (2007) The zebrafish erythropoietin: Functional identification and biochemical characterization. FEBS Letters 581:4265-4271

Dame C, Juul SE, Christensen RD (2001) The biology of Erythropoietin in the central nervous system and its neurotrophic and neuroprotective potential. Biol Neonate 79:228-235

Digicaylioglu M, Lipton SA (2001). Erythropoietin-mediated neuroprotection involves cross-talk between Jak2 and NF-$_K$B signalling cascades. Nature 412:641 -647

Digicaylioglu M, Bichet S, Marti HH, Wenger RH, Rivas LA, Bauer C, Gassmann M (1995) Localization of specific erythropoietin binding sites in defined areas of the mouse brain. Proc Natl Acad Sci USA 92:3717–3720

Digicaylioglu M & Lipton SA (2001) Erythropoietin-mediated neuroprotection involves cross-talk between Jak2 and NF-$_K$B signalling cascades. Nature 412:641–647

Ehrenreich H, Hasselblatt M, Knerlich F, von Ahsen N, Jacob S, Sperling S, Woldt H, Vehmeyer K, Nave KA, Sirén AL (2005) A hematopoietic growth factor, thrombopoietin, has a pro-apoptotic role in the brain. Proc Natl Acad Sci USA 102:862–867

Genc S, Koroglu TF, Genc K (2004) Erythropoietin and the nervous system. Brain Res 1000:19-31

Gocht D, Wagner S, Heinrich R (2009) Recognition, presence, and survival of locust central nervous glia *in situ* and *in vitro.* Mic Res Tech 72(5):385 - 397

Ivan M, Kondo K, Yang H, Kim W, Valiando J, Ohh M, Salic A, Asara JM, Lane WS, Kaelin WG (2001) HIF-targeted for VHL-mediated destruction by proline hydroxylation: implications for O2 sensing. Science 292:464–468

Jaakkola P, Mole DR, Tian JM, Wilson MI, Gielbert J, Gaskell SJ, Kriegsheim von A, Hebestreit HF, Mukherji M, Schofield CJ, Maxwell PH, Pugh CW, Ratcliffe PJ (2001) Targeting of HIF-α to the von Hippel-Lindau Ubiquitylation Complex by $O_2$-Regulated Prolyl Hydroxylation. Science 292 (5516):468-472

Junk AK, Mammis A, Savitz SI, Singh M, Roth S, Malhotra S, Rosenbaum PS, Cerami A, Brines M, Rosenbaum DM (2002) Erythropoietin administration protects retinal neurons from acute ischemia-reperfusion injury. Proc Natl Acad Sci USA 99:10659 - 10664

Kapuscinski I, Szer W (1979) interactions of 4', 6-diamidine-2-phenylindole with synthetic polynucleotides. Nucleic Acid Res 6:3535-3542

Keswani SC, Chander B, Hasan C, Griffin JW, McArthur JC, Hoke A (2003) FK506 is neuroprotective in a model of antiretroviral toxic neuropathy. Ann Neurol 53:57–64

Keswani SC, Buldanlioglu U, Fischer A, Reed N, Polley M, Liang H, Zhou C, Jack C, Leitz GJ, Hoke A (2004) A novel endogenous erythropoietin mediated pathway prevents axonal degeneration. Ann Neurol 56:815–826

Kawakami M, Sekiguchi M, Sato K, Kozak S, Takahashi M (2001) Erythropoietin receptor-mediated inhibition of axocytotic glutamate release confers neuroprotection during chemical ischemia. J Biol Chem 276(42):39469-39475

Kilic E, Kilic U, Soliz J, Bassetti CL, Gassmann M, Hermann DM (2005) Brain-derived erythropoietin protects from focal cerebral ischemia by dual activation of ERK-1/-2 and Akt pathways. FASEB J 19:2026–2028

Kotani Y, Matsuda S, Sakanaka M, Kondoh K, Ueno S, Sano A (1996) Prosaposin facilitates sciatic nerve regeneration *in vivo*. J Neurochem 66:2019–2025

Kretz A, Happold CJ, Marticke JK, Isenmann S (2005) Erythropoietin promotes regeneration of adult CNS neurons via Jak2/Stat3 and PI3K/AKT pathway activation. Mol Cell Neurosci 29:569-79

Lacombe C, Mayeux P (1999) The molecular biology of erythropoietin. Nephrol Dial Transplant 14:22-28

Lewczuk P, Hasselblatt M, Kamrowski-Kruck H, Heyer A, Unzicker C, Sirén AL, Ehrenreich H (2000) Survival of hippocampal neurons in culture upon hypoxia: effect of erythropoietin. Neuroreport 11:3485-3488

Liu J, Narasimhan P, Yu F, Chan PH (2005) Neuroprotection by Hypoxic Preconditioning Involves Oxidative Stress-Mediated Expression of Hypoxia-Inducible Factor and Erythropoietin. Stroke 36:1264-1269

Liu R Suzuki A Guo Z, Mizuno Y, Urabe T (2006) Intrinsic and extrinsic erythropoietin enhances neuroprotection against ischemia and reperfusion injury *in vitro.* J neurochem 96(4):1101-1110

Marti HH, Wenger RH, Rivas LA, Straumann U, Digicaylioglu M, Henn V, Yonekawa Y, Bauer C, Gassmann M (1996) Erythropoietin gene expression in human, monkey and murine brain. Eur J Neurosci 8:666-676

Marti HH (2004) Erythropoietin and the hypoxic brain. J Exp Biol 207:3233-3242

Maxwell PH, Wiesener MS, Chang GW, Clifford SC, Vaux EC, Cockman ME, Wykoff CC, Pugh CW, Maher ER, Ratcliffe PJ (1999) The tumour suppressor protein VHL targets hypoxia-inducible factors for oxygen-dependent proteolysis. Nature 399:271-275

Meloni BP, Tilbrook PA, Boulos S, Arthur PG, Knuckey NW (2006) Erythropoietin preconditioning in neuronal cultures: signaling, protection from in vitro ischemia, and proteomic analysis. J Neurosci Res 83:584–93

Metzen E, Berchner-Pfannschmidt U, Stengel P, Marxsen JH, Stolze I, Klinger M, Huang WQ, Wotzlaw C, Hellwig-Bürgel T, Jelkmann W, Acker H, Fandrey J (2003) Intracellular localisation of human HIF-1α hydroxylases: implications for oxygen sensing. J Cell Sci 116:1319-1326

Metzen E, Ratcliff PJ (2004) HIF hydroxylation and cellular oxygen sensing. J Biol Chem 385(3):223-230

Morishita E, Masuda S, Nagao M, Yasuda Y & Sasaki R. (1997) Erythropoietin receptor is expressed in rat hippocampal and cerebral cortical neurons, and erythropoietin prevents *in vitro* glutamate-induced neuronal death. Neuroscience 76:105−116

Morrison RS, Sharma A, deVellis J, Bradshaw RA (1986) Basic fibroblast growth factor supports the survival of cerebral cortical neurons in primary culture. Proc Natl Acad Sci USA 83:7537–7541

Mosmann (1983) Rapid colorimetric assay for cellular growth and survival: application to proliferation and cytotoxicity assays. J Immunol Methods 65(1-2):55-63

Northington FJ, Ferriero DM, Graham EM, Traystman RJ, Martin LJ (2001a) Early neurodegeneration after hypoxia-ischemia in neonatal rat is necrosis while delayed neuronal death is apoptosis. Neurobiol Dis 8:207–19

Northington FJ, Ferriero DM, Martin LJ (2001b) Neurodegeneration in the thalamus following neonatal hypoxia-ischemia is programmed cell death. Dev Neurosci 23:186–91

Paffett-Lugassy N, Hsia N, Fraenkel PG, Paw B, Leshinsky I, Barut B, Bahary N, Caro J, Handin R, Zon LI (2009) Epo-EpoR signaling not required for cardiovascular or neural development. Blood 110:2718-2726

Renzi MJ, Farrell FX, Bittner A, Galindo JE, Morton M, Trinh H and Jolliffe LK (2002) Erythropoietin induces changes in gene expression in PC-12 cells. Brain Res Mol 104: 86–95

Rousselet A, Fetler L, Chamak B, Prochiantz A (1988) Rat mesencephalic neurons in culture exhibit different morphological traits in the presence of media conditioned on mesencephalic or striatal astroglia. Dev Biol 129:495–504

Ruscher K, Freyer D, Karsch M, Isaev N, Megow D, Sawitzki B, Priller J, Dirnagl U, Meisel A (2002) Erythropoietin is a paracrine mediator of ischemic tolerance in the brain: evidence from an in vitro model. J Neurosci 22:10291–301

Sakanaka M, Wen T-C, Matsuda S, Masuda S, Morishita E, Nagao M & Sasaki R. (1998) *In vivo* evidence that erythropoietin protects neurons from ischemic damage. Proc Natl Acad Sci USA 95:4635−4640

Semenza GL, Wang GL (1992) A nuclear factor induced by hypoxia via de novo protein synthesis binds to the human erythropoietin gene enhancer at a site required for transcriptional activation. Mol Cell Biol 12(12): 5447-5454

Semenza GL (2001a) HIF-1 and mechanisms of hypoxia sensing. Curr Opin Cell Biol 13:167–171

Semenza GL (2001b) HIF-1, O-2, and the 3 PHDs: how animal cells signal hypoxia to the nucleus. Cell 107:1–3

Shang Y, Wu Y, Yao S, Wang X, Feng D, Yang W (2007) Protective effect of erythropoietin against ketamine-induced apoptosis in cultured rat cortical neurons: involvement of PI3K/Akt and GSK-3 beta pathway. Apoptosis 12:2187–95

Silva M, Grillot D, Benito A, Richard C, Nunez G, Fernandez-Luna JL (1996) Erythropoietin can promote erythroid progenitor survival by repressing apoptosis through bcl-$x_L$ and bcl-2. Blood 88:1576-1582

Sinor AD, Greenberg DA (2000) Erythropoietin protects cultured cortical neurons, but not astroglia, from hypoxia and AMPA toxicity. Neurosci Lett 290:213-215

Sirén AL, Fratelli M, Brines M, Goemans C, Casagrande S, Lewczuk P, Keenan S, Gleiter C, Pasquali C, Capobianco A, Mennini T, Heumann R, Cerami A, Ehrenreich H, Ghezzi P (2001a) Erythropoietin prevents neuronal apoptosis after cerebral ischemia and metabolic stress. Proc Natl Acad Sci USA 98:4044 -4049

Sirén AL, Knerlich F, Poser W, Gleiter CH, Brück W, Ehrenreich H (2001b) Erythropoietin and erythropoietin receptor in human ischemic/hypoxic brain. Acta Neuropathol 1001:271-276

Sugawa M, Sakurai Y, Ishikawa-Ieda Y, Suzuki H, Asou H (2002) Effects of erythropoietin on glial cell development; oligodendrocyte maturation and astrocyte proliferation. Neurosci Res 44:391-403

Ui-Tei K, Nagano M, Sato S, Miyata Y (2000) Calmodulin-dependent and independent apoptosis in cells of a *Drosophila* neuronal cell line. Apoptosis 5:133–140.

Volpe JJ (2001) Perinatal brain injury: from pathogenesis to neuroprotection. Ment Retard Dev Disabil Res Rev 7:56–64

Weishaupt JH, Rohde G, Polking E, Sirén AL, Ehrenreich H, Bähr M (2004) Effect of erythropoietin axotomy-induced apoptosis in rat retinal ganglion cells. Invest. Ophthalmol Visual Sci 45:1514–1522

Wen TC, Sadamoto Y, Tanaka J, Zhu PX, Nakata K, Ma YJ, Hata R, Sakanaka M (2002) Erythropoietin protects neurons against chemical hypoxia and cerebral ischemic injury by up-regulating Bcl-$x_L$ expression. J Neurosci Res 67:795 -803

Wenger R (2002) Cellular adaptation to hypoxia: $O_2$-sensing protein hydroxylases, hypoxia-inducible transcription factors, and $O_2$-regulated gene expression. FASEB J 16:1151-1162

Wu Y, Shang Y, Sun S, Liang H, Liu R (2007) Erythropoietin prevents PC12 cells from 1-methyl-4-phenylpyridinium ion-induced apoptosis via the Akt/GSK-3beta/caspase-3 mediated signaling pathway. Apoptosis 12:1365–1375

Yamaji R, Okada T, Moriya M, Naito M, Tsuruo T, Miyatake K & Nakano Y. (1996) Brain capillary endothelial cells express two forms of erythropoietin receptor mRNA. Eur J Biochem 239:494−500

Yoshimura A, Misawa H (1998) Physiology and function of the erythropoietin receptor. Curr Opin Hematol 5:171–176

Zipfel GJ, Babcock DJ, Lee JM, Choi DW (2000) Neuronal apoptosis after CNS injury: the roles of glutamate and calcium. J Neurotrauma 17:857–69

Zhong Y, Yao H, Deng L, Cheng Y, Zhou X (2007) Promotion of neurite outgrowth and protective effect of erythropoietin on the retinal neurons of rats. Graefes Arch Clin Exp Ophthalmol 245:1859–1867

# Summary

This doctoral study provided substantial evidences for the presence of the EPO/EPOR signalling system in the CNS of invertebrates from different phyla (chapter 2) and demonstrated neuroprotective and neuroregenerative functions of EPO on neuronal cells of insects both *in vivo* (chapter 3) and *in vitro* (chapter 4). Since glia is a major player in mammalian central nervous EPO/EPOR signalling and relatively little information about insect glia is available, the glia distribution and glia-to-neuron ratio were determined in locust brains. Furthermore, glial cell survival, morphology and functions were studied in primary cell cultures from locust brains (chapter 1).

Chapter 1: In central brains of fourth nymphal stage of *L. migratoria* the glia-to-neuron ratio was determined to be 1:2 both *in situ* and in dissociated primary cell cultures. Further analysis of primary cultured locust brain cells revealed a progressive reduction of glial cells within the first 5-6 days of cultivation. Analysis of primary cell cultures provided evidence for mobility and phagocytotic activity of glial cells. Furthermore, DAPI nuclear staining was established as a reliable marker to distinguish living from dead or dying cultured cells and indicated that dead cells detach from the substrate and vanish from the analysis.

Chapter 2: Antibodies raised against mammalian EPO and EPOR provided reproducible patterns of distinctly labelled cell bodies and neurites in the CNS of annelids (*Hirudo medicinalis*), crustaceans (*Procambarus spec.*) and insects (*Drosophila melanogaster*, *Locusta migratoria*). Furthermore, Western blot analysis indicated that the antigenic proteins detected in invertebrate nervous tissues had molecular sizes that were similar to those detected in mouse brain tissues and matched the range of sizes reported for mammalian EPO and EPOR proteins.

Chapter 3: Peripheral nerve crush injury of the leg nerve N5 of the grasshopper *Chorthippus biguttulus* caused increased *ia*EPOR immunoreactivity in central neuropil regions of the metathoracic ganglion, whereas *ia*EPO expression remained unchanged. Application of recombinant human EPO accelerated axonal regeneration of crushed auditory receptor fibres leading to a faster and more complete functional regeneration of acoustic orientation.

Chapter 4: The application of recombinant human EPO increased cell vitality of primary cultured locust brain cells and cultured *Drosophila* BG2 cells. EPO reduced hypoxia-induced cell death in cultures of locust brain neurons and the *Drosophila* derived neuronal cell line. Dose-dependency of this beneficial effect followed a typical optimum curve. In addition, EPO promoted the elongation of regenerating neurites without contributing to the initiation of neurite formation by cultured dissociated neuronal cell bodies.

Although EPO was initially described as the main regulator of vertebrate erythropoiesis, the results of my doctoral studies indicate that a ligand/receptor system similar to the vertebrate EPO/EPOR signalling system is expressed in the nervous systems of invertebrates. As in the

mammalian nervous systems, the invertebrate analogue of EPO/EPOR signalling (i) promotes neuronal survival in hypoxic conditions and following mechanical damage and (ii) supports neuroregeneration and the reestablishment of previous functions. A function in the nervous system of invertebrates suggests that the EPO/EPOR signalling system was already present before vertebrates emerged in evolution and that a protective role against invading pathogens and other harmful stimuli might have been its original function.

# References mentioned in the introduction


Belayev L, Khoutorova L, Zhao W, Vigdorchik A, Belayev A, Busto R, Magal E, Ginsberg MD (2005) Neuroprotective effect of darbepoetin alfa, a novel recombinant erythropoietic protein, in focal cerebral ischemia in rats. Stroke 36:1071–1076

Bernaudin M, Bernaudin M, Marti HH, Roussel S, Divoux D, Nouvelot A, MacKenzie ET, Petit E (1999) A potential role for erythropoietin in focal permanent cerebral ischemia in mice. J Cereb Blood Flow Metab 19:643–651

Böcker-Meffert S, Rosenstiel P, Röhl C, Warneke N, Held-Feindt J, Lucius R (2002) Erythropoietin and VEGF promote neural outgrowth from retinal explants in postnatal rats. Invest Ophthalmol Vis Sci 43:2021–2026

Brines A, Grasso G, Fiordaliso F, Sfacteria A, Ghezzi P, Fratelli M, Latini R, Xie QW, Smart J, Su-Rick C, Pobre E, Diaz D, Gomez D, Hand C, Coleman T, Cerami A (2004) Erythropoietin mediates tissue protection through an erythropoietin and common β-subunit heteroreceptor. Proc Nat Acad Sci USA 101(41):14907-14912

Campana WM, Myers RR (2001) Erythropoietin and erythropoietin receptors in the peripheral nervous system: changes after nerve injury. FASEB J 15:1804–1806

Chou CF, Tohari S, Brenner S, Venkatesh B (2004) Erythropoietin gene from a teleost fish, *Fugu rubripes*. Blood 104:1498-1503

Chu CY, Cheng CH, Chen GD, Chen YC, Hung CC, Huang KY, Huang CJ (2007) The zebrafish erythropoietin: Functional identification and biochemical characterization. FEBS Letters 581:4265-4271

Coleman TR, Westenfelder C, Togel FE, Yang Y, Hu Z, Swenson L, Leuvenink HG, Ploeg RJ, d'Uscio LV, Katusic ZS, Ghezzi P, Zanetti A, Kaushansky K, Fox NE, Cerami A, Brines M (2006) Cytoprotective doses of erythropoietin or carbamylated erythropoietin have markedly different procoagulant and vasoactive activities. Proc Nat Acad Sci USA 103:5965–5970

Dame C, Fahnenstich H, Freitag P, Hofmann D, Abdul-Nour T, Bartmann P, Fandrey J (1998) Erythropoietin mRNA expression in human fetal and neonatal tissue. Blood 92:3218-3225

Erbayraktar S, Grasso G, Sfacteria A, Xie QW, Coleman T, Kreilgaard M, Torup L, Sager T, Erbayraktar Z, Gokmen N, Yilmaz O, Ghezzi P, Villa P, Fratelli M, Casagrande S, Leist M, Helboe L, Gerwein J, Christensen S, Geist MA, Pedersen LO, Cerami-Hand C, Wuerth JP, Cerami A, Brines M (2003) Asialoerythropoietin is a nonerythropoietic cytokine with broad neuroprotective activity *in vivo*. Proc Natl Acad Sci USA 100:6741–6746

Erslev A (1953) Humoral regulation of red cell production. Blood 8:349-357

Jelkmann W (1992) Erythropoietin: structure, control of production, and function. Physiol Rev 72:449-489

Juul SE, Yachnis AT, Rojiani AM, Christensen RD (1999) Immunohistochemical localization of erythropoietin and its receptor in the developing human brain. Pediatr Dev Pathol 2:148-158

Juul S (2002) Erythropoietin in the central nervous system, and its use to prevent hypoxic-ischemic brain damage. Acta Paediatr Suppl 438:36-42

Knabe W, Knerlich F, Washausen S, Kietzmann T, Siren AL, Brunnett G, Kuhn HJ, Ehrenreich H (2004) Expression patterns of erythropoietin and its receptor in the developing midbrain. Anat Embryol (Berl) 207:503-512

Kretz A, Happold CJ, Marticke JK, Isenmann S (2005) Erythropoietin promotes regeneration of adult CNS neurons via Jak2/Stat3 and PI3K/AKT pathway activation. Mol Cell Neurosci 29:569-79

Lewczuk P, Hasselblatt M, Kamrowski-Kruck H, Heyer A, Unzicker C, Sirén AL, Ehrenreich H (2000) Survival of hippocampal neurons in culture upon hypoxia: effect of erythropoietin. Neuroreport 11:3485-3488

Leist M, Ghezzi P, Grasso G, Bianchi R, Villa P, Fratelli M, Savino C, Bianchi M, Nielsen J, Gerwien J, Kallunki P, Larsen AK, Helboe L, Christensen S, Pedersen LO, Nielsen M, Torup L, Sager T, Sfacteria A, Erbayraktar S (2004) Derivatives of erythropoietin that are tissue protective but not erythropoietic. Science 305:239–242

Li XQ, Gonias SL, CampanaWM (2005) Schwann cells express erythropoietin receptor and represent a major target for Epo in peripheral nerve injury. Glia 51:254–265

Masuda S, Okano M, Yamagishi K, Nagao M, Ueda M, Sasaki R (1994) A novel site of erythropoietin production. Oxygen-dependent production in cultured rat astrocytes. J Biol Chem 269:19488-19493

Morishita E, Masuda S, Nagao M, Yasuda Y, Sasaki R (1997) Erythropoietin receptor is expressed in rat hippocampal and cerebral cortical neurons and erythropoietin prevents in vitro glutamate-induced neuronal death. Neuroscience 76:105-116

Ruscher K, Freyer D, Karsch M, Isaev N, Megow D, Sawitzki B, Priller J, Dirnagl U, Meisel A (2002) Erythropoietin is a paracrine mediator of ischemic tolerance in the brain: evidence from an in vitro model. J Neurosci 22:10291–301

Sasaki H, Bothner B, Dell A, Fukuda M (1987) Carbohydrate structure of erythropoietin expressed in Chinese hamster ovary cells by a human erythropoietin cDNA. J Biol Chem 262:12059-12076

Sinor AD, Greenberg DA (2000) Erythropoietin protects cultured cortical neurons, but not astroglia, from hypoxia and AMPA toxicity. Neurosci Lett 290:213 -215

Sirén AL, Knerlich F, Poser W, Gleiter CH, Brück W, Ehrenreich H (2001) Erythropoietin and erythropietin receptor in human ischemic/hypoxic brain. Acta Neuropathol 1001:271-276

Tan C, Eckardt KU, Firth JD, Ratcliffe PJ (1992) Feedback modulation of renal and hepatic erythropoietin mRNA in response to graded anemia and hypoxia. Am J Physiol Renal Physiol 263: F474-F481

Toth C, Martinez JA, Liu WQ, Diggle J, Guo GF, Ramji N, Mi R, Hoke A, Zochodne DW (2008) Local erythropoietin signaling enhances regeneration in peripheral axons. J of Neurosci 154(2):767-783

Villa P, van BJ, Larsen AK, Gerwien J, Christensen S, Cerami A, Brines M, Leist M, Ghezzi P, Torup L (2007) Reduced functional deficits, neuroinflammation, and secondary tissue damage after treatment of stroke by nonerythropoietic erythropoietin derivatives. J Cereb Blood Flow Metab 27:552–563

Wang L, Zhang Z, Wang Y, Zhang R, Chopp M (2004) Treatment of stroke with erythropoietin enhances neurogenesis and angiogenesis and improves neurological function in rats. Stroke 35:1732–1737

Wang Y, Zhang ZG, Rhodes K, Renzi M, Zhang RL, Kapke A, Lu M, Pool C, Heavner G, Chopp M (2007) Post-ischemic treatment with erythropoietin or carbamylated erythropoietin reduces infarction and improves neurological outcome in a rat model of focal cerebral ischemia. Br J Pharmacol 151:1377–1384

Weber A, Maier R F, Hoffmann U, Grips M, Hoppenz M, Aktas AG, Heinemann U, Obladen M, Schuchmann S (2002) Erythropoietin improves synaptic transmission during and following ischemia in rat hippocampal slice cultures. Brain Res 958:305-311

Yu X, Shacka JJ, Eells JB, Suaret-Quian C, Przygodzki RM, Beleslin-Cokic B, Lin CS, Nikodem VM, Hempstead B, Flanders KC, Constantini F, Noguchi CT (2002) Erythropoietin receptor signalling is required for normal brain development. Develop 129:505-516

Zanjani ED, Poster J, Burlington H, Mann LI, Wasserman LR (1977) Liver as the site of Epo formation in the fetus. J Lab Clin Med 89:640

Zhong Y, Yao H, Deng L, Cheng Y, Zhou X (2007) Promotion of neurite outgrowth and protective effect of erythropoietin on the retinal neurons of rats. Graefes Arch Clin Exp Ophthalmol 245:1859–1867

# List of Abbreviations

| | |
|---|---|
| % | percent |
| α- | anti- |
| α | alpha |
| βcR | common β receptor |
| A | adenine |
| Ad | adult |
| AL | antennal lobe |
| AN | antennal nerve |
| aqua dest. | *aqua destillata* |
| ARNT | aryl hydrocarbon receptor nuclear translocator |
| bcl-2 | B-cell lymphoma 2 |
| bcl-xL | B-cell lymphoma-extra large |
| BSA | bovine serum albumin |
| ℃ | celcius |
| C57BL/6 | C57 black 6 – commonly used inbred strain of mice |
| Ca | calyces of mushroom bodies |
| CA | *Cornu ammonis* |
| $CaCl_2$ | calcium dichloride |
| CB | central body |
| CBP | CREB binding protein |
| CCD | charge coupled device |
| *Ch.* | *Chorthippus* |
| CNS | central nervous system |
| cm | centimetre |
| $CO_2$ | carbon dioxide |
| CREB | cyclic-AMP-response element-binding protein |
| C-TAD | C-terminal transactivation domain of HIF-1α |
| Cy2 | cyanine |
| Cy3 | indocarbocyanine |
| *D.* | *Drosophila* |
| DAPI | 4´-6-diamino-2-phenylindole |
| 2-DG | 2-deoxyglucose |
| DMSO | dimethyl sulfoxide |
| DNA | deoxyribonucleic acid |
| DRG | dorsal root ganglion |
| E13 | embryonic day 13 |
| e.g. | *exempli gratia* (for example) |

| | |
|---|---|
| ECL | enhanced chemiluminescence |
| EPO | erythropoietin |
| EPOR | erythropoietin receptor |
| ERK | extracellular signal-regulated kinase |
| FBS | fetal bovine serum |
| FCS | fetal calf serum |
| FCSG | fetal calf serum gold |
| g | gravity |
| GABA | γ-aminobutyric acid |
| GM | gentamicin |
| GmbH | Gesellschaft mit beschränkter Haftung |
| h | hour |
| $H_2O$ | water |
| HBBS | Hank`s balanced salt solution |
| HIF-1 | hypoxia-inducible-factor-1 |
| HIV | human immunodeficiency virus |
| HRE | hypoxia-responsive elements |
| HRP | horseradish peroxidase |
| HSP70-2 | heat shock protein 70-2 |
| HSP70-5 | heat shock protein 70-5 |
| hNT | human neuroteratocarcinoma neurons |
| *ia*EPO | *invertebrate analog* of Erythropoietin |
| *ia*EPOR | *invertebrate analog* of Erythropoietin receptor |
| IGF-I | insulin-like growth factor-I |
| IL | Interleukin |
| JAK | Janus-tyrosine kinase |
| KCl | potassium chloride |
| kDa | kilodalton |
| *L.* | *Locusta* |
| L15 | Leibovitz medium |
| LAL | lateral accessory lobe |
| LH | lateral horn |
| LO | lobula |
| ME | medulla |
| min | minute |
| ML-DmBG2-c2 | neuronal cell line from the larval *Drosophila* nervous system |
| ml | millilitre |
| mm | millimetre |
| mM | millimolar |
| mRNA | messenger ribonucleic acid |
| MTT | 3-(4,5-dimethylthiazol-2-yl)2,5-diphenyl tetrazolium bromide |

| | |
|---|---|
| n | number |
| $N_2$ | nitrogen gas |
| N5 | leg nerve of the metathoracic ganglion |
| N6 | tympanal nerve of the metathoracic ganglion |
| $Na_2HPO_4$ | disodium hydrogen phosphate |
| NaCl | sodium chloride |
| $NaH_2PO_4$ | monosodium phosphate |
| $NF_KB$ | nuclear factor kappa-light-chain-enhancer of activated B cells |
| NGS | normal goat serum |
| nm | nanometre |
| NO | nitric oxide |
| NPC | neuronal progenitor cell |
| NT2 | human teratocarcinoma cell line |
| $O_2$ | oxygen |
| OD | optical density |
| ODD | oxygen-dependent degradation domain of HIF-1α |
| OL | olfactory lobe |
| P19 | mouse embryonic carcinoma cells |
| P | pedunculus of mushroom body |
| *P.* | *Procambarus* |
| P5 | postnatal day 5 |
| p-value | expectation value |
| PB | phosphate buffer |
| PB | protocerebral bridge |
| PBS | phosphate buffered saline |
| PC12 | cancer cell line derived from a pheochromocytoma of the rat adrenal medulla |
| PI(3)K | phosphatidylinositol-3-kinase |
| pM | picomolar |
| PMSF | phenylmethylsulphonyl fluoride |
| PNS | peripheral nervous system |
| R | retina |
| Ras-MAPK | Ras mitogen-activated protein kinase |
| Ras | Rat sarcoma |
| RBX1 | ring box protein 1 |
| Repo | reversed polarity |
| RGC | retinal ganglion cell |
| rhEPO | recombinant human erythropoietin |
| rpm | rounds per minute |
| RT | room temperature |
| SaGl | satellite glia |

| | |
|---|---|
| SD | standard deviation |
| SDS-PAGE | sodium dodecyl sulphate polyacrylamide gel electrophoresis |
| sEPOR | soluble EPO receptor |
| SGN | spiral ganglion cells |
| SK-N-MC | neuroepithelioma cell line derived from a metastatic supra- |
| SN6 | cholinergic neuronal cell line derived from a fusion of mouse |
| STAT | signal transducer and activator of transcription |
| SubEG | subesophageal ganglion |
| SupraEG | supraesophageal ganglion |
| T | thymine |
| TBS | Tris buffered saline |
| TBS-T | Tris buffered saline with Tween |
| TNF-α | tumor necrosis factor alpha |
| TPO | thrombopoietin |
| TPOR | thrombopoietin receptor |
| UK | United Kingdom |
| VAC | anterior ventral association center |
| VHL | von Hippel Lindau protein |
| VIT | ventral intermediate tract |
| VMT | ventral median tract |
| µg | microgram |
| µl | microlitre |
| µm | micrometre |

# Acknowledgements

First of all my special graditude goes to my supervisor Prof. Dr. **Ralf Heinrich** for providing me the opportunity to work in his laboratory. Thanks a lot for your constant support in all aspects of my research, for giving me the chance to work independently and for your unfailing will to discuss any problems.

I owe many thanks to Prof. Dr. Dr. **Hannelore Ehrenreich**, my second thesis committee member, for her collaboration, support and her confidence in my work.

I also thank the other members of my defense committee Prof. Dr. **Andreas Stumpner**, Prof. Dr. **Norbert Elsner**, Prof. Dr. **Rüdiger Hardeland** and Prof. Dr. **André Fiala** for their interest in my doctoral thesis.

Sincere thanks go to **Marianne Fischer** of the Marianne & Dr. Fritz Walter Fischer-foundation for the financial funding of my doctoral studies.

I am very thankful to my ´labmoms` **Margret Winkler** and **Patricia Sprysch** for their ambitious help in small and large technical problems.

Many thanks also go to **Simone Wagner**, a busy bee, with a lot of effort to understand the life of cultured locust brain cells.

I also would like to thank all **members of diverse biological companies** that consistently supplied me with free samples.

Furthermore, I am very grateful to all my **colleagues of the neurobiology** and **cell biology department** that made the institute to a second home for me during my conferral of a doctorate.

I want to express my gratitude to my **family** for their constant support, their confidence in my decisions and their encouragement in frustrating periods. I greatly appreciate to have such a lovely family!

Last but not least, I would like to thank my ´future husband` **Tim**, who often saved me from drowning. I am looking forward to our common future starting in the USA!

# Curriculum Vitae

Daniela Gocht
Mauerstr. 21
37073 Göttingen

phone: +49(0)173-5602310
E-Mail: DaniGocht@gmx.de
Date of birth: February 17th, 1982
Place of birth: Dresden
Marital status: unmarried

## Education

| | |
|---|---|
| 1988 - 1993 | Elementary school Herbert Warnke, Dresden |
| 1993 - 2000 | Secondary school (Gymnasium) Julius-Ambrosius-Hülße, Dresden<br>Final secondary-schools examination (Abitur): 2.2 |

## Academic studies

| | |
|---|---|
| 2000 - 2005 | Georg-August-University, Göttingen<br>Subject: Biology |
| August 31th, 2005 | Diploma in Biology:<br>major subject: zoology (1.0)<br>1. minor subject: pharmacology (1.3)<br>2. minor subject: human genetics (1.0)<br>Diploma thesis: „Untersuchung elektrophysiologischer Eigenschaften spontanaktiver Serotoninzellen des Blutegels *Hirudo medicinalis*“ (1.0) |

## Conferral of a doctorate

| | |
|---|---|
| since December 2005 | Georg-August-University, Göttingen<br>Institute for Zoology, Department of Neurobiology<br>(supervisor Prof. Dr. Ralf Heinrich)<br>PhD thesis: „Expression and function of erythropoietin and its receptor in invertebrate nervous systems“ |

## Stipend

| | |
|---|---|
| February 2007 - March 2009 | PhD-scholarship of the Marianne und Dr. Fritz Walter Fischer-Foundation |

## Teaching Experience

| | |
|---|---|
| February 2004 | Georg-August-University, Göttingen<br>Student assistant for the basic course in zoology |
| September 2005 | International Max Planck Research School, Göttingen<br>Student assistant for the Neuroanatomy course |
| April - July 2006 | Georg-August-University, Göttingen<br>Lecturer of an undergraduate students tutorial |
| October 2006 - January 2007 | Professional school for assistant medical technicians, Göttingen<br>Teaching activity, subject: biology |
| September 2007 | Georg-August-University, Göttingen<br>Graduate assistant for the advanced neuropharmacology course |
| August 2007 - February 2008 | Georg-August-University, Göttingen<br>Supervisor of a undergraduate student<br>Thesis title: “The neuroprotective and neuroregenerative effect of erythropoietin on primary cultured locust neurons” |
| February - April 2009 | Georg-August-University, Göttingen<br>Graduate assistant for the advanced neurophysiology course |

## Research Experience

| | |
|---|---|
| August - October 2001 | Georg-August-University, Göttingen<br>Department of Neurobiology (Prof. Dr. N. Elsner)<br>Student research assistant (Immunocytochemical studies in the locust brain) |
| August - September 2003 | Georg-August-University, Göttingen<br>Centre for Internal Medicine, Department of Haematology and Oncology (PD Dr. rer. nat. Dieter Kube)<br>Student research assistant (Genotype analysis of patients with agressive Non-Hodgkin´s Lymphoma) |
| November - December 2003 | Max Planck Institute of Molecular Cell Biology and Genetics, Dresden<br>(Prof. Dr. M. Brand)<br>Student research assistant (Cellular analysis of protein trafficing in the zebrafish) |
| September - December 2005 | Georg-August-University, Göttingen<br>Department of Neurobiology (Prof. Dr. R. Heinrich)<br>Research assistant (Protein analysis by Western blot) |

Date: _____ Signature: _____

# Publications

**Articles in peer-reviewed journals:**

Gocht D, Wagner S, Heinrich R (2009) Recognition, presence and survival of locust central nervous glia *in situ* and *in vitro*. Microscopy and Research Technique 72(5): 385-397

Kube D, Hua T-D, Bonin F, Schoof N, Zeynalova S, Klöss M, Gocht D, Potthoff B, Tzvetkov M, Brockmöller J, Löffler M, Pfreundschuh M, Trümper L (2008) Effect of interleukin-10 gene polymorphisms on clinical outcome of patients with aggressive non-Hodgkin's lymphoma: an exploratory study. Clinical Cancer Research 14(12): 3777-3784

Hoffmann K, Wirmer A, Kunst M, Gocht D, Heinrich R (2007) Muscarinic excitation in grasshopper song control circuits is limited by acetylcholinesterase activity. Zoological Science 24: 1028-1035

Gocht D, Heinrich R (2006) Postactivation inhibition of spontaneously active neurosecretory neurons in the medicinal leech. Journal of Comparative Physiology A 193: 347–361

**Poster presentations:**

Gocht D, Wagner S, Heinrich R (2009) Recognition, presence and survival of locust central nervous glia *in situ* and *in vitro*. 32nd Göttingen Neurobiology Conference - 8th Meeting of the German Neuroscience Society in Göttingen, Germany

Gocht D, Sargin D, Sperling S, Ehrenreich H, Heinrich R (2007) Expression and function of human erythropoietin-responsive receptors in invertebrate nervous systems. 37th annual meeting of the Society for Neuroscience in San Diego, USA

Gocht D, Sargin D, Sperling S, Ehrenreich H, Heinrich R (2007) Expression and function of erythropoietin and its receptor in invertebrate nervous systems. 31nd Göttingen Neurobiology Conference - 7th Meeting of the German Neuroscience Society in Göttingen, Germany

Kube D, Hua T-D, Kulle B, Gocht D, Kloess M, Brockmöller J, Wojnowski L, Löffler M, Pfreundschuh M, Trümper L (2005) Interleukin-10 gene promoter polymorphisms in aggressive Non-Hodgkin lymphoma. 9th International Conference on Malignant Lymphoma in Lugano, Switzerland

Gocht D, Heinrich R (2005) Postactivation inhibition of spontaneously active serotonin-releasing neurosecretory cells in the medicinal leech. 30nd Göttingen Neurobiology Conference - 6th Meeting of the German Neuroscience Society in Göttingen, Germany